MAREES TERRESTRES

BULLETIN D'INFORMATIONS

105

15 MAI 1989

Association Internationale de Geodesie

Commission Permanente des Marees Terrestres

Editeur Prof. Paul MELCHIOR

Observatoire royal de Belgique

Avenue Circulaire 3

1180 Bruxelles

TABLE DES MATIERES

BIM 105

THE PRECISION OF THE DEVELOPMENT OF THE TIDAL GENERATING POTENTIAL AND SOME EXPLANATORY NOTES

XI QINWEN

Center for Analysis and Prediction
State Seismological Bureau
Beijing

A development of the tidal generating potential (TGP) is a fundamental theoretical problem in research and analytical calculation for earth tides. With arising and renewal of instruments for high precision observation of earth tides, especially superconducting gravimeter, the precision of earth tides observations come up to advanced standards. These data of observations have included much informations and materials about earth interior. In order to analyse and extract the informations effectively, a high precise development of TGP has been required.

At present there are two methods for obtained the development of TGP. One is spectrum method, the other is deductive method for formula, also called analytical method. The former requires to compute a long series of theoretical value of generating potential or gravity, and to design a spectrum method which can separate the tidal waves from the data series. It's precision is not only depend on the precision of theoretical value but the method for separating tidal waves. And the precision of the deductive method developed by us is principally depended on the precision of the ephemeris used for the moon and the sun (generally the ephemeris is simplified). The arguments obtained by the rigorous and perfect deductive program are absolutely reliable. The error of amplitudes are depended on the ephemeris error.

At first, let us do a mathematical analysis and error evaluation to find out the effect of ephemeris error. As an example, we take the expression of gravity included only the second order potential. it can be writen

$$\Delta g = -165.16\frac{\rho}{a}\left(\frac{c}{R}\right)^3\left(Cos^2\theta - \frac{1}{3}\right) \tag{1}$$

where

$$Cos\theta = Sin\varphi Sin\delta + Cos\varphi Cos\delta Cosl \tag{2}$$

from (1) we get

$$d(\Delta g)=\frac{\partial \Delta g}{\partial \theta}\frac{\partial \theta}{\partial \alpha}d\alpha+\frac{\partial \Delta g}{\partial \theta}\frac{\partial \theta}{\partial \delta}d\delta+\frac{\partial \Delta g}{\partial\left(\frac{c}{R}\right)}d\left(\frac{c}{R}\right) \tag{3}$$

where α is the right ascension of the moon and δ ,the declination.

We should consider a maximal effect of errors. When the celestial body is at the place of the upper culmination, then $\theta=\varphi-\delta$, so $\frac{\partial\theta}{\partial\delta}=-1$; When $\varphi=0$ and the celestial body is in the sky above the equator, due to $\delta=0$ and $\theta=l=\Theta-\alpha$, so $\frac{\partial\theta}{\partial\alpha}=-1$. By the law of error propagation , from (3) we get

$$m_{\Delta g}^2=(165.16)^2m_\alpha^2+(165.16)^2m_\delta^2+(330.32)^2m_{\frac{c}{R}}^2 \tag{4}$$

According to the principle of equality of error effect,

$$m_\alpha=m_\delta=m_{\frac{c}{R}}=m \tag{5}$$

then

$$m_{\Delta g}=404.54m \tag{6}$$

if we expect

$$m_{\Delta g}=0.001^{\mu gal}$$

corresponding to that

$$m=2.47\times10^{-6}\qquad(0''.5) \tag{7}$$

In other words, if one wishes the error of Δ g less than 1^{ngal}, thus the error of right ascension and declination of the moon must less than $0''.5$, that of $\frac{c}{R}$ less than 2.47×10^{-6}. We can see that the precision of 1^{ngal} requires very high precision for calculation of the ephemeris of the moon.

We have presented some papers [1] [2] on the development of TGP , [1] is a development obtained by the deductive program and Doodson's original method and data. The results show that the deductive program has a perfect function. in [2] we added some harmonic terms to calculate the ephemeris of the moon. But this results only have the amplitudes in the units of the 5th place of decimals.

We have improved that development once again. The fundamental dada are the same in [2]. The amplitudes are in the units of the 6th place of decimals. We got altogether 3070 waves in the new complete development. There are something we should give more details of explanation. In the new development we have 136 terms with long period in semidiurnal band, 12 terms with diurnal period in terdiurnal band and 2 terms with long period in fourth diurnal band. Although the amplitudes are not greater than 6×10^{-6}, but this phenomenon gives us much food for thought. In fact, it is really not difficult to comprehend if one understands the beat frequency and multiple frequency in physics. We can as well give an explanation on the basis of the formulas related to the amplitudes of waves in [1]. For example

$$H_{22} = Sin^2\delta Cos2I = 2Cos^2\zeta + Sin^2\delta - 1 \tag{8}$$

where $Sin^2\delta$ only has long period terms. That means the argument number a corresponding τ is equal to 0. The third term in the formula (8) is undoubtedly long period. The expression of $Cos\zeta$ has included the diurnal terms, it means the argument number a corresponding τ is equal to 1. Of course, we had to transform the products of trigonometric function into their sums or differences and use a formula

$$Cos\alpha Cos\beta = \frac{1}{2}[Cos(\alpha+\beta) + Cos(\alpha-\beta)]$$

Therefore the semidiurnal waves were derived from the first term, the long period terms were derived from the second term in the above formula. The long period terms can not completely offset the last two terms in formula (8), so it left 136 terms with long period in semidiurnal band in the new development. In addition, there is a numerical example. Since

$$Cos\zeta = -0.953772\,Cos\tau$$

this is an principal term in the expression of $cos\zeta$.
Therefore

$$Cos^2\zeta = 0.4548405Cos(2\tau) + 0.4548405Cos(0\tau) \tag{9}$$

it shows that the expression of $cos^2\zeta$ included a long periodic term and a semidiurnal periodic term.

The origins producing diurnal terms in the terdiurnal band and the long period

in fourth diurnal band are the same as that above—mentioned.

Besides that there are some explanatory notes on the new complete development.

(1) On the local mean lunar time τ

Up to now the formula

$$\tau = t + h - s + \lambda \tag{10}$$

have been continually used to calculate a local mean lunar time. It derived from local sidereal time θ^* (suppose it is measured from the lower culmination)

$$\theta^* = \tau + s = t + h + \lambda \tag{11}$$

where the universal time t was defined by the mean velocity of the diurnal apparent motion of the sun, the aberration was included in it. Generally, in (11) h did not include the aberration. Therefore, in the strict sense, h should be replaced by $\bar{\alpha}_s$, the right ascension of the mean equatorial sun for universal time. The discrepancy between $\bar{\alpha}_s$ and h is caused, besides the aberration, by a long periodic acceleration of the sun and a difference of a long periodic change for the general precession in right ascension and that in longitude. It can be expressed by $(\lambda_2+h_2)t^2-m_2t^2$ [3].

Therefore the strict expression for τ is

$$\tau = t + \bar{\alpha}_s - s + \lambda \tag{12}$$

$$\bar{\alpha}_s = 18^h.6973746 + 2400^h.0513369T_u + 0^h.0000258622T_u^2 - 1^h.7222 \times 10^{-9}T_u^3 \tag{13}$$

where T_u is the Julian century measured from Jan. 1. 2000. 12^h UT1 (JD = 2451545.0).

In [4] we have used a similar means to process the time angle of the moon and the sun. [5] has mentioned that as well, but it seems the author mixed up the mean lunar time, aberration of the sun and the true position.

(2) On the correction for dynamical time

To calculate a celestial position the dynamical time is used.. In the expressions of the arguments (s,h,p,n,p_s) for calculation of earth tides, the parameter T_d should be referenced Barycentric Dynamical Time (abbreviated TDB in French). The difference between Terrestrial Dynamical Time (TDT) and universal time UT1 is given by

$$\Delta T = TDT - UT1 = 32^s.184 + TAI - UT1 \tag{14}$$

where TAI is the International Atomic Time. The difference between the TDB and TDT only has same small periodic changes, the maximal term is the anniversary term, it's amplitude is about $0^s.001658$. For our purpose the difference between TDB and TDT can be neglected.

Generally, ΔT is obtained by compare the TAI with UT1. For example the reckoned value is about 56^s in 1988.

(3) On Doodson's normalization

In order to compare the relative importance of the amplitudes of tidal waves and determine to accept or reject a amplitude in the deductive processing of the development of TGP, Doodson had ingeniously used a normalization for the geodetic coefficients, so that the maximal values of all geodetic coefficients are equal to ± 1. But there was a mistake, the coefficient for G_{30}should be 0.5. We still adopt the original value 1.11803 established by usage.

(4) On the correction for nutation

To obtain a development by a spectrum method, of course,one should consider an effect of the nutation. But as we obtained the development of TGP by the deductive method, the effect of the nutation was not temporarily included. Therefore, for calculation of earth tides we should adopt a correction for nutation in longitude as follows

$$\Delta l = -0^\circ.00478 Sin N - 0^\circ.00037 Sin 2h \tag{15}$$

the values are between ± $1^s.2$. The correction can be added to the arguments (s,h,p,N,p_s) directly.

The nutation in obliquity is given

$$\Delta\varepsilon = 0^\circ.00256 Cos N + 0^\circ.00016 Cos 2h \tag{16}$$

(5) On the periodic variations in the arguments

The arguments just mentioned above must be added some corrections for periodic variations, called 《additive terms》[6], [7]

$$\Delta s = 0^\circ.00396 Sin(60^\circ.57 - 132^\circ.87 T_d) + 0^\circ.00202 Sin N$$

$$\Delta h = 0^\circ.00178 Sin(251^\circ.39 + 20^\circ.20 T_d) + (1''.866 - 0''.016 T_d) Sin(207^\circ.51 + 150^\circ.27 T_d)$$

$$
\begin{aligned}
&-0^\circ.00479T_d(1+0.003T_d)Sin(h-p_s)\\
\Delta p=&-0^\circ.00058Sin(71^\circ.40+20^\circ.20T_d)-0^\circ.00058SinN\\
\Delta N=&\,0^\circ.02666SinN+0^\circ.00433Sin(N+272^\circ.75-2^\circ.30T_d)\\
&+0^\circ.00052Sin(N+288^\circ.75-0^\circ.90T_d)\\
\Delta P_s=&\cdots\cdots
\end{aligned}
\qquad (17)
$$

The first two corrections Δs and Δh directly gave an effect to the longitudes of the moon and the sun. Therefore we must consider them in calculation for earth tides. The others can be neglected.

(6) On the corrections for planetary perturbations and that for geocentric coordinates of the sun

The corrections of planetary perturbations added to the coordinates of the sun were given by Newcomb. Generally they must be added to the longitude,latitude and the radius vector of the sun. But the correction for the latitude is very small, it can be neglected for our purpose. Considering to the geometrical mean longitude, it is a principal term of a expression for the longitude of the sun, for calculation of earth tides one can directly add the corrections for the sun's longitude to the principal term h, geometrical mean longitude of the sun. They were given by Meeus as follows [7]

$$
\begin{aligned}
&-0^\circ.00200Sin(67^\circ.20+32964^\circ.47T_d) && \textit{by Jupiter}\\
&-0^\circ.00154Sin(16^\circ.85-45036^\circ.89T_d)\\
&+0^\circ.00134Sin(81^\circ.51+22518^\circ.44T_d) && \textit{by Venus}\\
&+\cdots\cdots
\end{aligned}
$$

The sun's coordinates obtained from the proceeding of formulas were referenced to the centre–mass of the Earth–Moon system. So we have to add the corection of perturbations produced by the moon, in order to obtain the geocentric coordinates of the sun. According to Newcomb, it is

$$+0^\circ.00179\ \mathrm{Sin}(s-h)$$

Therefore, a total of the corections for the geometrical mean longitude must be

$$
\begin{aligned}
\Delta h=&\,0^\circ.00178Sin(251^\circ.39+20^\circ.20T_d)\\
&+(1''.866-0''.016T_d)Sin(207^\circ.51+150^\circ.27T_d)\\
&-0^\circ.00479T_d(1+0.003T_d)Sin(h-p_s)
\end{aligned}
$$

$$-0^\circ.00200Sin(67^\circ.20+32964^\circ.47T_d)$$
$$-0^\circ.00154Sin(16^\circ.85-45036^\circ.89T_d)$$
$$+0^\circ.00134Sin(81^\circ.51+22518^\circ.44T_d)$$
$$+0^\circ.00179Sin(s-h) \qquad (18)$$

In this section and last one T_d denotes the time interval measured from epoch J2000.0 TDB.

(7) On the geodetical coefficients and the phase corrections

In the table of the development of TGP we started a special column P_{ij}, they indicated that the tidal waves derived from potential P_{ij} and the geodetic coefficient G_{ij} must be used correspondingly. If i+j is equal to a even number, then the tidal wave is expressed in Cosine, so the phase correction for calculation of the gravitational theoretical value equals 0. If i+j is equal to a odd number, then it is expressed in Sine ,then the phase correction must be $-\frac{\pi}{2}$.

(8) On the ephemeris for the moon and the sun

Since the action of the attraction is related to the true distance between masses. Therefore the calculation of the tidal generating force must be referenced to a true position of the moon and the sun, not a apparent position.

Appendix 1. The arguments for epoch J2000.0

$$s=218^\circ.31643+481267^\circ.88128T_d-0^\circ.00161T_d^2+0^\circ.000005T_d^3$$
$$h=280^\circ.46607+36000^\circ.76980T_d+0^\circ.00030T_d^2$$
$$p=83^\circ.35345+4069^\circ.01388T_d-0^\circ.01031T_d^2-0^\circ.00001T_d^3$$
$$N=125^\circ.04452-1934^\circ.13626T_d+0^\circ.00207T_d^2+0^\circ.000002T_d^3$$
$$p_s=282^\circ.93835+1^\circ.71946T_d+0^\circ.00046T_d^2+0^\circ.000003T_d^3$$
$$\varepsilon=23^\circ.43929-0^\circ.01300T_d-0^\circ.00000016T_d^2+0^\circ.0000005T_d^3$$

where T_d is measured from 12^h Jan. 1. 2000. (JD = 2451545.0 TDB).

Appendix 2. Applied constants [8] , formulas and the new Doodson's constant

Equatorial radius of the earth a	6378140 m
Flatting factor of the earth α	1 / 298.257
Geocentric gravitational constant fE	3.986005×10^{20} cm^3 / sec^2
Mean value of gravity g_0	978.0318 cm / sec^2
Sine parallax of the moon $\mathrm{Sin}\pi = \frac{a}{c}$	0.01659251(3422″.451)
Ratio of mass of the moon to that of the earth $\mu = M / E$	0.01230002
Solar parallax $\pi_s (\mathrm{Sin}\pi_s = \frac{a}{c_s})$	8″.794148
Ratio of mass of the sun to that of the earth S / E	332946.0

Corresponding the a and the α ,

$$\frac{\rho}{a} = 1 - 0.00332479 \sin^2\varphi + \frac{H}{a}$$

The correction for geocentric latitude

$$\Delta\varphi = \varphi - \psi = 0^\circ.192424 \sin 2\varphi$$

where φ is geographical latitude. h, the elevation.

The definition of new Doodson's constant

$$G = G(\rho) = \frac{3}{4} f M \frac{\rho^2}{c^3} = \frac{3}{4} f E \frac{M}{E} \left(\frac{a}{c}\right)^3 \frac{1}{a} \left(\frac{\rho}{a}\right)^2 = G(a)\left(\frac{\rho}{a}\right)^2$$

$$D = G(a) = \frac{3}{4} f E \frac{M}{E} \left(\frac{a}{c}\right)^3 \frac{1}{a} = 26335.838 \quad cm^2 / sec^2$$

$$G(\rho) = \frac{3}{4} f S \frac{\rho^2}{c_s^3} = \left(\frac{c}{c_s}\right)^3 \frac{S}{M} G(\rho) = \frac{\left(\frac{a}{c_s}\right)^3 \frac{S}{E}}{\left(\frac{a}{c}\right)^3 \frac{M}{E}} G(\rho) = 0.45923780 G(\rho)$$

Appendix 3. A floppy diskette with the table of the new complete development of TGP

References

[1] Xi Qinwen, The algebraic deduction of harmonic development for the tide–generating potential with the IBM–pc, Earthquake research in China, Vol 3, No 2, p16– 28, Jan. 1987.

[2] Xi Qinwen, and Hou Tianhang, A new complete development of the tide–generating potential for the epoch J2000.0, Acta Geophysica Sinica, Vol 30, No 4, p349–362, July. 1987.

[3] E.W.Woolard, G.M.Clemence., Spherical astronomy, Survey press,1984 (in Chinese).

[4] Xi Qinwen, A calculation of theoretical value of earth tides, Acta Geophysica Sinica, Vol 25, Supp., p632–643, Dec. 1982.

[5] Tamura.Y., A harmonic development of the tide–generating potential, The meeting of the working group on high precision tidal data processing. 1986. Bonn.

[6] Eckert,W.J. et. al., Improved lunar ephemeris,1952–1959. U.S.Government Printing Office Washington,1954.

[7] Meeus,J., Tables of the moon and the Sun, Kesselderg Sterrenwacht, Belgium, 1962.

[8] MERIT Standards, U.S.Naval Observatory Circular, No 167.

DIRECT AND INDIRECT METHODS FOR CALCULATING THEORETICAL VALUES OF THE STRESS EARTH TIDE

Sun Wenke
(Earthquake Research Institute, The University of Tokyo)

ABSTRACT

This paper discusses both direct and indirect methods for calculating theoretical values of stress earth tide. Indirect method includes two sets of formulas -- closed and wave-summarized ones, which are valid in any depth of the earth. The paper specially discusses the problem of derivatives of Love functions. Geodetic coefficients and phase corrections of the stress earth tide are developed, which can be used for both calculating theoretical values and making harmonic analysis of the stress earth tide. The methods of the paper are suitable for the stress deformations caused by any external forces.

The theoretical calculation of the stress earth tide can be used not only for the study of earth stress field, but also for that of trigger effects of tidal force on earthquakes.

INTRODUCTION

Much study about the problem of stress responses of the earth to tide generating force has been made by many scientists in past decades. T. Heaton (1975), X. Gao (1981) and Q. Xi (1983) calculated respectively the stress tide field of a homogeneous sphere. P. Varga (1985) and Z. Ding et al (1986) studied the one of a layered sphere. This problem not only has theoretical values, but also has significance for understanding the stress field of the earth and studying trigger effects of the stress tide on an earthquake. Therefore, calculating the stress earth tide tensor is an important problem. An ideal calculating mode should include a reasonable earth model and assumptions as well as practical and convenient formulas. Like the gravity tide or strain tide, when time and position are provided, the stress tide tensor should be easily calculated.

In this paper, the earth models G-D1066A and PREM are adopted. From basic solutions of the equation of motion of the earth, direct and indirect methods for calculating stress tide under external forces (such as the tidal-generating force and loading force) are studied and discussed. As an example, for the Moon-Sun' s attraction, two sets of calculating formulas -- closed and wave- summarized ones -- are presented. All of the geodetic coefficients and the phase corrections of stress tide tensor are developed, which can be used in both calculating theoretical values and making harmonic analysis of the stress tide tensor. All of the formulas are valid everywhere in the earth. The problem of derivatives of Love functions is given a special discussion.

DIRECT METHOD

We assume that the earth deforms perfectly elastic under external forces. Its displacement and disturbing potential are usually expressed as (Alterman et al, 1959; Longman, 1962):

$$(u_r, u_\theta, u_\varphi)=(y_1(r), y_3(r)\frac{\partial}{\partial\theta}, y_3(r)\frac{\partial}{\sin\theta\,\partial\varphi})Y_n(\theta, \varphi) \tag{1a}$$

$$\phi=y_5(r)Y_n(\theta, \varphi) \tag{1b}$$

where $Y_n(\theta, \varphi)$ is a spherical harmonic function, (r, θ, φ) the radius and colatitude and longitude, respectively. $y_1(r)$ is the radial displacement factor, $y_3(r)$ the tangential one, and $y_5(r)$ the disturbed potential factor. $y_i(i=1, 3, 5)$ can be obtained by solving the following six-order equations

$$\underset{6\times1}{\dot{Y}}=\underset{6\times6}{A}\,\underset{6\times1}{Y} \tag{2}$$

where $Y=y_i(i=1, 2, \ldots, 6)$. $y_i(i=2, 4, 6)$ represent the radial stress, tangential stress and gravity change, respectively. Coefficient Matrix A is a function of elastic constants, density, gravity and radius of the earth. Dot '·' means the derivative $\frac{d}{dr}$.

Equation (2) has solutions only under certain boundary conditions. It is physically natural to adopt $y_i(a)(i=2, 4, 6)$ as the boundary conditions. Its general forms are

$$y_2(a)=\alpha \tag{3a}$$

$$y_4(a)=\beta \tag{3b}$$

$$y_6(a)=\gamma \tag{3c}$$

α, β *and* γ express boundary values. Different combinations correspond different natural phenomena and have certain determined solutions. For example, if $\alpha=\beta=0$, it is the tidal solution which is familiar to us; if $\beta=0$, it is the load solution studied in recent years; if $\alpha=0$, it is shear load solution, and so on. Although only three solutions are independent basic ones, each one has its physical meaning and theoretical value. Any way, once the boundary condition provided, the solution $y_i(i=1, 2, \ldots, 6)$ of equations (2) is determined.

When the solution of equations (2) is determined, strain

tensor $\overleftrightarrow{\varepsilon}$ can be obtained from displacement (1a):

$$\overleftrightarrow{\varepsilon}=(\nabla u+u\nabla)/2 \tag{4}$$

where ∇ is Hermitian operator, $u\nabla=(\nabla u)^{\top}$. Then according to the stress-strain relationship, we can easily get the stress tensor $\overleftrightarrow{T}$ at any point $P(r, \theta, \varphi)$ in or on the earth:

$$\overleftrightarrow{T}=\lambda\Theta\overleftrightarrow{I}+2\mu\overleftrightarrow{\varepsilon} \tag{5}$$

where $\overleftrightarrow{I}$ is a unit tensor, Θ the dilatation, $\lambda(r)$ *and* $\mu(r)$ Lame's constants. Components of the stress tide tensor can be easily written out (H. Takeuchi et al, 1972) as

$$\sigma_{rr}=y_2Y_n(\theta, \varphi) \tag{6a}$$

$$\sigma_{r\theta}=y_4\frac{\partial Y_n}{\partial\theta} \tag{6b}$$

$$\sigma_{r\varphi}=y_4\frac{\partial Y_n}{\sin\theta\,\partial\varphi} \tag{6c}$$

$$\sigma_{\theta\theta}=\left[y_2+2\mu(-\dot{y}_1+\frac{y_1}{r})\right]Y_n+\frac{2\mu y_3}{r}\frac{\partial^2 Y_n}{\partial\theta^2} \tag{6d}$$

$$\sigma_{\varphi\varphi}=\left[y_2+2\mu(-\dot{y}_1+\frac{y_1}{r})\right]Y_n+\frac{2\mu y_3}{r}(ctg\theta\frac{\partial Y_n}{\partial\theta}+\frac{1}{\sin^2\theta}\frac{\partial^2 Y_n}{\partial\varphi^2}) \tag{6e}$$

$$\sigma_{\theta\varphi}=2\mu\frac{y_3}{r\sin\theta}(\frac{\partial^2 Y_n}{\partial\theta\partial\varphi}-ctg\theta\frac{\partial Y_n}{\partial\varphi}) \tag{6f}$$

where

$$y_2=(\lambda+2\mu)\dot{y}_1+\frac{\lambda}{r}[2y_1-n(n+1)y_3] \tag{7a}$$

$$y_4=\mu(\dot{y}_3-\frac{1}{r}y_3+\frac{1}{r}y_1) \tag{7b}$$

The calculation of derivatives $\dot{y}_1$ *and* $\dot{y}_3$ will be discussed later. y_i can be gotten directly from the earth model. Therefore above method is a direct one, and suitable to calculating the deformations caused by any external forces.

In practical calculation, we may use the potential function instead of $Y_n(\theta, \varphi)$. For example, the Moon's tidal-generating potential is (Melchior, 1978):

$$V=\Sigma V_n=GM_m\sum_{n=2}^{\infty}\frac{r^n}{d_m^{n+1}}P_n(\cos Z_m) \tag{8}$$

where G is the gravitational constant, M_m the mass of the Moon, d_m the distance of the Moon and Earth, $P_m(cosz_m)$ Legendre function, z_m the zenith distance of the Moon relevant to point P.

In the case of the Sun, it is almost the same. What difference is to change the subscript m to s in equation (8). On the other hand the load potential is (Okubo, 1983):

$$U=\Sigma U_n=4\pi Ga\sigma\sum(\frac{r}{a})^n\frac{Y_n(\theta,\varphi)}{(2n+1)} \tag{9}$$

Where σ is the surface mass on the earth. As a special case, this paper will only study the calculation of theoretical values of the stress tide under the Moon-Sun's attraction.

INDIRECT METHOD

Above direct method is reasonable and useful in both theory and calculation. However, the problem is that, for different points, we have to calculate the six-order equations (2) according to the earth model each time. Then calculate the stress tide tensor by equation (6) according to potential function. Thus the calculating amount is very large. So we may use the intermediate results -- Love functions -- to simplify the calculation. Because Love functions have nothing to do with time and position, and can be gotten on by an earth model. With Love functions, the calculation of equations (2) does not need to repeat every time. So that the calculation becomes simple.

Here we define Love functions as

$$H_n(r)=g(a)y_1(r) \tag{10a}$$

$$L_n(r)=g(a)y_3(r) \tag{10b}$$

$$K_n(r)=y_5(r)-1 \tag{10c}$$

At the surface of the earth, r=a, equations (10) are the well-known Love numbers

$$H_n(a)=h_n \tag{11a}$$

$$L_n(a)=l_n \tag{11b}$$

$$K_n(a)=k_n \tag{11c}$$

Then we let

$$A_n=y_2(r)=(\lambda+2\mu)\frac{\dot{H}_n(r)}{g(a)}+\frac{\lambda}{rg(a)}[2H_n(r)-n(n+1)L_n(r)] \tag{12a}$$

$$B_n=y_4(r)=\frac{\mu}{g(a)r}[r\dot{L}_n(r)-L_n(r)+H_n(r)] \tag{12b}$$

$$C_n=y_2+2\mu(-\dot{y}_1+\frac{y_1}{r})$$
$$=\frac{\lambda}{g(a)r}[r\dot{H}_n(r)+\frac{2(\lambda+\mu)}{\lambda}H_n(r)-n(n+1)L_n(r)] \tag{12c}$$

$$D_n=\frac{2\mu y_3}{r}=\frac{2\mu}{g(a)r}L_n(r) \tag{12d}$$

With above Love functions and constants A_n, B_n, C_n, D_n (for degree n and radius of the earth r), and considering the summarization, the stress tide tensor (6) becomes following simple forms

$$\sigma_{rr}=\sum_{n=2}^{\infty}A_nY_n \tag{13a}$$

$$\sigma_{r\theta}=\sum_{n=2}^{\infty}B_n\frac{\partial Y_n}{\partial\theta} \tag{13b}$$

$$\sigma_{r\varphi}=\sum_{n=2}^{\infty}B_n\frac{\partial Y_n}{\sin\theta\,\partial\varphi} \tag{13c}$$

$$\sigma_{\theta\theta}=\sum_{n=2}^{\infty}[C_nY_n+D_n\frac{\partial^2Y_n}{\partial\theta^2}] \tag{13d}$$

$$\sigma_{\varphi\varphi}=\sum_{n=2}^{\infty}[C_nY_n+D_n(\frac{1}{\sin^2\theta}\frac{\partial^2Y_n}{\partial\varphi^2}+ctg\theta\frac{\partial Y_n}{\partial\theta})] \tag{13e}$$

$$\sigma_{\theta\varphi}=\sum_{n=2}^{\infty}\frac{D_n}{\sin\theta}[\frac{\partial^2Y_n}{\partial\theta\partial\varphi}-ctg\theta\frac{\partial Y_n}{\partial\varphi}] \tag{13f}$$

And the hydrostatic stress P can be obtained

$$P=\sigma_{rr}+\sigma_{\theta\theta}+\sigma_{\varphi\varphi}=(A_n+2C_n-n(n+1)D_n)Y_n$$

Because of the fast convergence of the potential function (8), in practical calculation of formula (7), the potential is taken up to the 3rd order for the Moon and the 2nd order for the Sun. Therefore the indirect method in this section is simple than direct one. Following we will further discuss the indirect method and give two sets of practical formulas.

CLOSED FORMULA

In calculating potentials of the Moon and Sun, the zenith distances Z_m of the Moon and Z_s of the Sun must be known. They are:

$$cosZ_m=sin\theta'\sin\delta_m+\cos\theta'\cos\delta_m\cos\tau_m \tag{14a}$$

$$cosZ_s=sin\theta'\sin\delta_s+\cos\theta'\cos\delta_s\cos\tau_s \tag{14b}$$

where δ_m is a geocentric latitude of the Moon, δ_s the one of the Sun, τ_m the hour angle of the Moon, τ_s the one of the Sun, θ' the latitude, $\theta'=\frac{\pi}{2}-\theta$. Toexpress clearly, let

$$Y_{m2}=GM_m\frac{r^2}{d_m^3}\frac{1}{ag(a)} \tag{15a}$$

$$Y_{m3}=GM_m\frac{r^3}{d_m^4}\frac{1}{ag(a)} \tag{15b}$$

$$Y_{s2}=GM_s\frac{r^2}{d_s^3}\frac{1}{ag(a)} \tag{15c}$$

Then formula (13) can be written as following practical calculating formulas:

$$\begin{aligned}\sigma_{rr}=&\frac{1}{2}A_2[Y_{m2}(3cos^2Z_m-1)\\&+Y_{s2}(3cos^2Z_s-1)]+\frac{1}{2}A_3Y_{m3}cosZ_m(5cos^2Z_m-3)\end{aligned} \tag{16a}$$

$$\begin{aligned}\sigma_{r\theta}=&3B_2[Y_{m2}\cos Z_m(\sin\theta'\cos\delta_m\cos\tau_m-\cos\theta'\sin\delta_m)\\&+Y_{s2}\cos Z_s(\sin\theta'\cos\delta_s\cos\tau_s-\cos\theta'\sin\delta_s)]\\&+\frac{3}{2}B_3Y_{m3}(\cos\theta'\sin\delta_m-\sin\theta'\cos\delta_m\cos\tau_m)(-5cos^2Z_m+1)\end{aligned} \tag{16b}$$

$$\begin{aligned}\sigma_{r\varphi}=&-3B_2(Y_{m2}\cos Z_m\cos\delta_m\sin\tau_m+Y_{s2}\cos Z_s\cos\delta_s\sin\tau_s)\\&+\frac{3}{2}B_3Y_{m3}\cos\delta_m\sin\tau_m(-5cos^2Z_m+1)\end{aligned} \tag{16c}$$

$$\begin{aligned}\sigma_{\theta\theta}=&\frac{1}{2}C_2[Y_{m2}(3cos^2Z_m-1)+Y_{s2}(3cos^2Z_s-1)]+\frac{1}{2}C_3Y_{m3}\cos Z_m(5cos^2Z_m-3)\\&+3D_2[Y_{m2}(-cos^2Z_m+(\cos\theta'\sin\delta_m-\sin\theta'\cos\delta_m\cos\tau_m)^2)\\&+Y_{s2}(-cos^2Z_s+(\cos\theta'\sin\delta_s-\sin\theta'\cos\delta_s\cos\tau_s)^2)]\\&+\frac{3}{2}D_3Y_{m3}\cos Z_m[10(\cos\theta'\sin\delta_m-\sin\theta'\cos\delta_m\cos\tau_m)^2-5\cos^2Z_m+1]\end{aligned} \tag{16d}$$

$$\begin{aligned}\sigma_{\varphi\varphi}=&\frac{1}{2}C_2[Y_{m2}(3cos^2Z_m-1)+Y_{s2}(3cos^2Z_s-1)]+\frac{1}{2}D_3y_{m3}\cos Z_m(5cos^2Z_m-3)\\&+3D_2[Y_{m2}\frac{1}{\sin\theta}(-cosZ_m\cos\delta_m\cos\tau_m+\cos\theta'\cos^2\delta_m\sin^2\tau_m)\\&+\frac{Y_{s2}}{\sin\theta}(-cosZ_s\cos\delta_s\cos\tau_s+cos\theta'\cos^2\delta_s\sin^2\tau_s)\\&+Y_{m2}ctg\theta\cos Z_m(sin\theta'\cos\delta_m\cos\tau_m-cos\theta'\sin\delta_m)\end{aligned}$$

$$+Y_{s2}ctg\theta\cos Z_s(sin\theta'\cos\delta_s\cos\tau_s-cos\theta'\sin\delta_s)]$$

$$+\frac{3}{2}D_3Y_{m3}[\frac{1}{\sin\theta}(10cosZ_m\cos\theta'\cos^2\delta_m\sin^2\tau_m-5cos^2Z_m\cos\delta_m\cos\tau_m$$

$$+\cos\delta_m\cos\tau_m)+ctg\theta(cos\theta'\sin\delta_m$$

$$-sin\theta'\cos\delta_m\cos\tau_m)(-5cos^2Z_m+1)] \qquad (16e)$$

$$\sigma_{\theta\varphi}=3\frac{D_2}{\sin\theta}[Y_{m2}((cos\theta'\sin\delta_m-\sin\theta'\cos\delta_m\cos\tau_m)\cos\theta'\cos\delta_m\sin\tau_m$$

$$-\cos Z_m\sin\theta'\cos\delta_m\sin\tau_m)+Y_{s2}((cos\theta'\sin\delta_s$$

$$-\sin\theta'\cos\delta_s\cos\tau_s)\cos\theta'\cos\delta_s\sin\tau_s-\cos Z_s\sin\theta'\cos\delta_s\sin\tau_s)$$

$$+\cos\theta(Y_{m2}\cos Z_m\cos\delta_m\sin\tau_m+Y_{s2}\cos Z_s\cos\delta_s\sin\tau_s)]$$

$$+\frac{3}{2}\frac{D_3}{\sin\theta}Y_{m3}[10cosZ_m(\cos\theta'\sin d_m-\sin\theta'\cos\delta_m\cos\tau_m)\cos\theta'\cos\delta_m\sin\tau_m$$

$$-5cos^2Z_m\sin\theta'\cos\delta_m\sin\tau_m+\sin\theta'\cos\delta_m\sin\tau_m$$

$$-\cos\theta\cos\delta_m\sin\tau_m(-5cos^2Z_m+1)] \qquad (16f)$$

Formula (16) is a simple closed form. If the time and calculated position are provided, Y_{ij} can be easily calculated, and A_n, B_n, C_n, D_n can also be determined by radius r. Then the final results will be conveniently gotten by formula (16).

As mentioned above, A_n, B_n, C_n, D_n are functions of Love functions and their derivatives which must be calculated in advance. However, calculating Love functions , especially their derivatives, is a noticeable problem. Following it will be given a special discussion.

Derivatives of Love Functions

When calculating stress (or strain) tide tensor by indirect method, derivatives of Love functions must be known. This is a slight complicated problem. Because there is no analytic solutions about Love functions to get their derivatives. On the other hand, there are no enough results of Love functions in the inner earth to get numerical derivatives. Then P. Melchior (1966) adopted following assumption on the surface of the earth:

$$\frac{\dot{l}_n}{l_n}=\frac{\dot{h}_n}{h_n}=\frac{\dot{g}}{g} \qquad (17)$$

Since gradient of gravity can be known from gravity survey, it means $\frac{\dot{g}}{g}$ is known. Then other two derivatives can be determined. With this assumption, the calculation becomes simple. Although

P. Melchior(1978) cancelled (17) in his latter book "The Tides of the Planet Earth", it was still adopted by some authors (Luo M., et al, 1986). We will analyze and discuss the assumption to prove that it is not reasonable. Then give methods to resolve the problem.

1. Demonstration about Unreasonable Equation (17)

First, the demonstration is given in theory. Equation (7) equals to:

$$\dot{y}_1=\frac{1}{\lambda+2\mu}[y_2-\frac{\lambda}{r}(2y_1-n(n+1)y_3)] \tag{18a}$$

$$\dot{y}_3=\frac{1}{\mu}y_4+\frac{1}{r}y_3-\frac{1}{r}y_1 \tag{18b}$$

We will discuss the problem in the special case of the surface of the earth. In this case, $y_2=y_4=0$. Then taking into account definitions of Love numbers, equation (18) becomes to

$$\frac{\dot{h}_n}{h_n}=-\frac{2\lambda}{\lambda+2\mu}\frac{1}{a}+\frac{n(n+1)\lambda}{\lambda+2\mu}\frac{l_n}{ah_n} \tag{19a}$$

$$\frac{\dot{l}_n}{l_n}=\frac{1}{a}+\frac{h_n}{al_n} \tag{19b}$$

It is clear that the right hands of equation (19) are not equal. That means equation (17) is not right in theory.

Next, let's check numerical results. Here we adopt P. Melchior's (1978) data:

Theory:

$$h = 0.6199 \quad l = 0.088 \quad a\dot{h} = -1.472 \quad a\dot{l} = -0.7079$$

Observation:

$$h = 0.638 \quad l = 0.088 \quad a\dot{h} = -1.520 \quad a\dot{l} = -0.726$$

Then we have

Theory:

$$\frac{\dot{h}}{h}=-3.727*10^{-9}/cm \qquad \frac{\dot{l}}{l}=-12.626*10^{-9}/cm$$

Observation:

$$\frac{\dot{h}}{h}=-3.740*10^{-9}/cm \qquad \frac{\dot{l}}{l}=-12.949*10^{-9}/cm$$

While the gradient of gravity is

$$\frac{\dot{g}}{g}=-3.1425*10^{-9}/cm$$

It can be seen from above results that, $\frac{\dot{h}}{h} \neq \frac{\dot{l}}{l} \neq \frac{\dot{g}}{g}$. Especially $\frac{\dot{l}}{l}$ is 3.5 times of $\frac{\dot{h}}{h}$. Therefore, for accuracy calculation, the assumption (17) is not enough.

Finally, let's discuss the error magnitude caused by (17). The content in brackets of (12b) about B_n (on the surface of the earth) is

$$a\dot{l}_n - l_n + h_n$$

According to above data and results, we know that $a\dot{l}$ is almost one order larger than 1, while $a\dot{l}$ is the same order as h. So assumption (17) will cause the error of 100% to $\sigma_{r\theta}$ *and* $\sigma_{r\varphi}$. This error is very large, and shouldn't be neglected.

2. Methods to the Problem

To calculate correctly the stress (or strain) tide tensor in inner earth, derivatives of Love functions can be obtained by following two ways.

a. Calculation in theory. Love functions and their derivatives can be gotten from equations (2) directly. In fact, after resolving equations (2), derivatives of Love functions can be obtained from equation (18). We have calculated the results for earth model G-D1066A, shown in Figure 2. The results also indicate that (17) is not right.

b. Observation values. Practical observations of tilt and strain tides can present the results of $a\dot{h}$ *and* $a\dot{l}$ by the method of P. Melchior (1978). It has more practical meaning in calculating tidal tensor in a special area.

With derivatives of Love functions, we can easily calculate the coefficients A_n, B_n, C_n *and* D_n (for models 1066A and PREM), shown in Figure 1, and also list in table 1 and 2 for practical applications.

GEODETIC COEFFICIENTS AND PHASE CORRECTIONS OF STRESS EARTH TIDE

Besides above method, there also is another method to calculate theoretical values of the stress earth tide, that is summering harmonic waves. This method can be used not only in calculating theoretical values, but also in making harmonic analysis of the stress tide. Like gravity, tilt, and strain earth tides, geodetic coefficients and phase corrections of the stress earth tide must be given in advance.

As we know, tide generating potential can be divided into two parts according to its character. One is N_{ij} -- the function

of a latitude, and the other is M_{ij} -- the function of a longitude and an hour angle. That is, the tide-generating potential (8) of the Moon and Sun can be expressed as

$$V=\sum_{i=2}^{3}\sum_{j=0}^{3}N_{ij}M_{ij} \tag{20a}$$

Doodson (1922) and Q. Xi (1987) gave the harmonic development of the tide-generating potential, respectively. To have a generalized standard for comparing amplitudes of the harmonic waves, they set up normalized coefficients N_{ij} -- so called geodetic coefficients -- as following:

$$N_{20}=\frac{1}{2}D(r)(1-3sin^2\theta') \tag{20b}$$

$$N_{21}=D(r)\sin 2\theta' \tag{20c}$$

$$N_{22}=D(r)\cos^2\theta' \tag{20d}$$

$$N_{30}=1.11803D'(r)\sin\theta'(3-5sin^2\theta') \tag{20e}$$

$$N_{31}=0.72618D'(r)\cos\theta'(1-5sin^2\theta') \tag{20f}$$

$$N_{32}=2.59808D'(r)\sin\theta'\cos^2\theta' \tag{20g}$$

$$N_{33}=D'(r)\cos^3\theta' \tag{20h}$$

where $D(r)=D_0(\frac{r}{\bar{r}})^2$, $\bar{r}$ is the average radius of the earth. While $D_0=26335.838cm^2/\sec^2$ is Doodson's constant. $D'=D\frac{r}{a}$. At the same time M_{ij} can be expressed as

$$M_{ij}=K_k cos(\alpha_k+\beta_{ij}) \tag{20i}$$

In which K_k is the amplitude coefficient of a harmonic wave, α_k the phase relevant to K_k. k_k *and* α_k can be determined by the harmonic development of the tide-generating potential. β_{ij} is a phase correction. N_{ij} in formula (20a) and β_{ij} in formula (20i) are the geodetic coefficients and the phase corrections which are just what we want to obtain in the section.

Inserting equations (20b)-(20i) into (20a), then (20a) into (13), we can get calculating formulas of each components of the stress earth tide tensor as follows:

$$\sigma_{rr}=\sum_{i=2}^{3}\sum_{j=0}^{3}\sum_{k}T_{rr}(ij)K_k(ij)\cos(\alpha_k(ij)+\beta_{ij}) \tag{21a}$$

$$\sigma_{r\theta}=\sum_{i=2}^{3}\sum_{j=0}^{3}\sum_{k}T_{r\theta}(ij)K_k(ij)\cos(\alpha_k(ij)+\beta_{ij}) \tag{21b}$$

$$\sigma_{r\varphi}=\sum_{i=2}^{3}\sum_{j=0}^{3}\sum_{k}T_{r\varphi}(ij)K_k(ij)\cos(\alpha_k(ij)+\beta_{ij}) \tag{21c}$$

$$\sigma_{\theta\theta}=\sum_{i=2}^{3}\sum_{j=0}^{3}\sum_{k}T_{\theta\theta}(ij)K_k(ij)\cos(\alpha_k(ij)+\beta_{ij}) \tag{21d}$$

$$\sigma_{\varphi\varphi}=\sum_{i=2}^{3}\sum_{j=0}^{3}\sum_{k}T_{\varphi\varphi}(ij)K_k(ij)\cos(\alpha_k(ij)+\beta_{ij}) \tag{21e}$$

$$\sigma_{\theta\varphi}=\sum_{i=2}^{3}\sum_{j=0}^{3}\sum_{k}T_{\theta\varphi}(ij)K_k(ij)\cos(\alpha_k(ij)+\beta_{ij}) \tag{21f}$$

Where $T_{rr}(ij)$ are detailed geodetic coefficients of the component σ_{rr} of the stress earth tide, and so on. Then we can write out all of the geodetic coefficients of the stress earth tide in explicit formulas (in which $G(r)=D(r)\frac{1}{ag(a)}$, $G'(r)=G(r)\frac{r}{a}$):

σ_{rr}:

$$T_{rr}(20)=\frac{1}{2}A_2G(r)(1-3\sin^2\theta') \tag{22a}$$

$$T_{rr}(21)=A_2G(r)\sin2\theta' \tag{22b}$$

$$T_{rr}(22)=A_2G(r)\cos^2\theta' \tag{22c}$$

$$T_{rr}(30)=1.11803A_3G'(r)\sin\theta'(3-5\sin^2\theta') \tag{22d}$$

$$T_{rr}(31)=0.72618A_3G'(r)\cos\theta'(1-5\sin^2\theta') \tag{22e}$$

$$T_{rr}(32)=2.59808A_3G'(r)\sin\theta'\cos^2\theta' \tag{22f}$$

$$T_{rr}(33)=A_3G'(r)\cos^3\theta' \tag{22g}$$

$\sigma_{r\theta}$:

$$T_{r\theta}(20)=\frac{3}{2}G(r)B_2\sin2\theta' \tag{23a}$$

$$T_{r\theta}(21)=-2G(r)B_2\cos2\theta' \tag{23b}$$

$$T_{r\theta}(22)=G(r)B_2\sin2\theta' \tag{23c}$$

$$T_{r\theta}(30)=1.11803G'(r)3B_3\cos\theta'(5\sin^2\theta'-1) \tag{23d}$$

$$T_{r\theta}(31)=0.72618G'(r)B_3\sin\theta'(15\cos^2\theta'-4) \tag{23e}$$

$$T_{r\theta}(32)=2.59808G'(r)B_3\cos\theta'(3\sin^2\theta'-1) \tag{23f}$$

$$T_{r\theta}(33)=G'(r)3B_3\cos^2\theta'\sin\theta' \tag{23g}$$

$\sigma_{r\varphi}$:

$$T_{r\varphi}(20)=0 \tag{24a}$$

$$T_{r\varphi}(21)=G(r)2B_2\sin\theta' \tag{24b}$$

$$T_{r\varphi}(22)=G(r)2B_2\cos\theta' \tag{24c}$$

$$T_{r\varphi}(30)=0 \tag{24d}$$

$$T_{r\varphi}(31)=0.72618G'(r)B_3(1-5sin^2\theta') \tag{24e}$$

$$T_{r\varphi}(32)=2.59808G'(r)B_3\sin2\theta' \tag{24f}$$

$$T_{r\varphi}(33)=G'(r)3B_3\cos^2\theta' \tag{24g}$$

$\sigma_{\theta\theta}$:

$$T_{\theta\theta}(20)=G(r)[\frac{1}{2}C_2(1-3sin^2\theta')-3D_2cos2\theta'] \tag{25a}$$

$$T_{\theta\theta}(21)=G(r)(C_2-4D_2)sin2\theta' \tag{25b}$$

$$T_{\theta\theta}(22)=G(r)(C_2\cos^2\theta'-2D_2cos2\theta') \tag{25c}$$

$$T_{\theta\theta}(30)=1.11803G'(r)sin\theta'[C_3(3-5sin^2\theta') +3D_3(4-15cos^2\theta')] \tag{25d}$$

$$T_{\theta\theta}(31)=0.72618G'(r)cos\theta'[C_3(1-5sin^2\theta') +D_3(45sin^2\theta'-11)] \tag{25e}$$

$$T_{\theta\theta}(32)=2.59808G'(r)sin\theta'[C_3\cos^2\theta'+D_3(2-9cos^2\theta')] \tag{25f}$$

$$T_{\theta\theta}(33)=G'(r)cos\theta'[C_3\cos^2\theta'+3D_3(3sin^2\theta'-1)] \tag{25g}$$

$\sigma_{\varphi\varphi}$:

$$T_{\varphi\varphi}(20)=G(r)[\frac{1}{2}C_2(1-3sin^2\theta')+3D_2\sin^2\theta'] \tag{26a}$$

$$T_{\varphi\varphi}(21)=G(r)(C_2-2D_2)sin2\theta' \tag{26b}$$

$$T_{\varphi\varphi}(22)=G(r)[C_2\cos^2\theta'-2D_2(1+cos^2\theta')] \tag{26c}$$

$$T_{\varphi\varphi}(30)=1.11803G'(r)sin\theta'[C_3(3-5sin^2\theta') -3D_3(1-5sin^2\theta')] \tag{26d}$$

$$T_{\varphi\varphi}(31)=0.72618G'(r)cos\theta'[C_3(1-5sin^2\theta') +\frac{D_3}{\cos\theta'}(-1+16sin^2\theta'-15sin^4\theta')] \tag{26e}$$

$$T_{\varphi\varphi}(32)=2.59808G'(r)sin\theta'[C_3\cos^2\theta'+D_3(3sin^2\theta'-5)] \tag{26f}$$

$$T_{\varphi\varphi}(33)=G'(r)cos\theta'[C_3\cos^2\theta'-3D_3(cos^2\theta'+2)] \tag{26g}$$

$\sigma_{\theta\varphi}$:

$$T_{\theta\varphi}(20)=0 \tag{27a}$$

$$T_{\theta\varphi}(21)=-G(r)2D_2\cos\theta' \tag{27b}$$

$$T_{\theta\varphi}(22)=G(r)2D_2\sin\theta' \tag{27c}$$

$$T_{\theta\varphi}(30)=0 \tag{27d}$$

$$T_{\theta\varphi}(31)=0.72618G'(r)5D_3\sin2\theta' \tag{27e}$$

$$T_{\theta\varphi}(32)=-2.59808G'(r)2D_3\cos2\theta' \tag{27f}$$

$$T_{\theta\varphi}(33)=G'(r)3D_3\sin2\theta' \tag{27g}$$

The phase corrections are listed in table 3.

Table 3. Phase corrections

	2, 0	3, 0	2, 1	3, 1	2, 2	3, 2	3, 3
σ_{rr}	0	$-\pi/2$	$-\pi/2$	0	0	$-\pi/2$	0
$\sigma_{\theta\theta}$	0	$-\pi/2$	$-\pi/2$	0	0	$-\pi/2$	0
$\sigma_{\varphi\varphi}$	0	$-\pi/2$	$-\pi/2$	0	0	$-\pi/2$	0
$\sigma_{r\theta}$	0	$-\pi/2$	$-\pi/2$	0	0	$-\pi/2$	0
$\sigma_{r\varphi}$			0	$\pi/2$	$\pi/2$	0	$\pi/2$
$\sigma_{\theta\varphi}$			0	$\pi/2$	$\pi/2$	0	$\pi/2$

As an example, at last, using the closed formula (16), we have calculated the stress earth tide in Beijing with 300km depth, shown in figure 3.

ACKNOWLEDGMENTS

The author wishes to express his sincere thanks to Professor Y. Hagiwara for personal advice and helpness. The author is indebted to Doctor S. Okubo and Doctor K. Nagasawa for their helpful discussions.

REFERENCES

Alterman, Z., H. Jarosch, and C. L. Pekeris, Oscillations of the earth, Proc. Roy. Soc. London, Ser. A., 252, 80-95, 1959

Ding, Z. and R. Wang, Global displacement and stress fields due to tidal attraction, Acta Geophysica Sinica, V. 29, 578-596, 1986

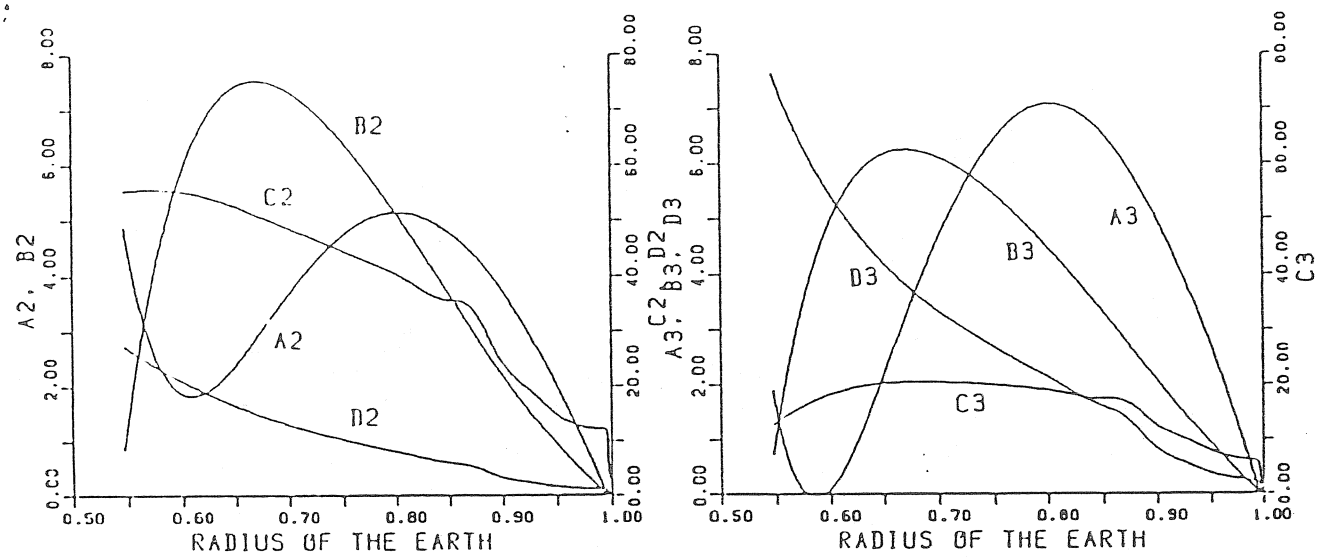

Fig. 1. Cueves of Constants A_n. B_n. C_n *and* D_n

Unit: $10^{11} dn/cm^2$ (Earth Model: 1066A)

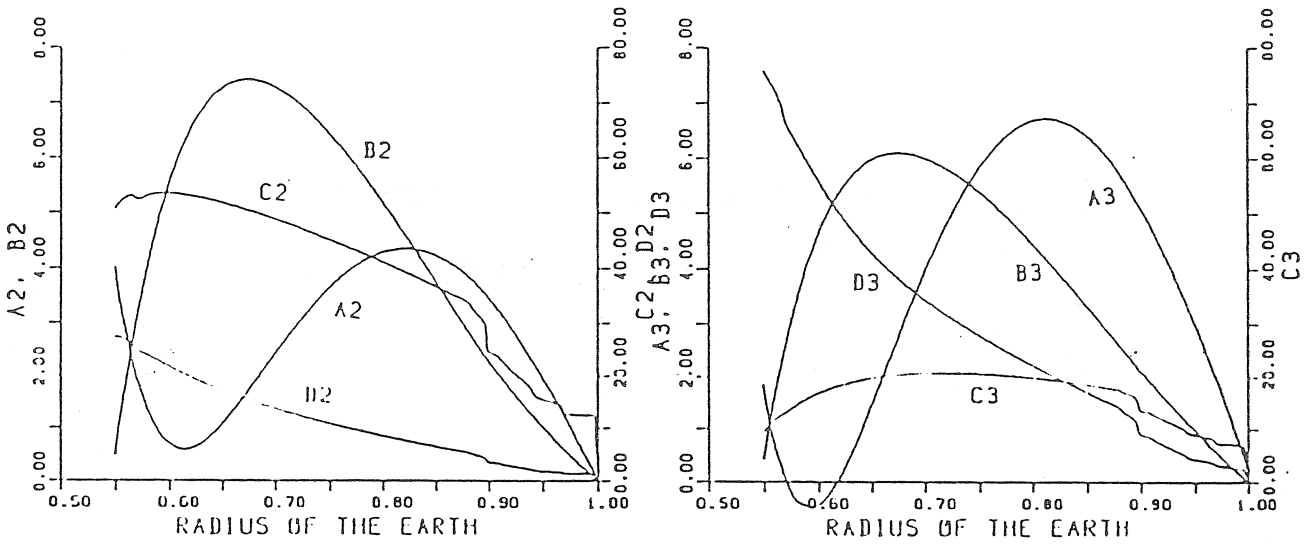

Fig. 1. Cueves of Constants A_n. B_n. C_n *and* D_n

Unit: $10^{11} dn/cm^2$ (Earth Model: PREM)

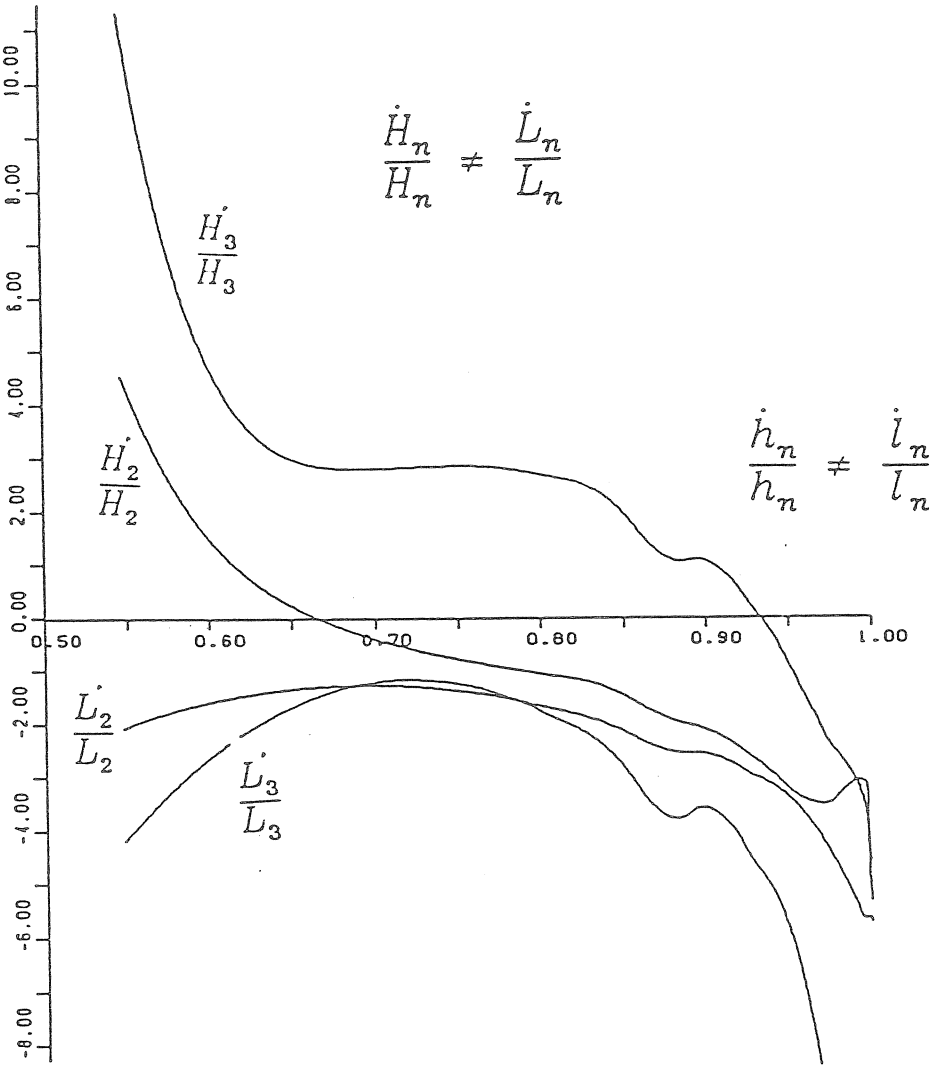

Fig. 2. Derivatives of Love Functions

Unit: $1/(6.371\times10^{8}cm)$ (1066A)

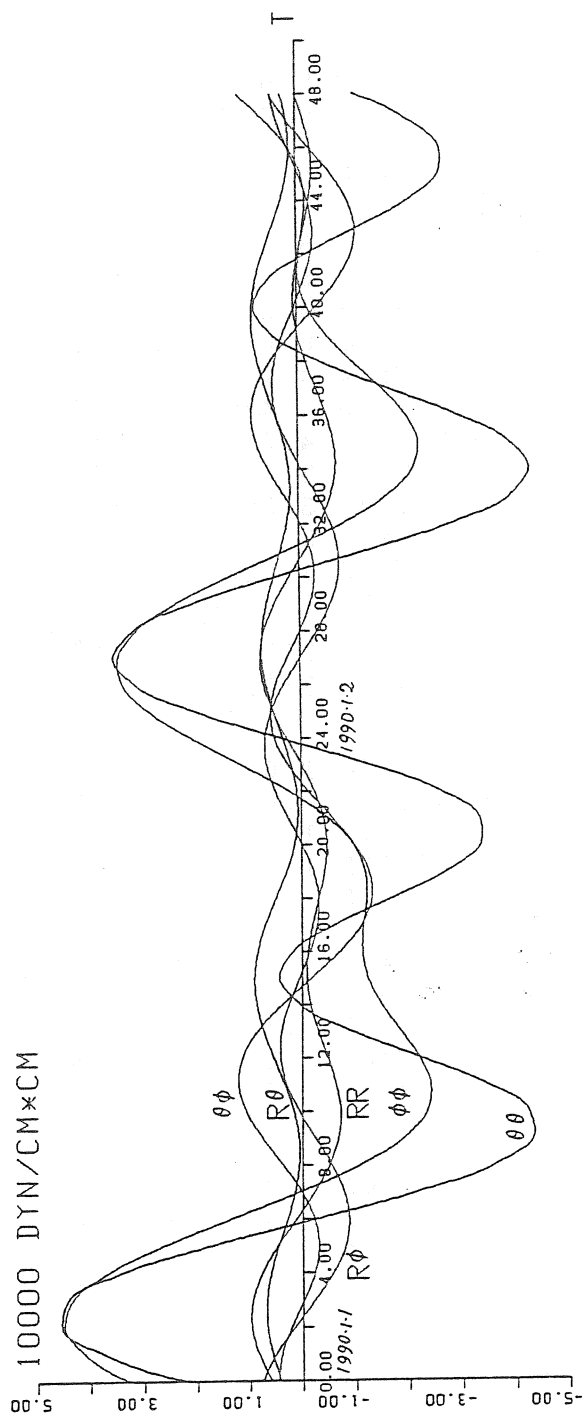

FIG.3 STRESS EARTH TIDE IN BEIJING

LAT.: 40, LØG.: 116, DEPTH: 300KM

TIME: 1990.1.1-1990.1.2

EARTH MØDEL: 1066A

Table 1. Coefficients An Bn Cn and Dn (Earth Model: PREM)
Unit: 1e11dyn/cm2

S	A2	B2	C2	D2	A3	B3	C3	D3
.5494	4.0249	.4899	50.554	27.377	1.5954	.4202	8.637	7.5937
.5651	2.3105	2.5922	53.050	25.989	.0460	2.1984	11.760	7.0060
.5698	1.9377	3.1216	52.352	24.930	-.2384	2.6394	12.276	6.6705
.5808	1.2784	4.1938	53.091	23.771	-.6427	3.5234	13.885	6.2625
.5965	.7540	5.3789	53.486	22.097	-.7263	4.4848	15.700	5.7192
.6121	.5927	6.2299	53.175	20.425	-.4061	5.1637	16.994	5.2185
.6278	.6839	6.8125	52.659	18.922	.1706	5.6225	17.974	4.7928
.6435	.9440	7.1794	51.986	17.563	.8961	5.9092	18.706	4.4266
.6592	1.3095	7.3722	51.173	16.321	1.6921	6.0602	19.234	4.1062
.6749	1.7323	7.4244	50.270	15.186	2.5020	6.1040	19.604	3.8237
.6906	2.1761	7.3631	49.279	14.137	3.2850	6.0625	19.838	3.5699
.7063	2.6138	7.2101	48.218	13.163	4.0120	5.9526	19.961	3.3388
.7220	3.0253	6.9832	47.100	12.256	4.6627	5.7878	19.989	3.1259
.7377	3.3955	6.6968	45.918	11.402	5.2233	5.5783	19.930	2.9260
.7534	3.7137	6.3629	44.699	10.600	5.6843	5.3325	19.800	2.7375
.7691	3.9724	5.9914	43.447	9.845	6.0401	5.0569	19.608	2.5580
.7848	4.1663	5.5903	42.151	9.128	6.2874	4.7567	19.354	2.3844
.8005	4.2922	5.1666	40.830	8.449	6.4250	4.4362	19.048	2.2164
.8162	4.3482	4.7258	39.472	7.800	6.4527	4.0987	18.686	2.0517
.8319	4.3336	4.2729	38.076	7.181	6.3715	3.7470	18.271	1.8897
.8476	4.2484	3.8118	36.646	6.589	6.1829	3.3835	17.805	1.7297
.8633	4.0933	3.3462	35.199	6.025	5.8891	3.0102	17.295	1.5723
.8790	3.8695	2.8790	33.702	5.481	5.4925	2.6288	16.728	1.4155
.8868	3.7295	2.6455	31.792	4.994	5.2556	2.4350	15.939	1.2806
.8948	3.5637	2.4081	30.163	4.573	4.9866	2.2349	15.254	1.1633
.9003	3.4386	2.2577	24.301	3.534	4.8094	2.1035	12.651	.8973
.9058	3.3056	2.1082	23.931	3.422	4.6192	1.9725	12.462	.8665
.9137	3.1008	1.8979	22.347	3.103	4.3271	1.7869	11.711	.7816
.9215	2.8776	1.6932	20.787	2.804	4.0128	1.6039	10.955	.7017
.9294	2.6372	1.4942	19.281	2.525	3.6773	1.4241	10.209	.6271
.9372	2.3805	1.3013	17.828	2.267	3.3214	1.2475	9.475	.5577
.9443	2.1439	1.1401	15.582	1.918	3.0012	1.0973	8.369	.4682
.9513	1.8989	.9817	15.091	1.821	2.6653	.9490	8.064	.4394
.9584	1.6458	.8261	14.616	1.727	2.3142	.8026	7.765	.4104
.9655	1.3848	.6732	14.143	1.634	1.9484	.6579	7.465	.3808
.9710	1.1716	.5613	12.395	1.415	1.6555	.5498	6.545	.3239
.9765	.9542	.4497	12.362	1.386	1.3529	.4417	6.471	.3105
.9819	.7327	.3383	12.312	1.353	1.0407	.3336	6.388	.2954
.9874	.5072	.2272	12.276	1.322	.7191	.2254	6.313	.2794
.9906	.3766	.1638	12.228	1.300	.5311	.1634	6.256	.2691
.9937	.2448	.1004	12.208	1.282	.3401	.1014	6.213	.2590
.9962	.1410	.0510	12.181	1.265	.1890	.0529	6.174	.2506
.9976	.0816	.0274	7.696	.810	.1073	.0289	3.896	.1584
.9995	.0083	.0021	4.735	.483	.0102	.0024	2.394	.0928
1.0000	.0000	.0000	.158	.015	.0000	.0000	.080	.0030

Table 2. Coefficients An Bn Cn and Dn (Earth Model: 1066A)
Unit: 1elldyn/cm2

S	A2	B2	C2	D2	A3	B3	C3	D3
.5578	4.2576	1.6108	54.866	26.618	1.3213	1.3854	13.175	7.3725
.5686	3.2760	2.9494	55.020	25.146	.5038	2.5193	14.574	6.8386
.5795	2.5960	4.0535	55.049	23.797	.0686	3.4413	15.763	6.3709
.5904	2.1590	4.9557	54.967	22.550	-.0705	4.1849	16.786	5.9574
.6012	1.9160	5.6839	54.781	21.393	.0170	4.7779	17.661	5.5898
.6121	1.8264	6.2616	54.451	20.302	.2746	5.2432	18.381	5.2574
.6230	1.8560	6.7091	54.005	19.276	.6563	5.6003	18.960	4.9568
.6338	1.9762	7.0441	53.411	18.294	1.1244	5.8656	19.390	4.6800
.6447	2.1630	7.2818	52.746	17.373	1.6484	6.0529	19.711	4.4285
.6556	2.3968	7.4352	51.968	16.488	2.2037	6.1739	19.914	4.1939
.6664	2.6613	7.5157	51.156	15.654	2.7703	6.2385	20.042	3.9783
.6773	2.9432	7.5329	50.301	14.859	3.3327	6.2549	20.105	3.7777
.6882	3.2318	7.4954	49.414	14.102	3.8784	6.2300	20.114	3.5899
.6991	3.5180	7.4106	48.549	13.394	4.3976	6.1697	20.100	3.4172
.7099	3.7947	7.2851	47.703	12.733	4.8827	6.0791	20.066	3.2575
.7208	4.0558	7.1249	46.853	12.107	5.3279	5.9625	20.006	3.1077
.7317	4.2965	6.9351	46.016	11.520	5.7285	5.8237	19.927	2.9675
.7425	4.5128	6.7200	45.138	10.953	6.0813	5.6655	19.809	2.8319
.7534	4.7013	6.4833	44.211	10.400	6.3835	5.4904	19.649	2.6989
.7643	4.8590	6.2280	43.284	9.874	6.6329	5.3003	19.468	2.5716
.7751	4.9835	5.9570	42.363	9.373	6.8277	5.0972	19.269	2.4491
.7860	5.0735	5.6731	41.480	8.903	6.9670	4.8827	19.067	2.3329
.7969	5.1280	5.3783	40.563	8.446	7.0501	4.6582	18.832	2.2178
.8077	5.1464	5.0748	39.549	7.989	7.0775	4.4249	18.537	2.1004
.8186	5.1279	4.7644	38.306	7.502	7.0502	4.1836	18.127	1.9732
.8295	5.0719	4.4487	36.971	7.012	6.9689	3.9353	17.660	1.8436
.8403	4.9795	4.1290	35.847	6.575	6.8345	3.6807	17.270	1.7260
.8512	4.8535	3.8053	35.177	6.226	6.6473	3.4205	17.072	1.6291
.8621	4.6967	3.4771	34.945	5.958	6.4070	3.1545	17.062	1.5500
.8729	4.5107	3.1442	34.239	5.606	6.1142	2.8823	16.838	1.4457
.8838	4.2899	2.8109	31.672	4.951	5.7744	2.6054	15.767	1.2630
.8947	4.0280	2.4855	27.435	4.069	5.3947	2.3282	13.905	1.0268
.9045	3.7556	2.2053	23.769	3.359	5.0240	2.0828	12.249	.8404
.9143	3.4541	1.9363	21.395	2.895	4.6244	1.8429	11.146	.7183
.9241	3.1281	1.6772	19.580	2.539	4.1949	1.6082	10.277	.6238
.9339	2.7810	1.4266	18.006	2.235	3.7359	1.3786	9.504	.5423
.9419	2.4828	1.2291	16.330	1.947	3.3416	1.1953	8.679	.4664
.9500	2.1734	1.0396	14.889	1.709	2.9328	1.0173	7.947	.4031
.9580	1.8521	.8573	13.701	1.520	2.5078	.8440	7.313	.3519
.9661	1.5186	.6812	12.829	1.392	2.0643	.6747	6.803	.3141
.9741	1.1719	.5100	12.209	1.308	1.5996	.5084	6.400	.2854
.9822	.8129	.3429	11.863	1.272	1.1134	.3443	6.117	.2654
.9902	.4435	.1795	11.681	1.262	.6070	.1821	5.921	.2478
.9982	.0658	.0189	11.645	1.248	.0824	.0206	5.828	.2261
1.0000	.0009	.0003	2.581	.247	.0012	.0003	1.309	.0438

Doodson, A. T., The harmonic development of the tide-generating potential, Proc. Roy. Soc. London. Ser. A., 100, 1922

Gao, X., Yin, Z., Wang, W., Huang, L. and Li, J., Triggering of earthquakes by the tidal stress tensor, Acta Seismologica Sinica, 3, 1981

Gilbert, F. and A. M. Dziewonski, An application of normal mode theory to the retrieval of structural parameters and source mechanisms from seismic spectra, Phil. Trans. Roy. Soc. London, A, V. 278, 187, 1975

Heaton, T. H., Tidal triggering of earthquakes, Geophys. J. R. astr. Soc., 43, 307-326, 1975

Longman, I. M., A Green's function for determining the deformation of the earth under surface mass loads, Part 1, J. Geophys. Res., 67, 845-850, 1962

Luo, M., Gu, M., Sui, J. and Li, A., Calculation of the theoretical values of the strain tide, Acta Geophysica Sinica, V. 29, 157-165, 1986

Melchior, P., The Earth Tides, Pergamon Press, 1966

Melchior, P., The tides of the planet earth, Pergamon Press, 1978

Okubo, S. and M. Saito, Partial derivatives of Love numbers, Bull. Geod. 57, 167-179, 1983

Takeuchi, H. and M. Saito, Seismic surface waves, in Methods in Computational Physics, 11, Academic Press, New York, 1972

Varga, P., Influence of external forces on the triggering of earthquakes, Earthq. Predict. Res. 1, 191-201, 1985

Xi, Q., Proc. of the Ninth International Symposium on Earth tides, 1983

Xi, Q., The algebraic deduction of harmonic development for the tide-generating potential with the IBM-PC, Earthquake Research in China, V. 3, 16-28, 1987

ON THE VARIATION OF TIDAL WAVE PARAMETERS IN TIME

Tadeusz Chojnicki
Space Research Centre, Polish Academy of Sciences, Warsaw

A number of recent publications suggest that tidal waves parameters obtained from observation analysis are variable in time (Dittfeld, 1980,1984; Richter, 1987; Volkov et al., 1986). Above all, there are two works presented at the meeting of the Working Group on "High Precision Tidal Data Processing" in Bonn, October 1988, (Dittfeld, 1988; Schwahn et al., 1988) that seem to provide convincing evidence, to support this idea.

All the publications we refer to concern the vertical component of the Earth tides. Since clinometric observations of the tides have been performed in Książ observatory continuosly since 1973, they provide enormous amount of data to be examined with respect to the time variations of the parameters obtained for the horizontal component of the Earth tides. The present paper is conceived as a clinometric illustration of the mentioned works by Dittfeld and Schwahn (1988).

For examination of the variation of tidal parameters in time, the Książ observations that have been done in 1973-86 were processed in two variants. In the first one the observational data were divided into 13 yearly series including the period from June of the year n til June of the year $(n+1)$. The central date of each series was 1st January of the year $(n+1)$. The preceding and the following series do not overlap. Table 1 presents the results of the first variant analysis for seven waves: O1, P1, K1, N2, M2, L2 and S2; each wave for two components: NS and EW.

In the second variant the observational data set was divided into 12 two-yearly series including the period from June of the year $(n-1)$ till June of the year $(n+1)$. The central date of each series was 1st July of the year n. The observations of the preceding and the following series overlap for one year. The results of the 2nd variant are presented in table 2 for the same waves as in table 1.

Figures 1-3 present in the analog form the results obtained in the 2nd variant for the chosen five waves: O1, K1, N2, M2 and S2 and two components NS and EW. Comparing individual diagrams we can notice some shape similarity of the curves representing the same component and the same wave groups: diur-

nal or semidiurnal. For instance: O1/NS resembled K1/NS, O1/EW resembled K1/EW and N2/NS resembled M2/NS etc. However, there was no similarity of the curve shape of the same component between diurnal and semidiurnal waves. Moreover, there was no similarity between N2 and M2 as compared to S2 in the semidiurnal waves group. All these remarks prove that calibration errors can be excluded as a possible reson for the variation of tidal parameters.

In order to estimate the character of the time changes of tidal parameters and their order of magnitude, the values of the individual parameters, treated as time functions, were approximated by polynomials from the zero up to the tenth order. The standard devioation of the polynomial points was accepted as a criterion for adjusting any individual polynomial to the character of changes of a given parameter. It is obvious that determination of the zero order polynomial means calculating the mean value of all yearly values of a given parameter for the whole period. A significant decrease of the standard deviation between zero and first order polynomials can be interpreted as an existance of changes of the examined parameters in time.

Fig. 4 presents the diagrams of the relations between the standard deviation of points for individual polynomials and their orders. Table 3 presents the approximate characteristics of the time variations of the parameters for individual waves. The order of polynomial which may represent a type of time variations of individual waves is presented in column "polynomial order". The asterisk denotes the possibility of existence of a polynomial higher than of the 2nd order. The approximate values of the parameter changes per year are presented in "ampl." and "$\Delta\varphi$" columns, assuming linear character of changes.

A very interesting fact was Schwahn's finding of the yearly modulation of the M2-wave (Schwahn, 1988). A method of calculation different prom that of Schwahn was applied here to prove the existance of such modulation in Książ as well. The method enabled verification of other waves in this respect. Our thirteen years observation data for each component NS and EW were divided into 12 parts. Each of them contained always the same month of the individual years. Each of these parts was separately analysed in order to determine parameters of 18 tidal waves. Thus, from individual analyses the parameters were obtained characteristic for the given months of the period 1973-86. Fig. 5 presents the diagram of the obtained values of the M2-wave in the polar coordinates system $[\gamma, \Delta\varphi]$. However the figure shows only the tip of the vector $M2[\gamma, \Delta\varphi]$, because modulation of this vector is very small compared to its magnitude. Fig.5 shows the yearly mo-

Table 1a. The results of the 1st variant analysis, north-south component, amplitude factors and phase lags /"-"/.

Year	O1	P1	K1	N2	M2	L2	S2
1973-74	0.7150 21.16	0.6311 25.55	0.9357 13.74	0.7161 -7.84	0.6739 -7.00	0.8359 -35.11	0.6580 -3.58
1974-75	0.7383 26.50	0.8859 29.14	0.8770 18.39	0.6902 -4.92	0.6754 -4.52	0.6432 -3.74	0.6663 -1.19
1975-76	0.7049 22.40	0.8252 24.44	0.8284 15.51	0.6659 -6.87	0.6591 -4.69	0.6753 -5.88	0.6545 -2.95
1976-77	0.6859 19.46	0.8143 16.13	0.8433 15.71	0.6677 -5.61	0.6650 -5.49	0.6382 1.08	0.6616 -2.27
1977-78	0.7420 22.90	0.8870 13.96	0.8272 13.20	0.6567 -5.41	0.6584 -4.75	0.6162 -0.67	0.6434 -3.09
1978-79	0.7834 21.92	0.9277 20.07	0.8924 13.94	0.7055 -7.53	0.6909 -5.39	0.5790 4.73	0.6884 -0.29
1979-80	0.6962 24.19	0.8437 20.56	0.8656 13.32	0.7026 -9.36	0.6947 -8.29	0.7152 12.74	0.6780 -3.00
1980-81	0.8122 23.57	0.8575 8.84	0.8717 14.77	0.7034 -5.64	0.6729 -5.34	0.8240 -2.16	0.6682 -1.76
1981-82	0.7047 22.68	0.8714 27.09	0.8566 18.45	0.6717 -8.24	0.6621 -6.64	0.6949 12.34	0.6591 -1.57
1982-83	0.7195 24.20	0.9626 16.84	0.8229 15.80	0.6938 -8.72	0.6690 -7.24	0.6726 -14.00	0.6536 -3.46
1983-84	0.7262 14.32	0.7911 15.38	0.7725 6.98	0.6725 -10.29	0.6667 -10.23	0.8474 -11.71	0.6419 -6.91
1984-85	0.6662 14.32	0.6326 8.07	0.7691 8.16	0.6791 -12.82	0.6610 -11.94	0.5501 -15.02	0.6445 -7.81
1985-86	0.6595 12.91	0.6878 12.70	0.7923 6.77	0.6930 -11.31	0.6576 -10.72	0.7242 -6.96	0.6391 -7.03
mean	0.7195 ±.0119 20.81 ±1.20	0.8168 ±.0294 18.37 ±1.88	0.8427 ±.0133 13.44 ±1.08	0.6860 ±.0051 -8.04 ±.67	0.6697 ±.0033 -7.10 ±.69	0.6986 ±.0264 -4.95 ±3.50	0.6582 ±.0040 -3.45 ±.66

Table 1b. The results of the 1st variant analysis, east-west component, amplitude factors an phase lags /"-"/.

Year	O1	P1	K1	N2	M2	L2	S2
1973-74	0.6664 -26.52	0.7308 -27.29	0.6820 -21.91	0.7741 -11.73	0.7460 -14.59	0.6133 -13.61	0.7316 -15.27
1974-75	0.6526 -22.31	0.7126 -21.33	0.6861 -19.18	0.7711 -11.80	0.7527 -12.05	0.6526 -5.28	0.7167 -14.44
1975-76	0.6364 -18.76	0.6785 -18.64	0.6743 -17.51	0.7796 -7.22	0.7496 -9.18	0.6905 -8.31	0.7125 -12.46
1976-77	0.6351 -19.17	0.7075 -21.19	0.6823 -16.88	0.7692 -7.55	0.7531 -9.20	0.7186 -7.47	0.7083 -11.84
1977-78	0.6589 -19.49	0.6910 -19.58	0.7026 -17.30	0.7779 -8.18	0.7526 -9.93	0.7398 -11.88	0.7085 -13.52
1978-79	0.6806 -19.58	0.7554 -19.61	0.7168 -16.91	0.7862 -9.16	0.7527 -9.71	0.7463 -6.86	0.6967 -12.70
1979-80	0.6760 -22.62	0.7375 -19.24	0.7376 -20.39	0.7678 -12.82	0.7400 -13.02	0.7277 4.18	0.6988 -16.62
1980-81	0.6854 -23.36	0.7503 -25.99	0.6992 -14.87	0.7426 -12.43	0.7341 -10.31	0.7659 -45.19	0.7058 -13.11
1981-82	0.6263 -20.84	0.8069 -21.69	0.7548 -17.20	0.7203 -10.66	0.7177 -11.84	0.6262 15.18	0.7467 -15.84
1982-83	0.7293 -21.08	0.7748 -13.16	0.7807 -17.97	0.7460 -7.38	0.7187 -11.53	0.6325 -0.20	0.7484 -14.13
1983-84	0.7262 -19.58	0.7480 -17.27	0.7742 -16.95	0.7574 -9.22	0.7340 -11.94	0.6827 -19.21	0.7771 -15.47
1984-85	0.7032 -21.02	0.8098 -20.53	0.7527 -18.60	0.7448 -11.85	0.7222 -13.23	0.9084 -15.66	0.7472 -15.97
1985-86	0.7076 -19.98	0.8217 -22.56	0.7407 -18.75	0.7704 -13.17	0.7322 -13.56	0.7557 -12.25	0.7659 -15.73
mean	0.6757 ±.0094 -21.10 ±.60	0.7481 ±.0126 -20.62 ±.99	0.7218 ±.0103 -18.03 ±.49	0.7623 ±.0053 -10.24 ±.61	0.7392 ±.0038 -11.55 ±.49	0.7123 ±.0218 -9.74 ±3.88	0.7280 ±.0074 -14.39 ±.43

Table 2a. The results of the 2nd variant analysis, north-south component, amplitude factors and phase lags /"-"/.

Year	O1	P1	K1	N2	M2	L2	S2
1973-75	0.7338 24.72	0.8373 24.31	0.8698 16.30	0.6981 -6.12	0.6748 -6.43	0.7004 -17.61	0.6620 -2.01
1974-76	0.7215 24.60	0.8543 26.95	0.8542 16.94	0.6766 -5.98	0.6671 -4.61	0.6654 -5.00	0.6599 -2.05
1975-77	0.6940 21.06	0.8201 20.35	0.8326 15.51	0.6651 -6.30	0.6619 -5.06	0.6446 -2.35	0.6584 -2.64
1976-78	0.7127 21.32	0.8517 14.99	0.8336 14.48	0.6627 -5.54	0.6618 -5.10	0.6127 0.13	0.6525 -2.75
1977-79	0.7636 22.29	0.9071 17.42	0.8615 13.63	0.6879 -6.68	0.6764 -5.12	0.5504 1.24	0.6674 -1.52
1978-80	0.7501 22.79	0.9100 19.91	0.8817 13.96	0.7013 -7.90	0.6921 -6.45	0.6088 4.95	0.6852 -1.35
1979-81	0.7515 24.42	0.8506 17.33	0.8676 13.84	0.6948 -7.87	0.6868 -7.12	0.7197 4.98	0.6710 -2.68
1980-82	0.7346 23.36	0.8671 22.13	0.8532 16.74	0.6824 -7.31	0.6658 -6.20	0.6947 7.25	0.6601 -1.63
1981-83	0.7117 23.60	0.9137 21.70	0.8389 16.87	0.6844 -8.47	0.6658 -6.95	0.6596 -2.87	0.6561 -2.57
1982-84	0.6730 19.02	0.8789 16.18	0.7946 11.38	0.6797 -9.58	0.6679 -8.70	0.7283 -11.09	0.6469 -5.17
1983-85	0.6526 14.15	0.7182 12.40	0.7717 7.37	0.6768 -11.47	0.6638 -11.07	0.7061 -13.04	0.6429 -7.38
1984-86	0.6622 13.58	0.6630 10.96	0.7809 7.35	0.6862 -12.10	0.6592 -11.32	0.6722 -8.62	0.6422 -7.41
mean	0.7134 ±.0105 21.24 ±1.10	0.8393 ±.0220 18.72 ±1.37	0.8367 ±.0104 13.70 ±.98	0.6830 ±.0034 -7.94 ±.62	0.6703 ±.0030 -7.01 ±.65	0.6636 ±.0152 -3.50 ±2.26	0.6587 ±.0035 -3.26 ±.63

dulation of the M2-wave for the NS but not for the EW component. For EW, on the other hand, there is quite clear half-yearly modulation. It is highly probable that such situation was physically determined by seasonal changes of the ocean loading effect, as suggested by Schwahn. Seasonal temperature changes of water on the meridian (NS) have different character then on the parallel (EW). There are some regions on the Earth where such changes have half-yearly period, e.g. equatorial area. Moreover, Ooe and Tamura (1985) found yearly and half-yearly modulation in the seas around Japan.

The other wave that proves unquestionably the existance of a yearly modulation is the S1-wave, which is demonstrated in Fig. 6. As opposed to Fig. 5, the S1$(\gamma, \Delta\varphi)$ vector was presented in its full magnitude, since the modulation of its phase includes the full range of 0° to 360°. The physical interpretation of the existence of S1-wave modulation is much easier than in case of the M2-wave. The S1-wave reflects in the first place the influence of the atmosphere temperature, therefore we might expect the vector S1$(\gamma, \Delta\varphi)$ to be longer in summer than in winter. Fig. 6 fully confirms this assumption.

The discovery of the S1-wave temperature modulation is a very important contribution to our 2 years' research on the mechanism and elimination of temperature influence on tidal measurements (Chojnicki, 1987, 1988). In agreement with our earlier suggestions on the influence of the S1-wave variation on the adjacent P1 and K1 waves and the lack of this influence on the more distant ones (e.g. O1 or N2), we can expect that the S1-wave modulation may induce K1-modulation but would have no such effect on O1 or N2 waves. Figures 7 and 8 confirm these predictions.

It's also interesting that the quasi-tidal S3-wave, also produced by secondary temperature influence - as demonstrated in Fig. 9 - clearly undergoes modulation.

Detection and determination of the tidal waves modulation have enormous consequences for the further research in two aspects:

1. It is necessary to undertake research in order to explain the reasons of the modulation. In the first place, one should analyse the possibility and estimate the magnitude of possible seasonal changes of the oceanic loading effect.

2. New methods of analysis of observations should be developed; they should take into account the variation of some, at least, determined parameters and, if possible, the magnitude of variations should be calculated. All the methods of analysis that have been used so far assume

Table 2b. The results of the 2nd variant analysis, east-west component, amplitude factors and phase lags /"-"/.

Year	O1	P1	K1	N2	M2	L2	S2
1973-75	0.6577 -23.74	0.7134 -21.97	0.6874 -20.54	0.7721 -11.68	0.7527 -12.91	0.6499 -9.21	0.7215 -14.65
1974-76	0.6448 -20.77	0.6950 -19.97	0.6798 -18.41	0.7731 -9.31	0.7530 -10.57	0.6856 -9.56	0.7147 -13.46
1975-77	0.6357 -18.99	0.6920 -19.75	0.6777 -17.29	0.7746 -7.39	0.7514 -9.17	0.7084 -8.11	0.7107 -12.13
1976-78	0.6472 -19.36	0.6966 -20.28	0.6920 -17.13	0.7742 -7.77	0.7528 -9.56	0.7323 -10.58	0.7088 -12.67
1977-79	0.6716 -19.58	0.7304 -19.72	0.7117 -16.99	0.7840 -8.70	0.7527 -9.82	0.7426 -9.68	0.7022 -13.11
1978-80	0.6784 -20.70	0.7535 -18.94	0.7253 -18.22	0.7781 -10.28	0.7476 -10.91	0.7248 -5.52	0.6971 -14.17
1979-81	0.6828 -23.09	0.7258 -20.10	0.7221 -18.84	0.7599 -12.01	0.7375 -11.90	0.6583 -10.00	0.6986 -15.40
1980-82	0.6468 -21.78	0.7771 -23.04	0.7365 -16.59	0.7324 -10.66	0.7231 -11.21	0.5640 -9.75	0.7299 -14.93
1981-83	0.6856 -21.12	0.7835 -16.78	0.7690 -17.58	0.7341 -8.88	0.7182 -11.70	0.6381 6.67	0.7472 -14.93
1982-84	0.7274 -20.24	0.7563 -15.12	0.7769 -17.40	0.7513 -8.43	0.7263 -11.72	0.6322 -9.65	0.7625 -14.83
1983-85	0.7142 -20.24	0.7754 -19.03	0.7644 -17.75	0.7517 -10.54	0.7278 -12.59	0.8256 -17.36	0.7620 -15.78
1984-86	0.7058 -20.45	0.8154 -21.58	0.7467 -18.72	0.7560 -12.46	0.7272 -13.40	0.8011 -13.36	0.7568 -15.92
mean	0.6748 ±.0086 -20.84 ±.41	0.7429 ±.0116 -19.69 ±.62	0.7241 ±.0102 -17.95 ±.31	0.7618 ±.0049 -9.84 ±.49	0.7392 ±.0040 -11.29 ±.39	0.6969 ±.0215 -8.84 ±1.63	0.7260 ±.0072 -14.33 0.36

invariability of determined parameters. It should also be examined, what deformations of the adjacent waves are caused by ignoring the modulation of S1-wave.

Table 3. The approximate characteristics of the time variations of the tidal parameters.

wave		polynomial order		ampl.		$\Delta\varphi$
		γ	$\Delta\varphi$	msec/y	%/y	°/y
O1	NS	1,2	1 *	-0.003	0.26	-0.70
	EW	1	0 *	+0.023	0.67	+0.05
P1	NS	2 *	1	-0.002	0.63	-1.12
	EW	1	0 *	+0.018	0.99	+0.18
K1	NS	1 *	1 *	-0.014	0.83	-0.65
	EW	1 *	2	+0.044	0.90	+0.08
N2	NS	0 *	1 *	-0.0003	0.01	-0.53
	EW	1 *	0 *	-0.006	0.32	-0.14
M2	NS	0	1 *	-0.004	0.06	-0.55
	EW	1	0 *	-0.025	0.34	-0.20
L2	NS	0 *	0 *	+0.0001	0.29	-0.20
	EW	0 *	0	+0.001	0.46	-0.16
S2	NS	2	1 *	-0.004	0.16	-0.42
	EW	1 *	1 *	+0.018	0.51	-0.25

References

Chojnicki T., 1987, Determination and consequences of variability of S1-wave parameters, B.I.M. no 99, Bruxelles, ss 6858-6872.

Chojnicki T., 1988, Results of gravimetric observations of Earth tides in 1985-86 at the Warszawa station no 0905, Publ. Inst. Geophys. Pol. Acad. Sc., no F-15 (215), ss 81-100.

Dittfeld H.-J., 1980, Earth tide registrations at Potsdam 1974-78. Results of standard analysis method. Study of the Earth tides, Bull. no 3, Budapest, ss 32-55.

Dittfeld H.-J., 1984, Final results of an eight years gravimetric registration series at Potsdam, B.I.M. no 92, Bruxelles, ss 6054-6068.

Dittfeld H.-J., 1988, Temporal trends in the variations of tidal parameters, Proceedings of the 6th International Symposium "Geodesy and Physics of the Earth", Potsdam, 1988.

Ooe M., Tamura L., 1985, Fine structures of tidal admittances and the fluid core resonance effect in the ocean tide around Japan, Manuscr. geod., Berlin, no 10/1, ss 37-49.

Richter B., 1987, Das supraleitende Gravimeter DGK, R.C, H. 329, Frankfurt/Main.

Schwahn W., Elstner Cl., Savin I., 1988, On the modulation of the M2 gravity tide, Proceedings of the 6th International Symposium "Geodesy and Physics of the Earth", Potsdam, 1988.

Volkov V. et al., 1986, Communication at the KAPG-Meeting, Potsdam.

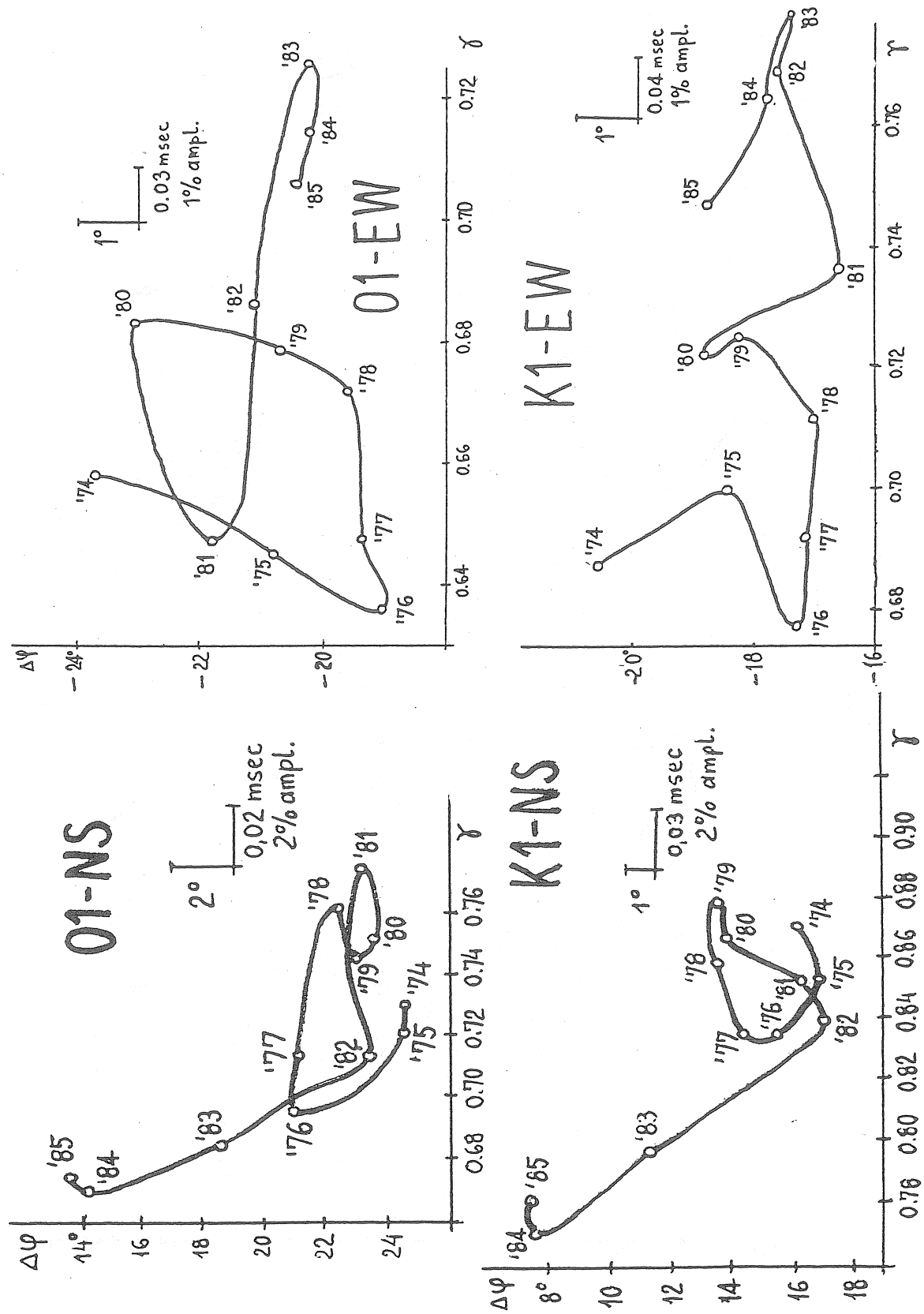

Fig. 1. The variation of 01 and K1 vectors at Książ station.

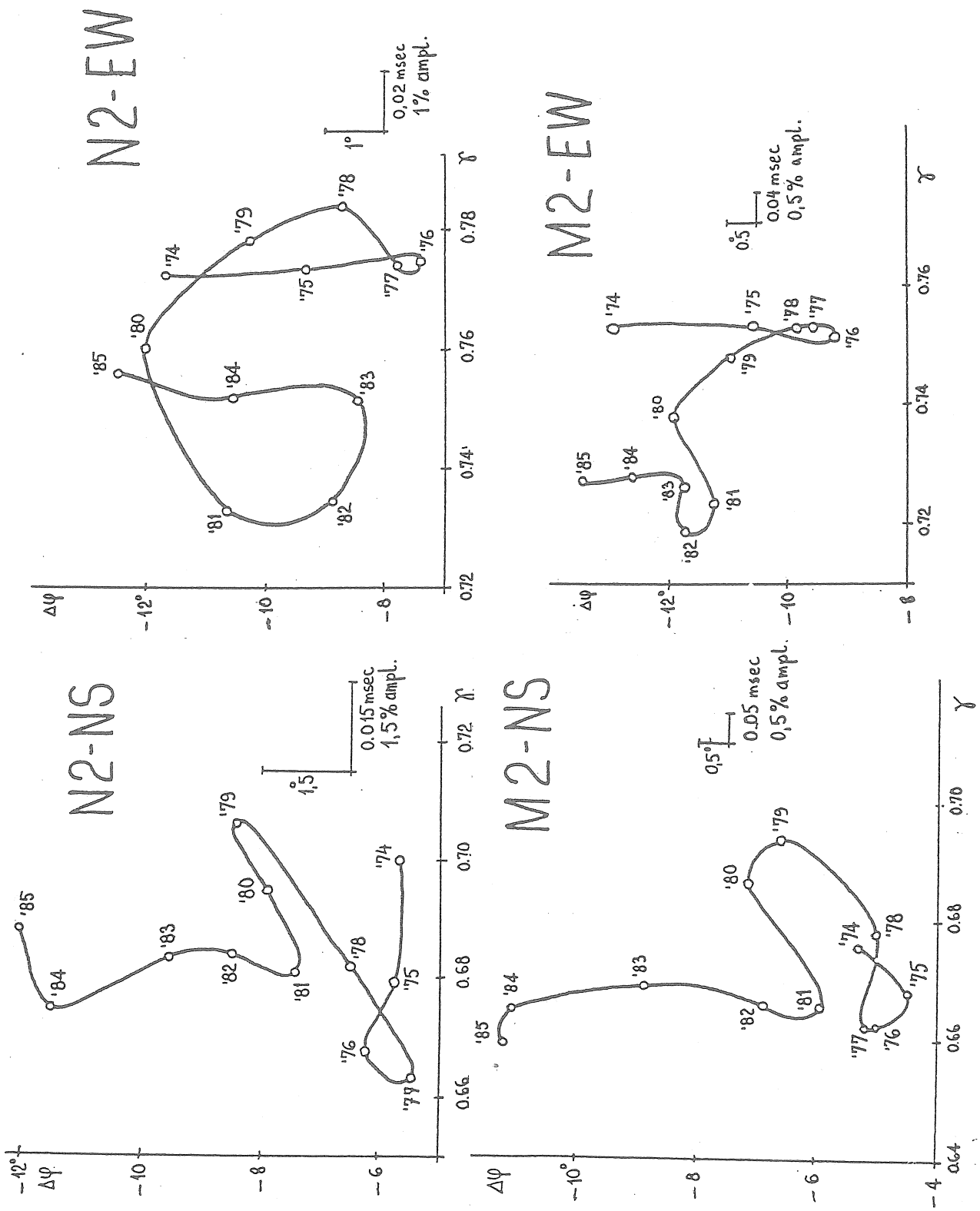

Fig. 2. The variation of N2 and M2 vectors at Książ station.

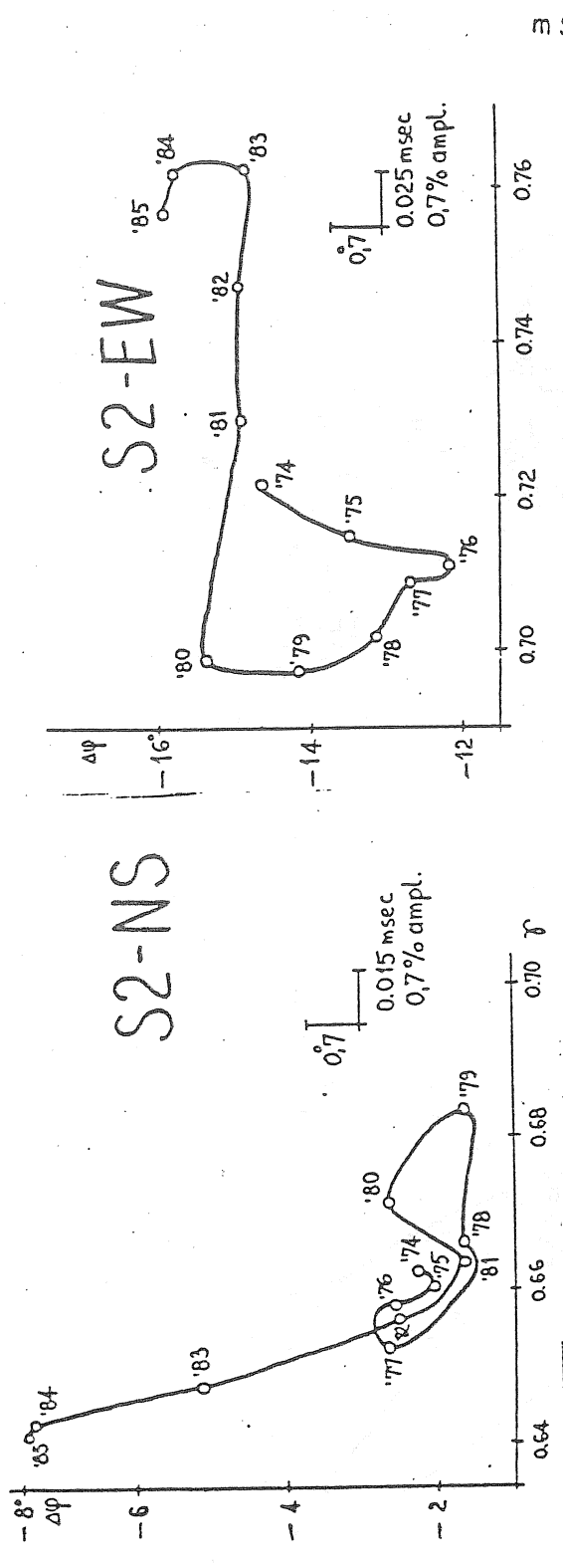

Fig. 3. The variation of S2 vector at Książ station.

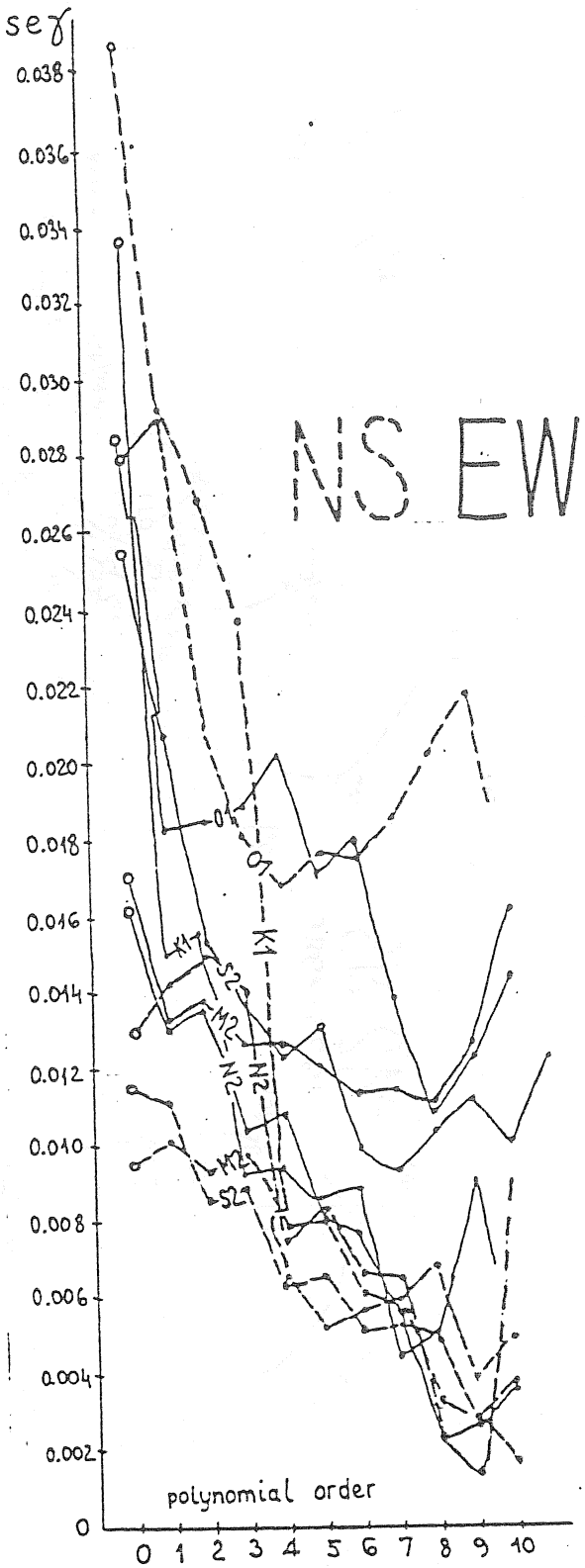

Fig. 4. The standard deviations of points of different approximation polynomials.

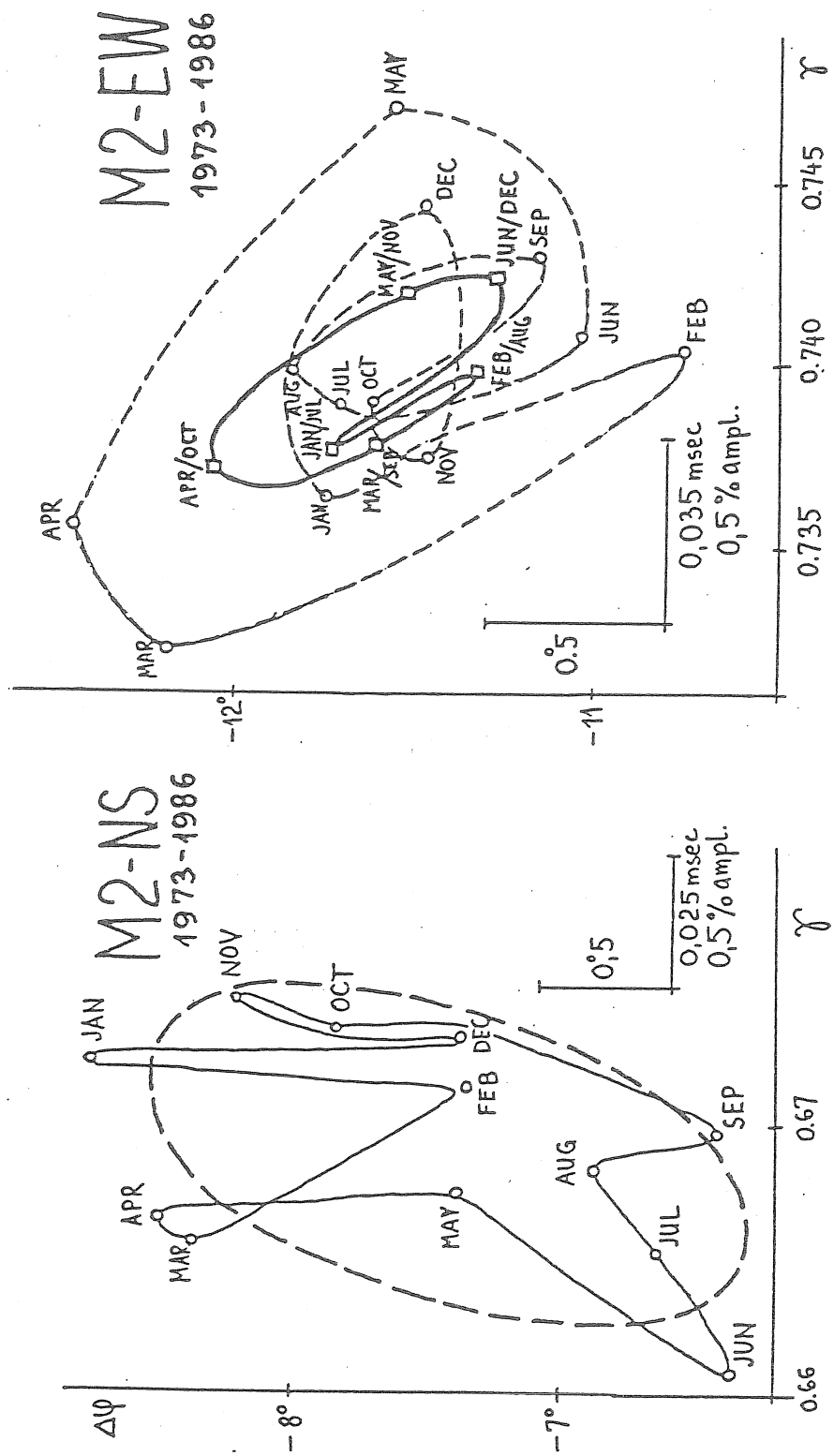

Fig. 5. The modulation of M2 vector at Książ station.

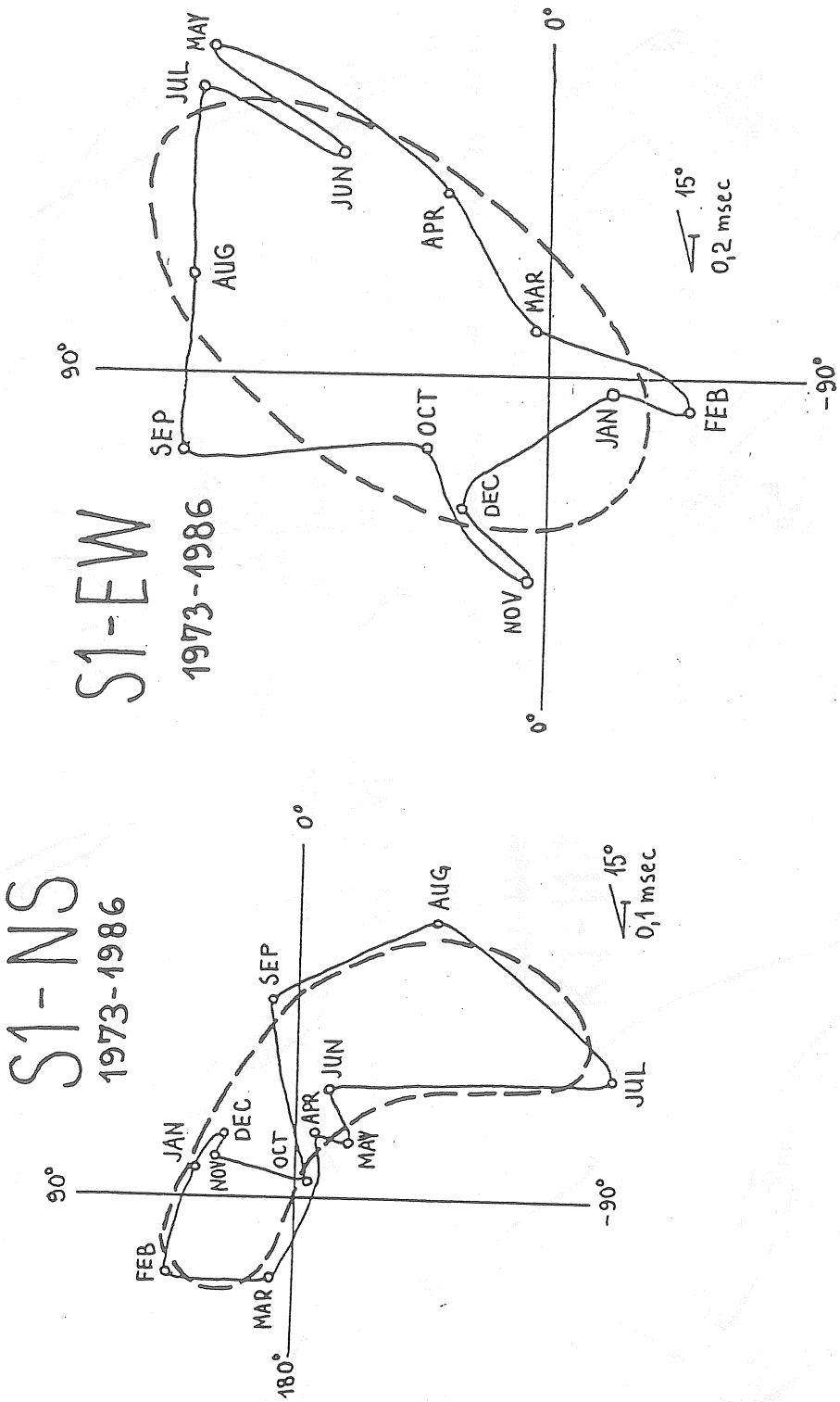

Fig. 6. The modulation of S2 vector at Książ station.

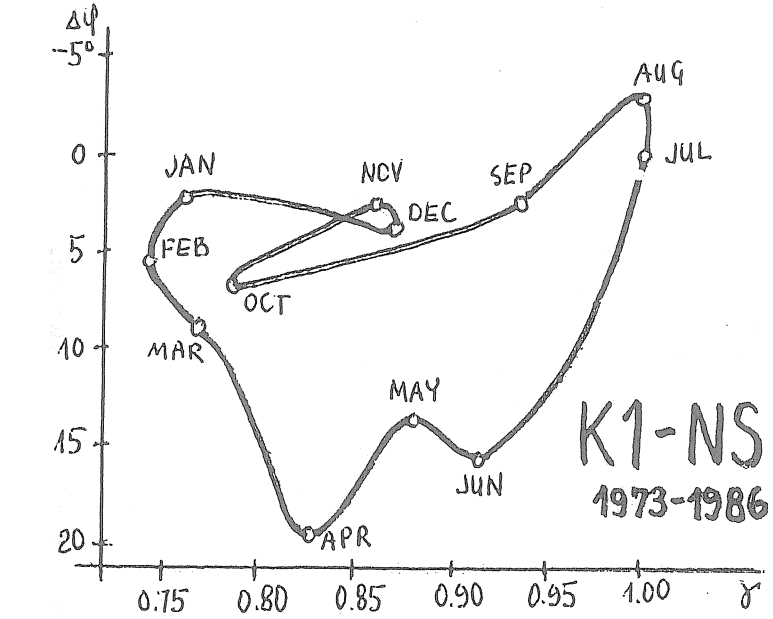

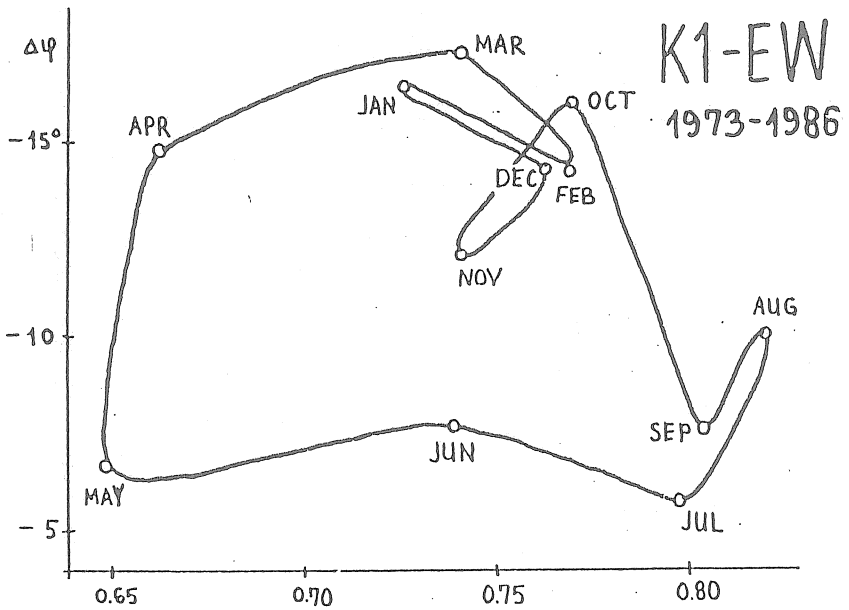

Fig. 7. The modulation of K1 vector at Książ.

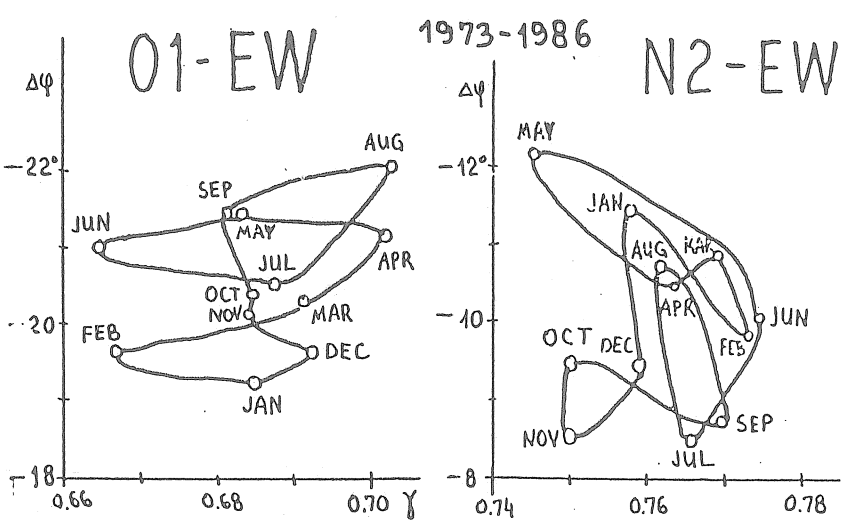

Fig. 8. The modulation of O1 and N2 vectors.

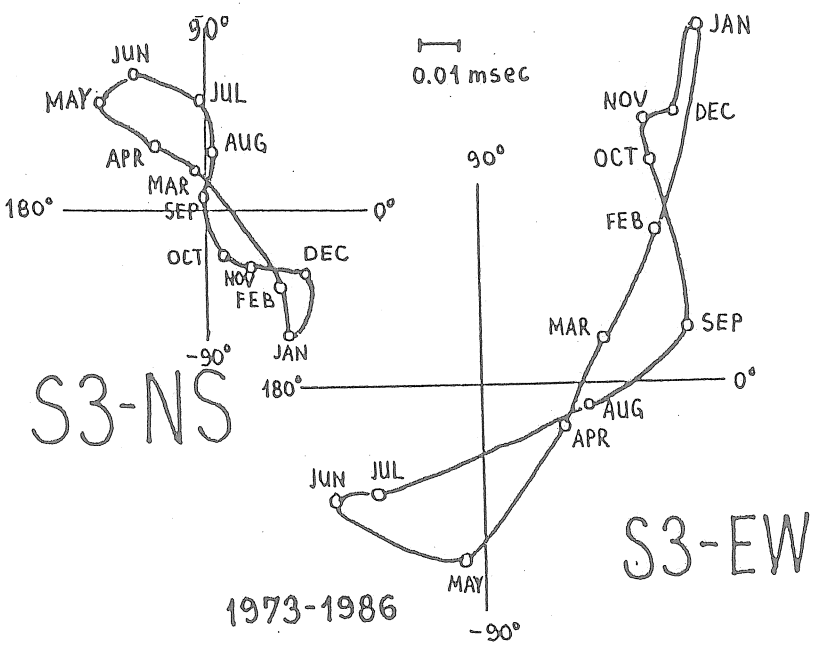

Fig. 9. The modulation of S3 vector at Książ.

TEMPORAL TRENDS in the VARIATIONS of TIDAL PARAMETERS

by Hans-Jürgen Dittfeld

Abstract
Time series of different gravimeters at several sites are analysed by uniform methods. Evident long-term trends of the amplitudes and phases of the resulting tidal parameters are discribed.
Especially for the waves M1,N2 and L2 very similar trends are observed, independently of the measuring conditions and of the analysis methods.
Object of the investigations are the measurements of two ASKANIA-GS15 and two GWR - superconducting gravimeters.
The considered variations are not confirmed by the Earth models and their reality is frequently called in doubt. Therefore the significance of the variations is critically discussed.

Zusammenfassung
Gravimetrische Gezeitenmessungen an vier Stationen wurden mit einheitlichen Methoden analysiert, wobei sich augenfällige Langzeitvariationen einiger Ergebnisparameter zeigten, die für verschiedene Stationen und Meßsysteme erhebliche Ähnlichkeiten aufweisen.
Unabhängig von Analysenmethoden und Beobachtungsbedingungen gilt dies besonders für die Wellengruppen M1,L2 und N2.
Derlei Variationen ergeben sich nicht aus den gültigen Erdmodellen und werden oft in Zweifel gezogen. Deshalb wurde die Signifikanz dieser Variationen besonders kritisch untersucht.
Der Arbeit liegen die Langzeitreihen von zwei ASKANIA-GS15 - und zwei Supraleitgravimetern zugrunde.

Already eight years ago we published first remarks concerning the temporal variations of tidal parameters within the Potsdam gravimetric results, giving a first impression of our intentions /1/. Temporal variations are also observed by RICHTER /3/ and VOLKOV et.al. /4/ for the stations Bad Homburg/FRG and Sofia/Bulgary respectively.

Of course such kind of variations are not predicted by the Earth models and so these results have been called in doubt in a number of discussions. But there seems to be more information in the results as generally supposed.

So we have been looking for temporal trends of the parameters within corresponding series of other stations and we found remarkable similarities with the trends inside the 12.5 years part of our series evaluated at present.

In the first picture is represented the amplitude factor of the wave L2. The points are showing results of overlapping analyses by CHOJNICKIs method A15K using the error estimation based on residuals. The analysis period is always about 480 days (16 monthes), the shift is 180 days or six monthes. A resolution of nineteen wave groups was used. There are compared four stations. At Potsdam/GDR and Pecny/CSSR are registrating the Askania GS15 gravimeters No.222 and No.228 but in Brussels/Belgium and Bad Homburg/FRG there are superconducting once (GWR type). The general trend found for these very different measurements is nearly the same.

The slope downward in 1983/84 is good confirmed by both the superconducting gravimeters and the result of the registration at Potsdam. Comparing the L2 DELTA factors resulting from the total series at Bad Homburg (1981/84) and Brussels (1982/86) we found a difference of about 10%. From former publications 3.9 or 5.1% difference may be calculated. These discrepancies can be fully explained by the temporal variations at Fig.1: The Bad Homburg series is measured mostly near to the maximum but the Brussels measurement is passing through the minimum of 1984. So the temporal variations may be the reason for different results of very precise measurements if these are not carried out contemporary.

Naturally the other series are not so long as in Potsdam. But also by parts the general trend is very similar if constant deviations are neglected which are caused by different influences of the indirect effects and the calibration problems of the superconducting gravimeters. So for instance follows from the averaged relations of the amplitude factors of seven main waves that the calibration factor of the gravimeter GWR TT40 at Bad Homburg is about 0.83% smaller than that of the instrument in Brussels. The corresponding relations to the Potsdam series are −0.55%(Bad Homburg) and +0.28%(Brussels) respectively. In the considered frequency bands the inner accuracy of these latter instruments is higher than those of the Potsdam series by a factor of about 1.5.

The Figure 2 represents the phase shift of the same tidal wave. The inner accuracy of the Pecny analyses is practically equal to that of the Potsdam series. But the Pecny series was often interrupted and therefore there seems to be a little bit more noise. Thats because of the seasonal effects. Owing to the missed contributions of not existing parts of the measurement the result is shifted somewhat in the direction towards the result of fulfilled seasons. So we have a scattering in comparison with uninterrupted series. The last point of the Pecny curve connected with a broken line represents the result of a yearly analysis after a break of two years in the registration but it is also situated within the general trend.

Fig.3 is a corresponding representation for the tidal wave N2 which has an amplitude of about six microgal at Potsdam. The variation in amplitude is much more significant and amounts to about two percent corresponding to nearly nine times the error of a single result. It is impossible to explain such variations by imperfections of the Cartwright-Tayler-Edden development of the tidal potential used for the analysis because the contributions of not regarded waves are almost

very small.

At the picture for the phase lag of the wave N2 very good is to be seen the decrease of the influence of the indirect effect of the ocean from near the coast (Brussels) to Pecny station which is situated near Prague. But without mentioning these differences the long term trends are very similar again.

So our statements concerning the temporal variations are consequently supported by the results of the investigations of the other series.

To be sure that these features are not a effect of the analysis method our series was also analysed by Prof.VENEDIKOV using his VM74 method. At Fig.4 are pictured the results of independent (not overlapping) yearly and biennial parts of the measurement. The other curve is showing the results of the CHOJNICKI method like on the foregoing Figures. The different level in the case of the amplitude factor is originated by the inertial effect which is corrected by the VM74 programme but not during the CHOJNICKI analysis. Both the methods are giving similar trends.Therefore the variations are not a failure of a singular method nor a phenomenon of a singular station.

The significance of the results was already discussed in /2/. (From other comparisons was estimated that for such kind of investigations a particular measuring accuracy is needed as for instance characterised by a mean square error of Mzero smaller than 1.0 microgal in the CHOJNICKI analysis.) Now we have these new results underlining the assertion concerning the temporal variations of the tidal parameters. Naturally these effects are very small and the errors are big in comparison with the variations itself. That holds also for the best series available at present. So a real congruence of the curves of different stations is not to be expected even if the local effects may be excluded. Just therefore the presented features are extremely astonishing.

We have been looking for especially remarkable trends and found these for the constituents M1, N2 and L2 which are connected in the development of the tidal potential with the perigeum of the moon.

A special software system was developed by our colleague Mrs.HARNISCH for the presentation of these variations inside the DELTA-KAPPA plane. So we get pictures showing the variation in amplitude as well as in phase at the same figure.

In the figures 5, 6 and 7 is demonstrated the way of the end of the DELTA-KAPPA vector during the time. Close to the dots is marked the central month of the corresponding analysis.

These figures for L2, N2 and M1 are showing a quasi circular behaviour having a comparable clear period : The vector returns to the vincinity of the starting point after nearly ten years. The total variations are 97; 110 and 252 nanogal respectively. Here we have some new experiences resulting from a fourteen years observation which was seldom interrupted (13 gaps only) and carried out almost without changing the used instruments.

Until now we don't have a determined explanation for the outlined features but we warrant for the significance of these variations. Corresponding pictures are available for nineteen constituents of the tidal potential.

The ten years period of the mentioned tides is within the error borders near to the eleven years sun freckles cyclus as well as near to the half of the 18.6 years period of the moon. But the explanation may lie also in the interferences of diurnal and semidiurnal features connected with non tidal amplitude variations of M2 or S1 acting on the neighboured bands. References therefore are already visible in the spectrum of the residuals /5/. In the figures 5, 6 and 7 the vector of L2 is turning counter-clockwise but for N2 and M1 we see a clockwise rotation. As pointed out by SCHWAHN et al /6/ the opposite rotation of the N2 and L2 vectors is a proof therefore that the variations are caused by a modulation of the M2 main wave which is producing satellites in the amplitude spectrum situated (symmetrically to the M2 line) in the N2 and L2 wave group respectively.

For the preparation of the showed pictures was needed a constant and precise measurement of about fourteen years. Of course in shorter series are such kind of long acting phenomena much more difficult to discover.

These variations are open for interpretation. First ideas are mentioned but other ideas for which we are waiting may be more acceptable.

One of the main tides, almost hold for very constant, is O1. It was making a flight between 1979 and 1982 (Fig.8). This variation was amounted to about 0.51% corresponding to 176.6 nanogal. That means that for instance yearly measurements carried out in 1977/78 or in 1981/82 will have a different result also for one of the biggest tidal waves.

In our experience the most stable wave of the tidal spectrum is M2. It shows anomalies of about 0.15 degree of the phase only, registrated in 1982 and practically not connected with an amplitude variation (Fig.9). The total M2 variation is about 95 nanogal or 0.28%.

To avoid misunderstandings - these latter are results of the Potsdam series only not ever underlined by corresponding results of the other stations. To compare several stations on this type of pictures is not yet possible at present.

Furthermore shall be remarked that the existence of other variations can be expected: If they are shorter as the analysis interval of 480 days used for the investigations they will not be clearly detected by the presented methods.

In every case it is shown that the tidal parameters are not so constant as ever believed. Therefore we have to measure and we have to observe the tidal parameters in order to get their real values for every epoch in which accurate tidal prognoses are needed.

Finally is listed the result of the 12.5 years tidal measurement at Potsdam. The last column gives the deviations against the WAHR model which are between 0.74 and 1.37%.

Gravimetric Observatory Potsdam / GDR
GS15 No.222 1974 - 1986
CHOJNICKI A15K
N = 103 640 hrs. Mzero = 0.603 microgal

WAVE	DELTA Observation	KAPPA	AMPLIT. Indirect effect	DELTA corrected	KAPPA	DT/DT(O1) (SCHWIDERSKI/ICET)	MODEL %
Q1	1.1503 14	-0.24 07	6.6594	1.1560	-0.056	0.99953	0.790
O1	1.1522 3	0.02 01	34.7984	1.1565	-0.086	1.00000	0.838
P1	1.1519 6	0.33 03	16.1101	1.1504	0.189	0.99474	0.746
K1	1.1398 2	0.16 01	48.1394	1.1376	0.041	0.98367	0.951
N2	1.1764 7	1.93 04	6.2238	1.1561	0.092	0.99964	0.942
M2	1.1845 1	1.20 01	32.5012	1.1559	-0.212	0.99944	0.922
S2	1.1878 3	0.40 01	15.1873	1.1609	-0.002	1.00383	1.366
K2	1.1822 11	0.17 06	4.1172	1.1564	-0.114	0.99991	0.969
DT(O1) - DT(K1) = 0.0124				0.0189			0.0200
DT(O1) - DT(M2) = -0.0323				0.0006			0.0016

Acknowledgement

For the hourly values of the series measured at Pecny, Brussels and Bad Homburg we are very indebted to Dr.Zd.Simon / VUGTK Zdiby - CSSR, Dr.B.Ducarme / ORB - Belgium and to Dr.B.Richter / IfAG, Frankfurt/M - FRG respectively.
Thanks are also du to Mrs.M.Harnisch for programming and preparation of the vector scetches as well as to Mr.W.Altmann who supported the tidal observation at Potsdam with continuity and care.

References

/ 1 / DITTFELD, H.-J.: Earth Tide Registrations at Potsdam 1974-78. Results of standard analysis methods Study of the Earth Tides, Bull.No.3, Budapest 1980,32-55

/ 2 / DITTFELD, H.-J.: Final results of an eight years gravimetric registration series at Potsdam B.I.M. No.92, Brussels 1984, 6054-6068

/ 3 / RICHTER, B.: Das supraleitende Gravimeter DGK, R.C, H.329, Frankfurt/Main 1987

/ 4 / VOLKOV, W.A.: Communication at the KAPG-Meeting Potsdam 1986

/ 5 / ASCH,G.; C. ELSTNER; G. JENTZSCH and H.-P. PLAG: On the Estimation of Significant Periodic and Aperiodic Gravity Variations in the Time Series of Neighbouring Stations - Part I ; Proc. 10th Int. Symp. on Earth Tides, Madrid 1985, 239-250

/ 6 / SCHWAHN, W.; C. ELSTNER and I.V. SAVIN: On the Modulation of M2 Gravity Tide. 6th Int. Symp."Geodesy and Physics of the Earth", Potsdam 1988

Figure captions

Fig 1 Temporal trends of the L2 amplitude factor at different stations

Fig. 2 Corresponding trends of the L2 phase lags

Fig. 3a Temporal trends of the N2 amplitude factor

Fig. 3b Temporal trends of the N2 phase lag

Fig. 4a Trends of the N2 amplitude factor in Potsdam calculated by different methods

Fig. 4b Corresponding trends of the L2 phase lag

Fig. 5 The variation of the L2 vector at Potsdam

Fig. 6 The variation of the N2 vector at Potsdam

Fig. 7 The variation of the M1 vector at Potsdam

Fig. 8 The variation of the O1 vector at Potsdam

Fig. 9 The variation of the M2 vector at Potsdam

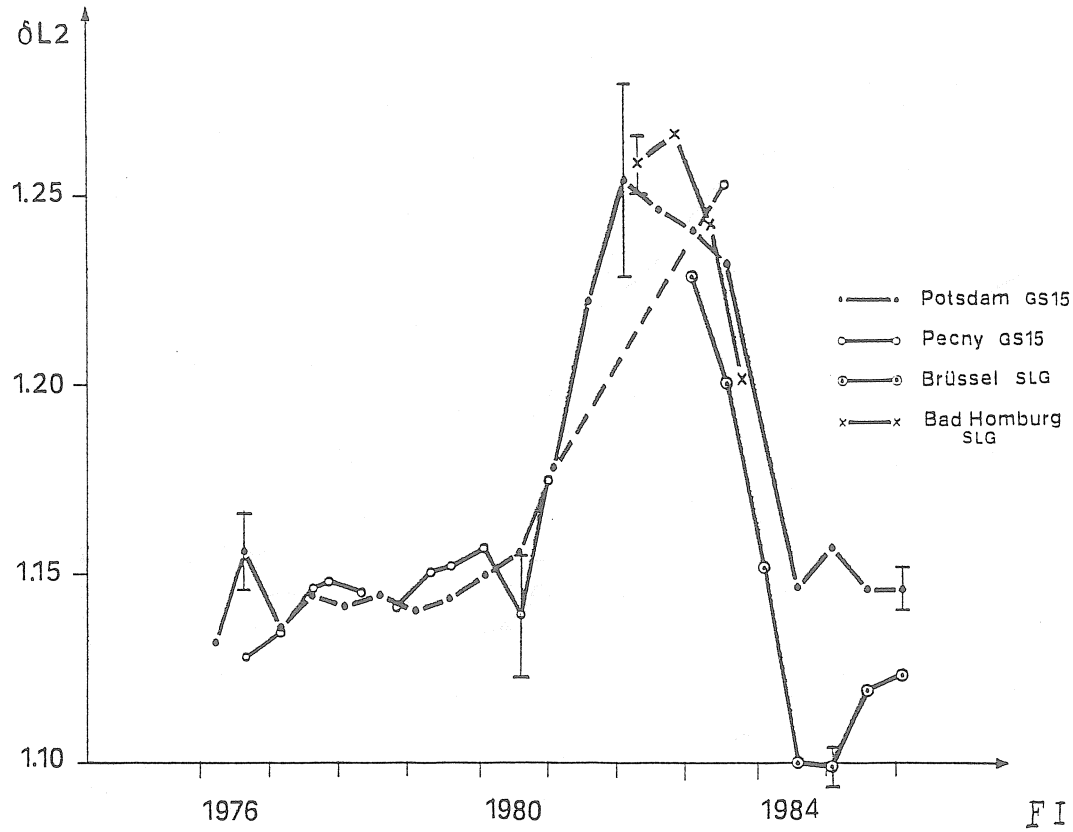
δL2
1.25
1.20
1.15
1.10
1976
1980
1984
Potsdam GS15
Pecny GS15
Brüssel SLG
Bad Homburg SLG

FIG. 1

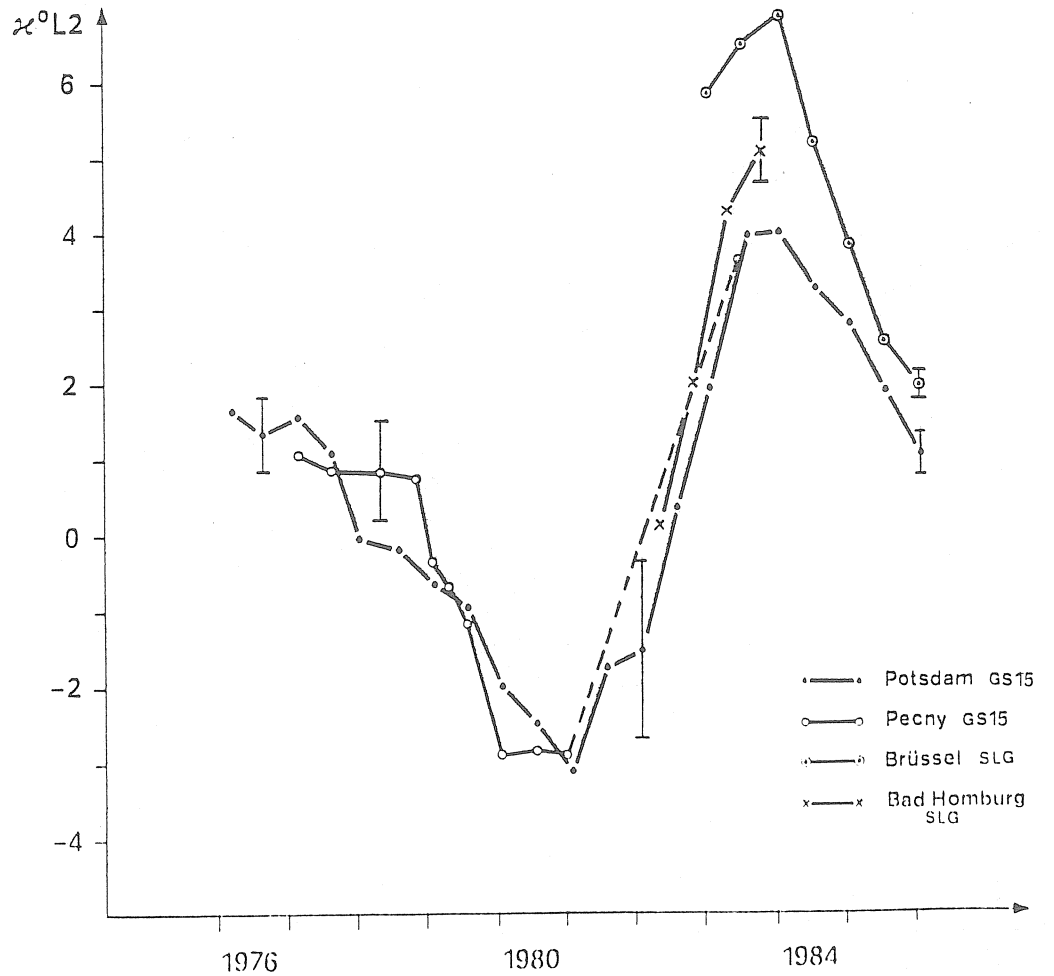
𝒳°L2
6
4
2
0
-2
-4
1976
1980
1984
Potsdam GS15
Pecny GS15
Brüssel SLG
Bad Homburg SLG

FIG. 2

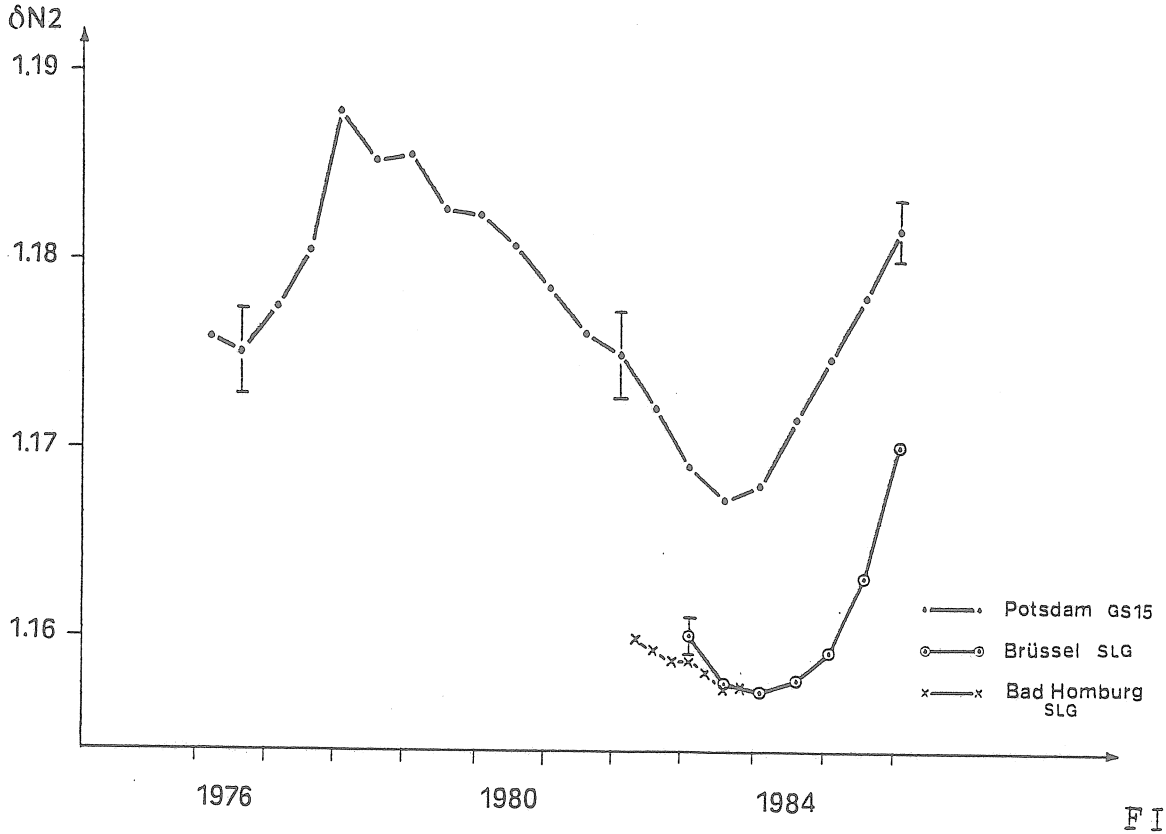
δN2
1.19
1.18
1.17
1.16
1976
1980
1984
Potsdam GS15
Brüssel SLG
Bad Homburg SLG

FIG. 3A

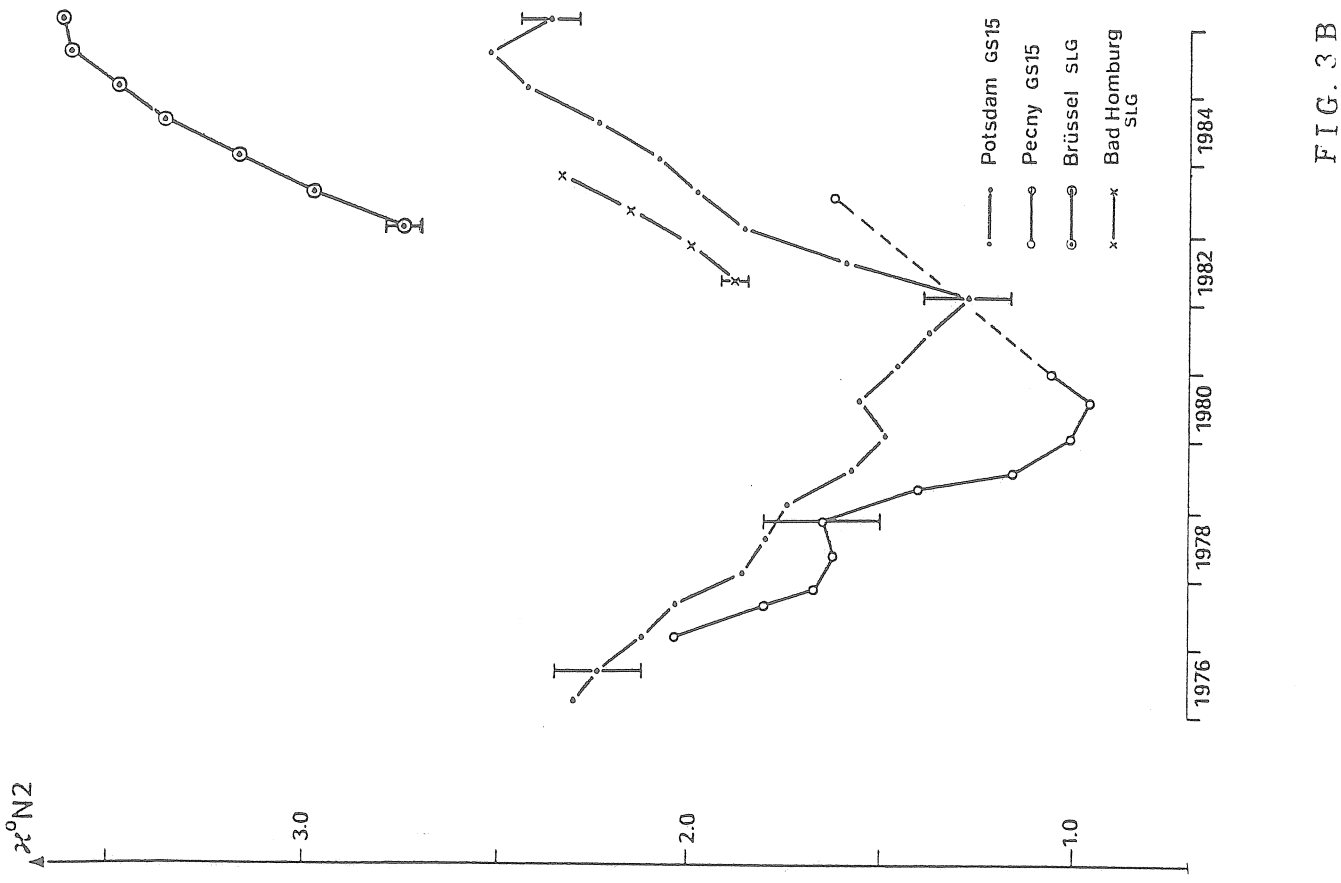
Potsdam GS15
Pecny GS15
Brüssel SLG
Bad Homburg SLG
1976
1978
1980
1982
1984
δ¹⁸O N2
3.0
2.0
1.0

FIG. 3B

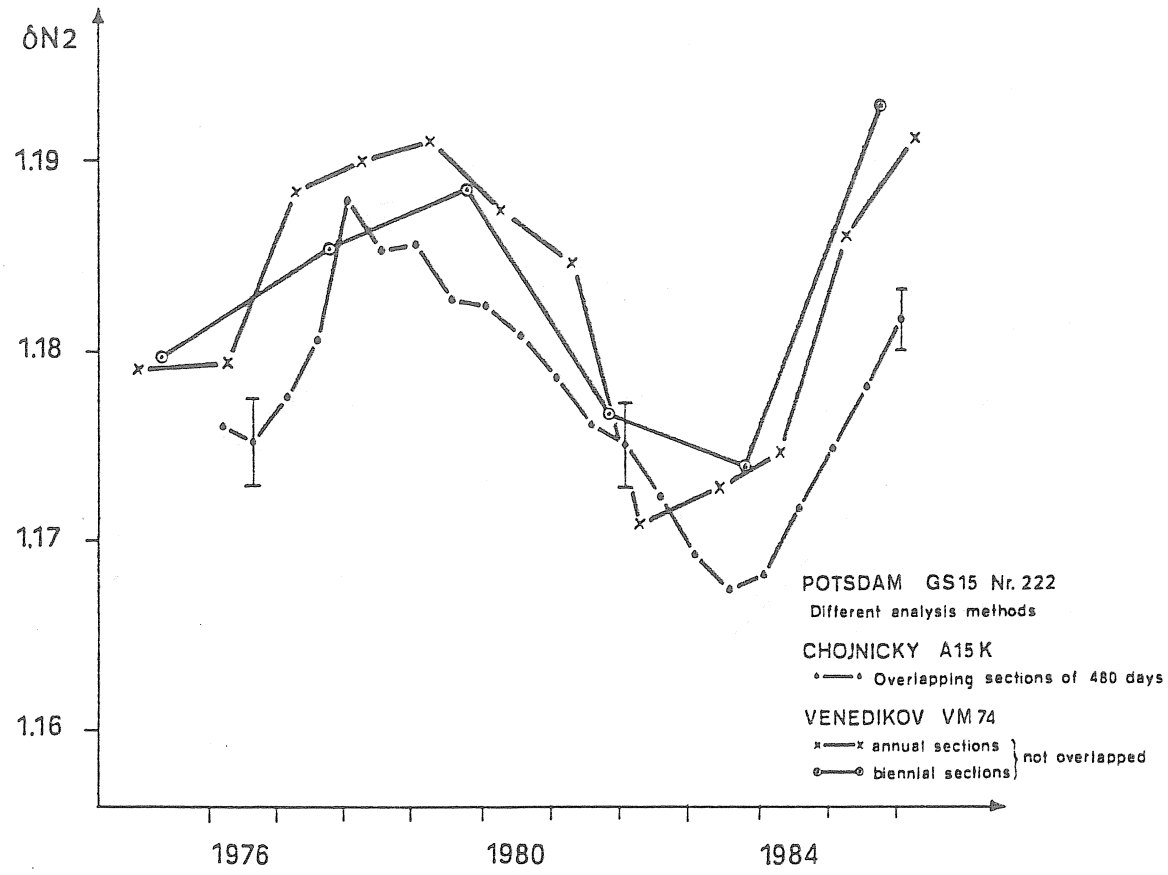
δN2
1.19
1.18
1.17
1.16
1976
1980
1984
POTSDAM GS15 Nr. 222
Different analysis methods
CHOJNICKY A15K
Overlapping sections of 480 days
VENEDIKOV VM74
annual sections
biennial sections
not overlapped

FIG. 4A

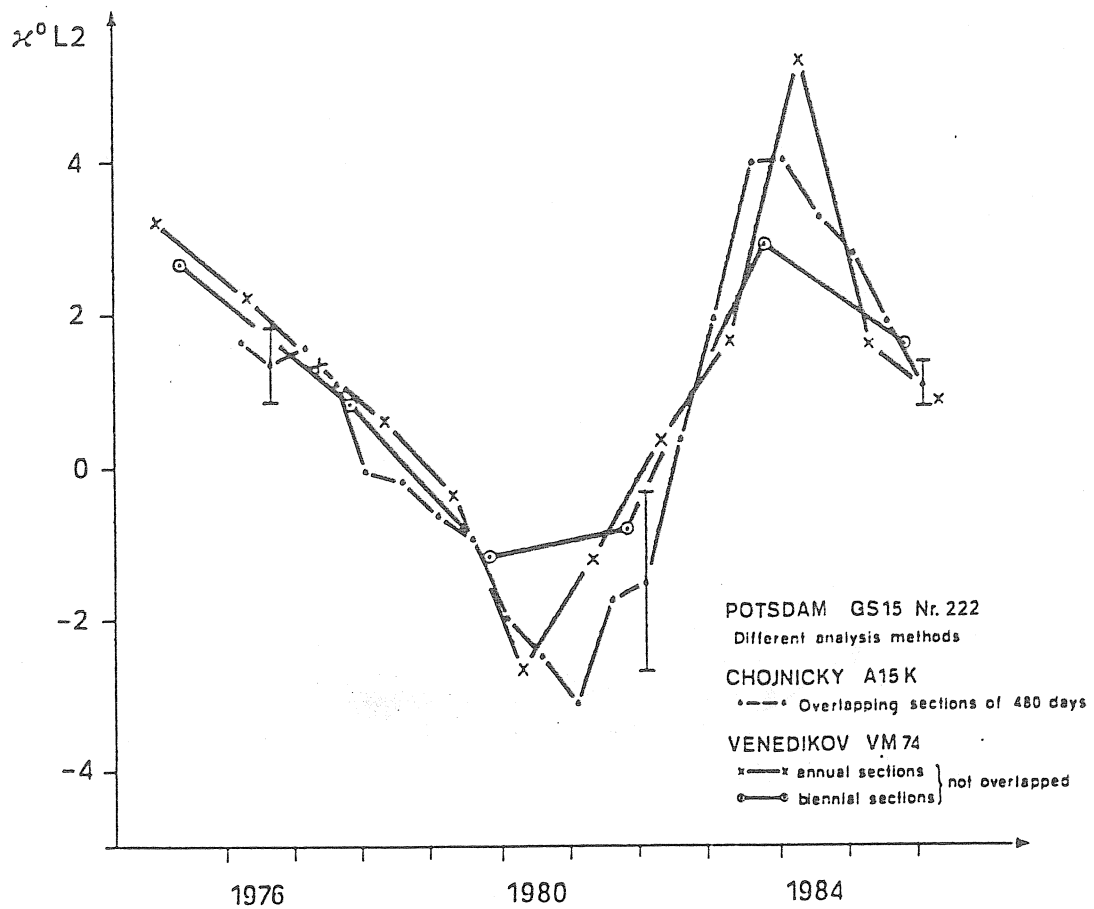
χ°L2
4
2
0
-2
-4
1976
1980
1984
POTSDAM GS15 Nr. 222
Different analysis methods
CHOJNICKY A15K
Overlapping sections of 480 days
VENEDIKOV VM74
annual sections
biennial sections
not overlapped

FIG. 4B

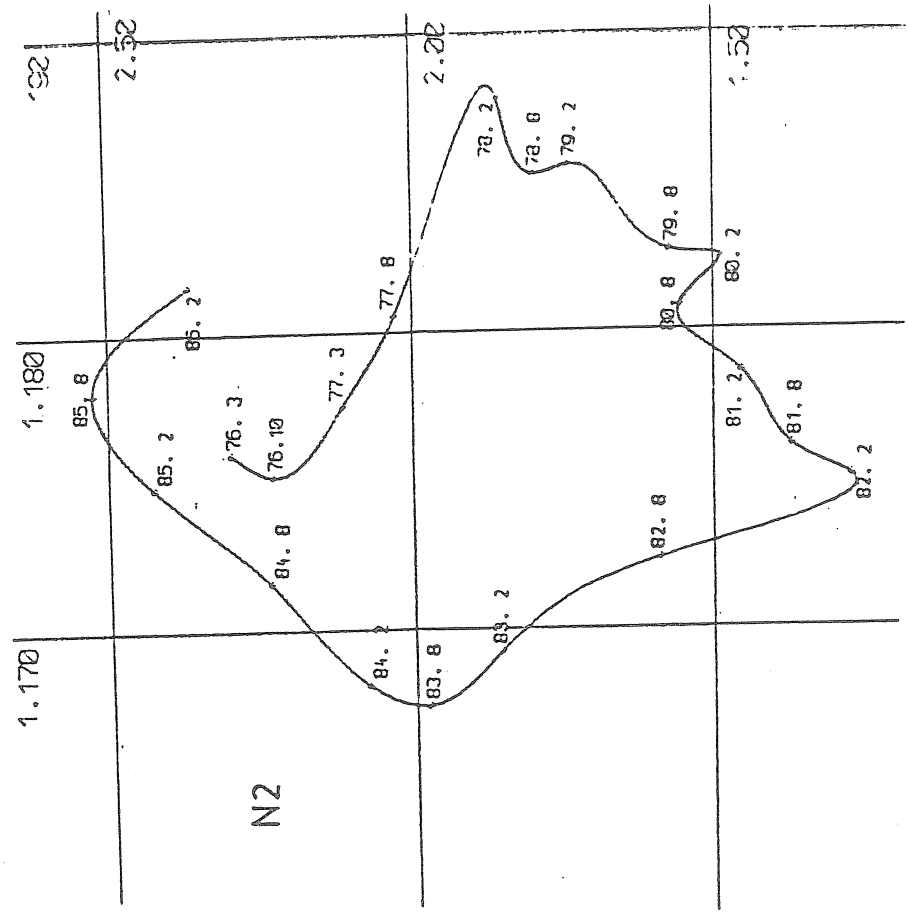

FIG. 6

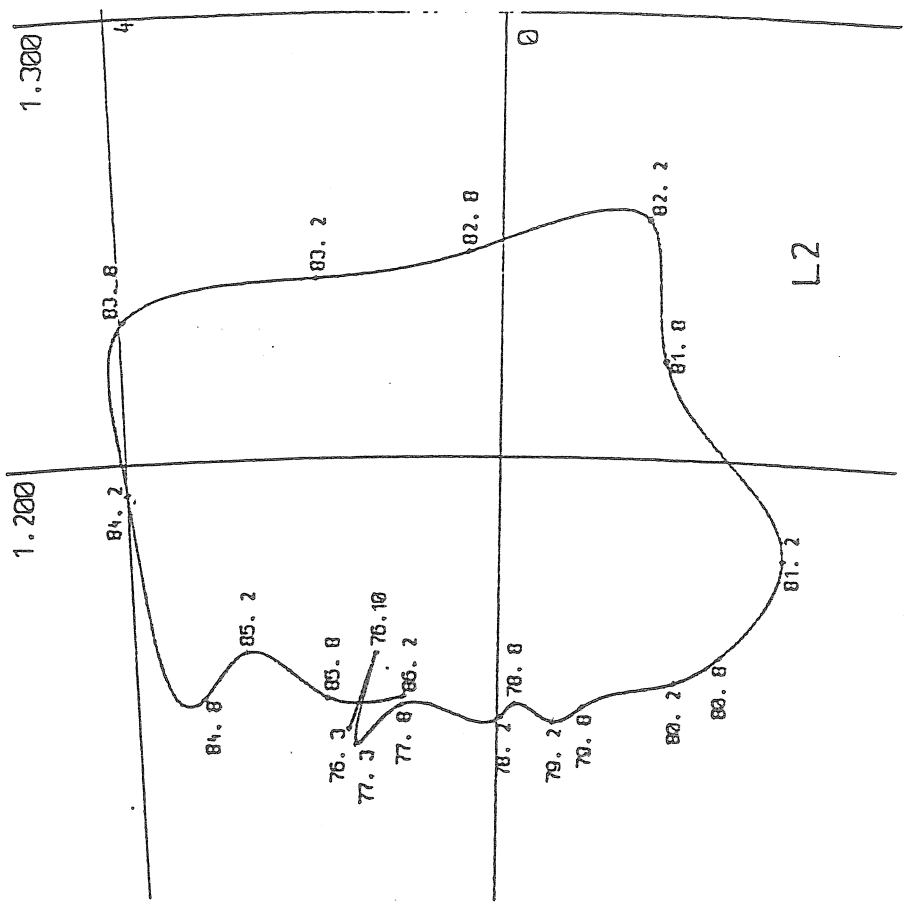

FIG. 5

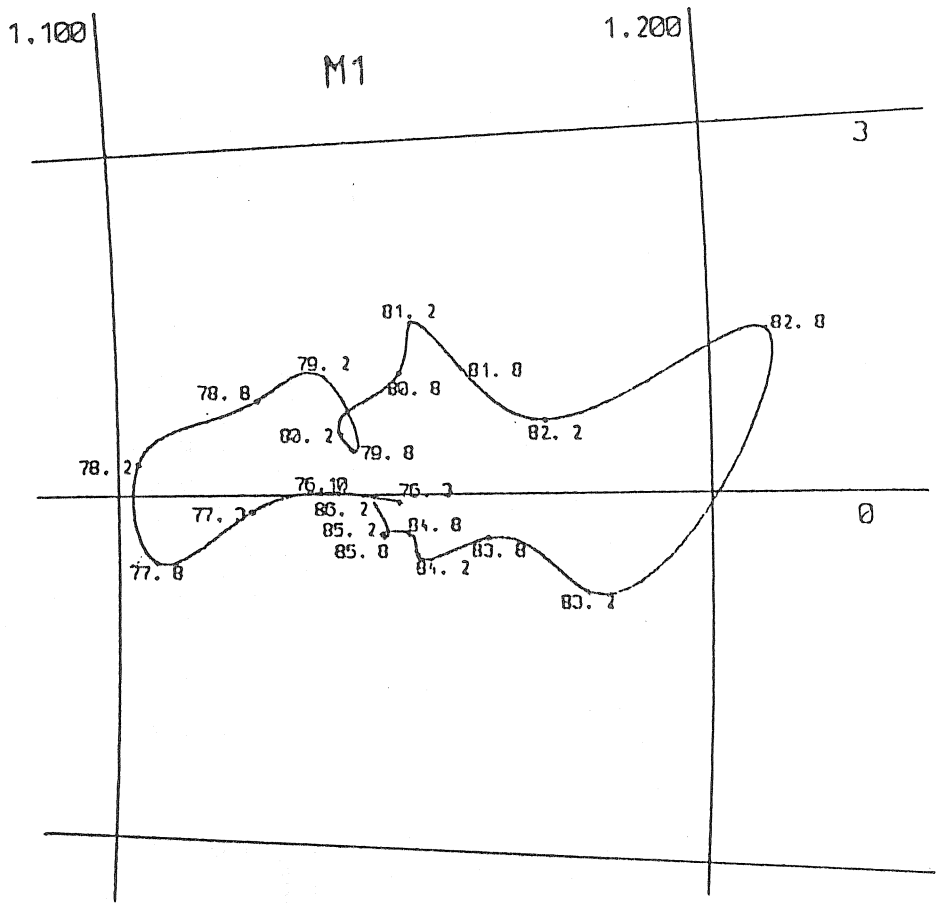
1.100
1.200
M1
3
0
78. 2
78. 8
79. 2
81. 2
82. 8
80. 8
81. 8
80. 2
79. 8
82. 2
76. 10
76. 3
77. 3
86. 2
85. 2
84. 8
85. 8
83. 8
84. 2
77. 8
83. 2

FIG.7

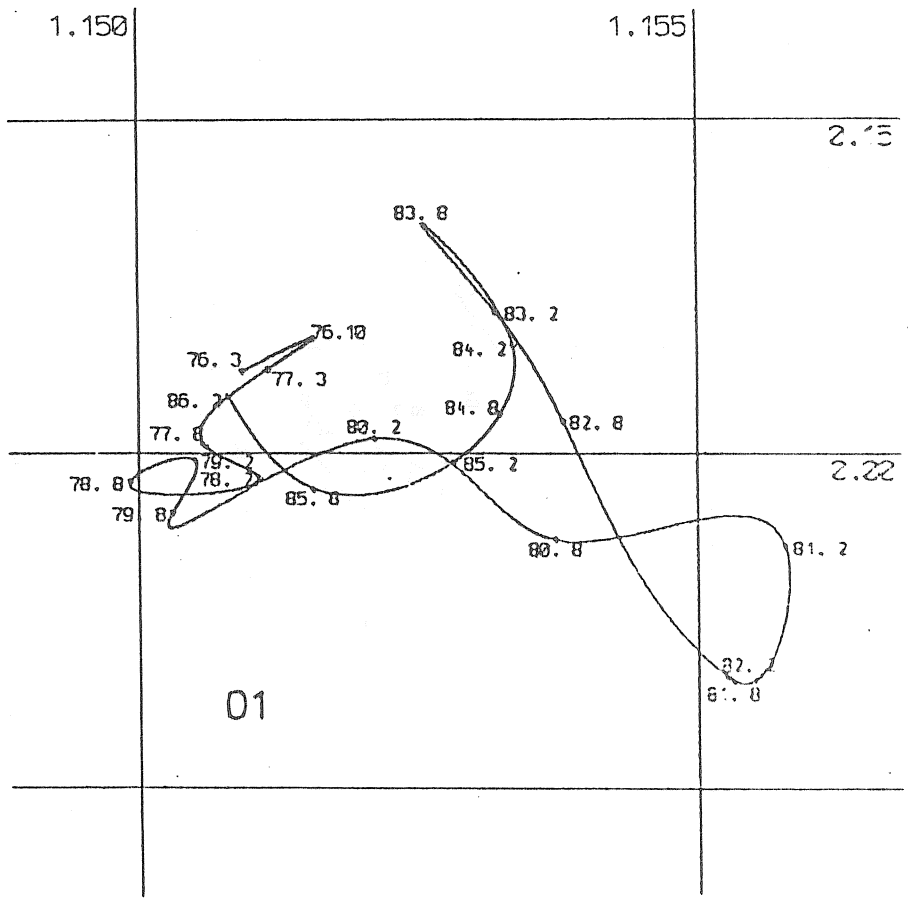
1.150
1.155
2.15
2.22
01
83. 8
83. 2
76. 10
76. 3
77. 3
84. 2
86. 2
84. 8
82. 8
77. 8
80. 2
79. 2
78. 8
78.
85. 2
85. 8
80. 8
81. 2
82. 1
81. 8

FIG 8

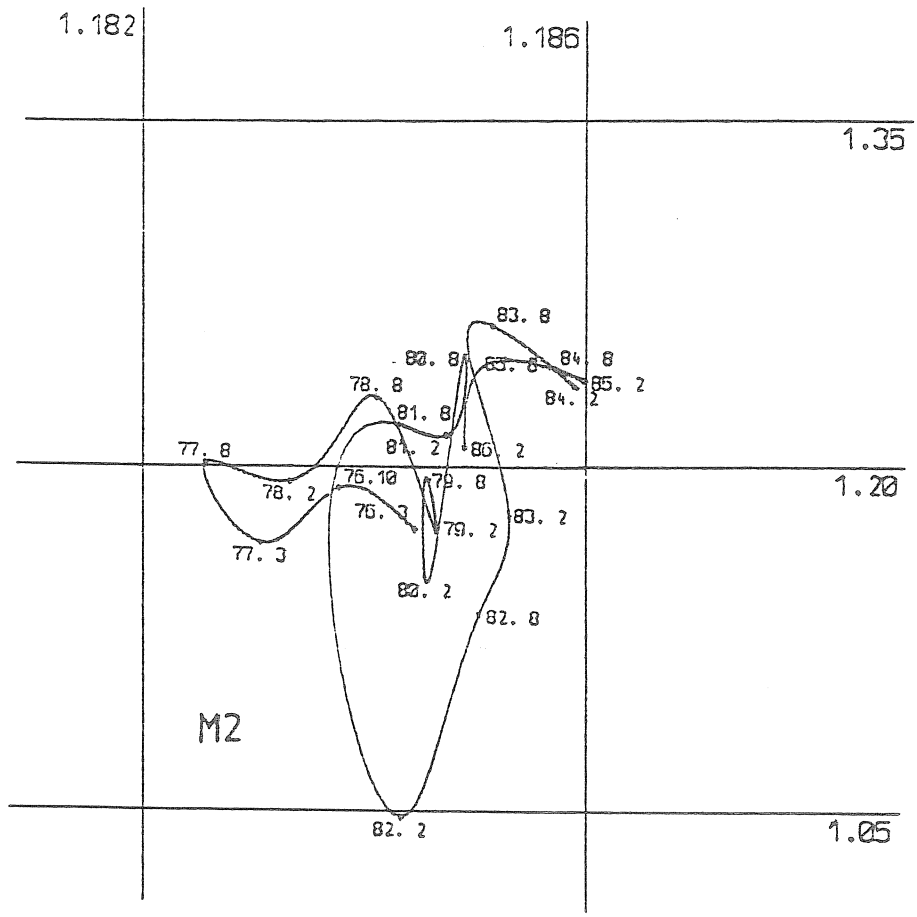

FIG. 9

Appendix

GS15 No. 222

Temporal Variations of 19 Tides as observed
at Potsdam 1976 - 1986

Legend
Each point in the $\delta - \varkappa$-plane corresponds to a result of a 480 days analysis.
The instrumental phase lag is corrected.
Other corrections are not applied.
As central epoch is given year.month beside the points.
Error crosses are marked for single points only.
The points are connected by cubic spline functions.

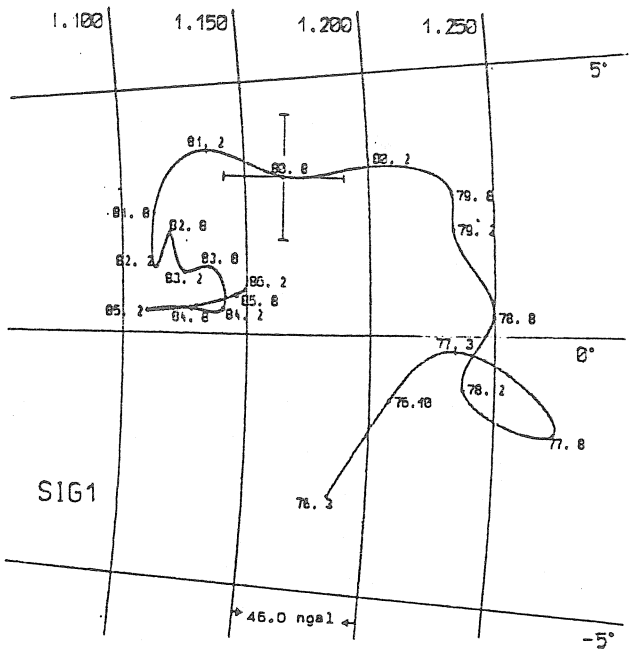
1.100
1.150
1.200
1.250
5°
0°
-5°
SIG1
46.0 ngal

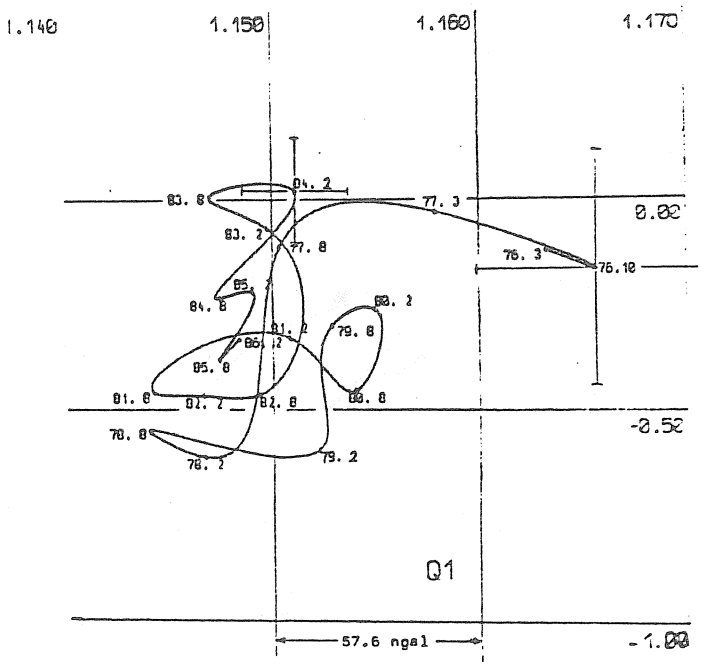
1.140
1.150
1.160
1.170
0.00
-0.52
-1.00
Q1
57.6 ngal

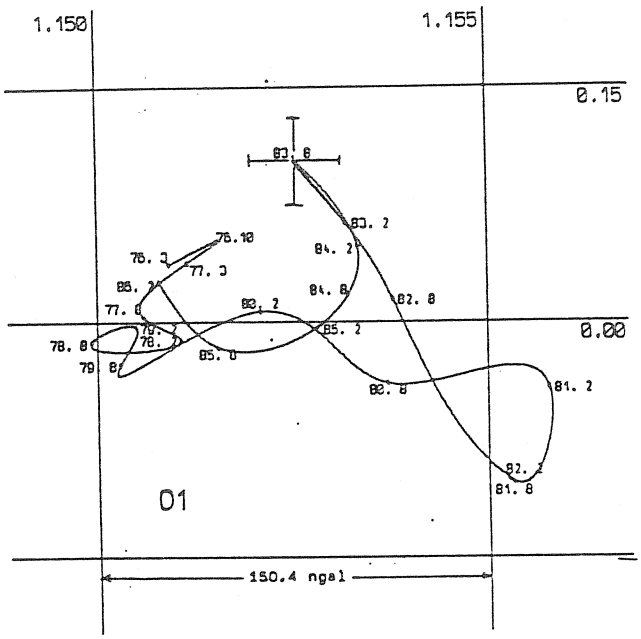
1.150
1.155
0.15
0.00
O1
150.4 ngal

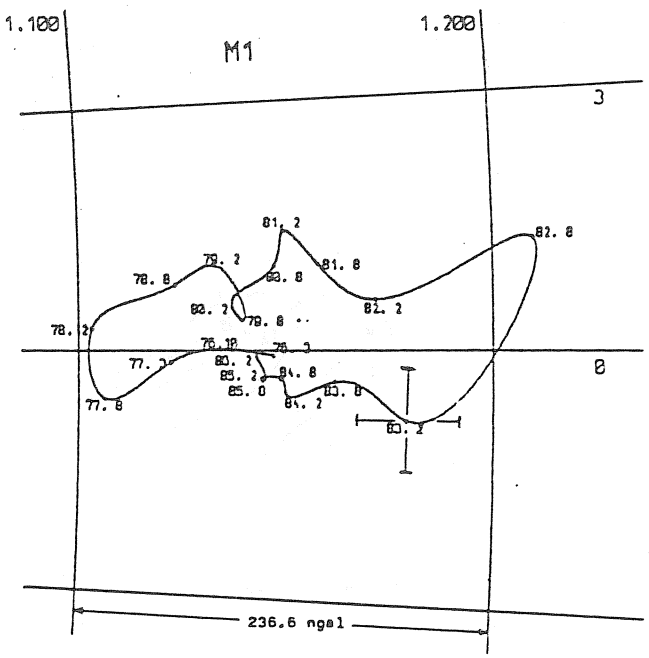
1.100
1.200
M1
3
0
236.6 ngal

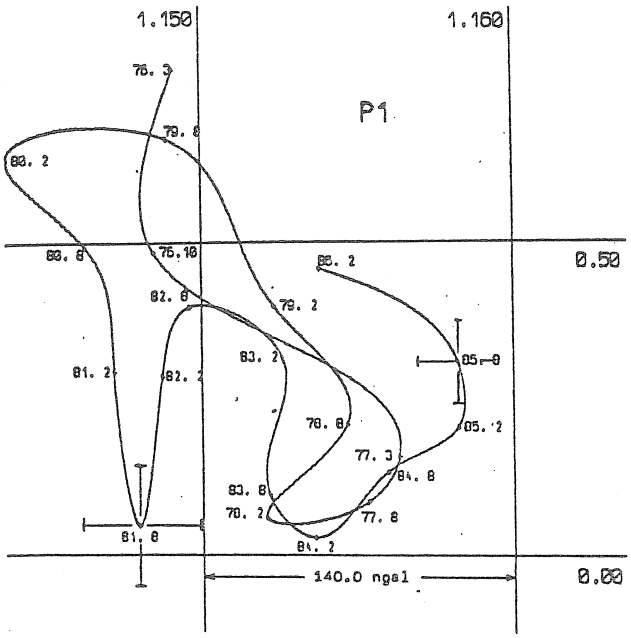
1.150
1.160
P1
0.50
0.00
140.0 ngal

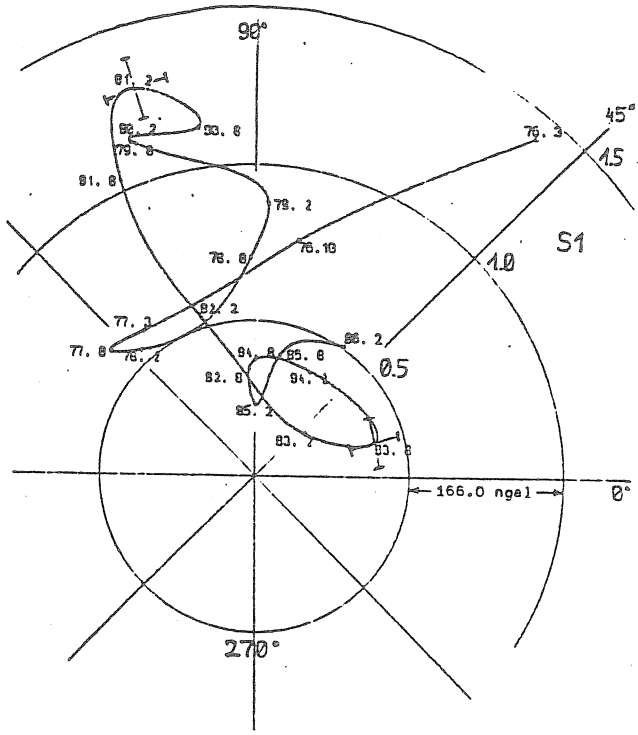
90°
45°
1.5
1.0
0.5
S1
166.0 ngal
0°
270°

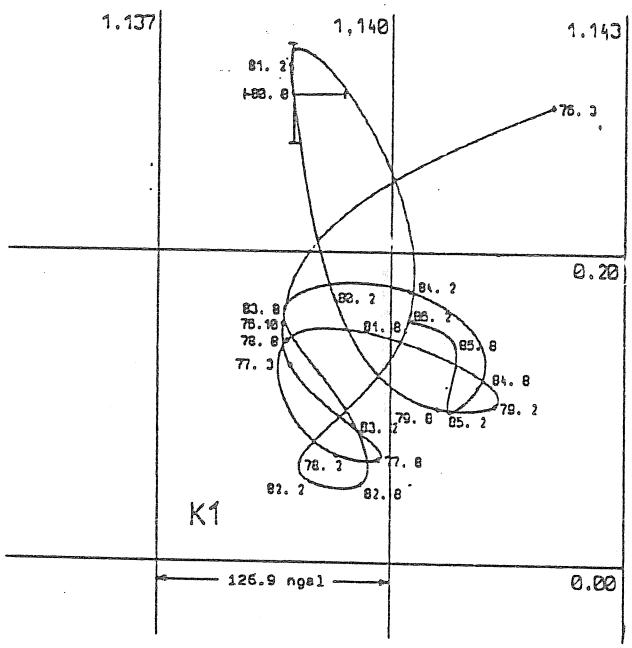
1.137
1,140
1.143
0.20
K1
126.9 ngal
0.00

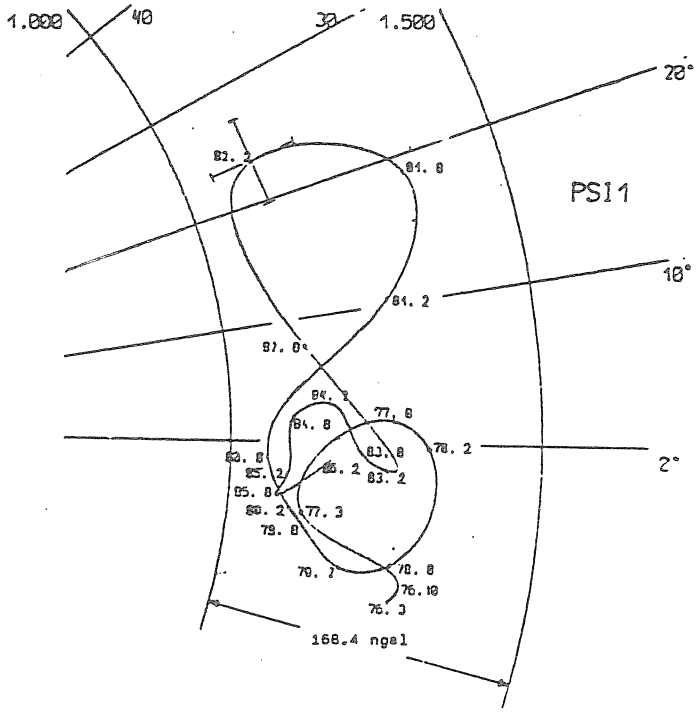
1.000
40
30
1.500
20°
10°
2°
PSI1
168.4 ngal

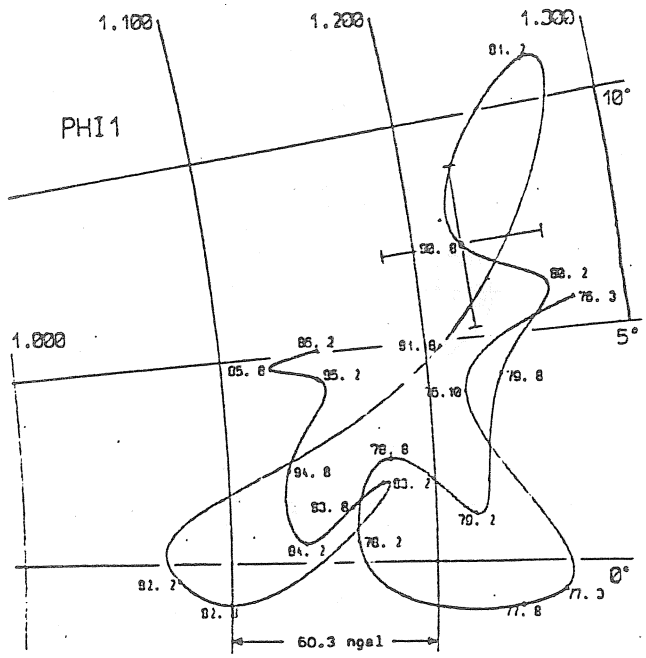
1.100
1.200
1.300
PHI1
10°
5°
0°
1.000
60.3 ngal

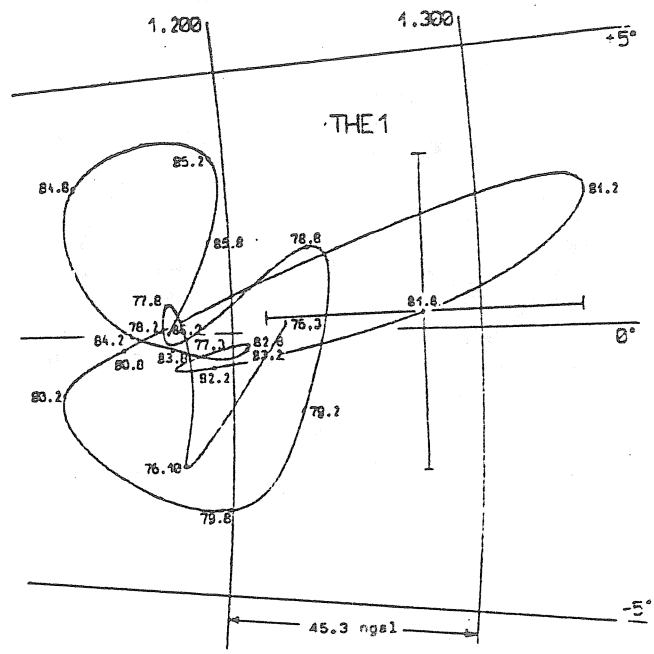
1.200
1.300
THE1
+5°
0°
-5°
45.3 ngal

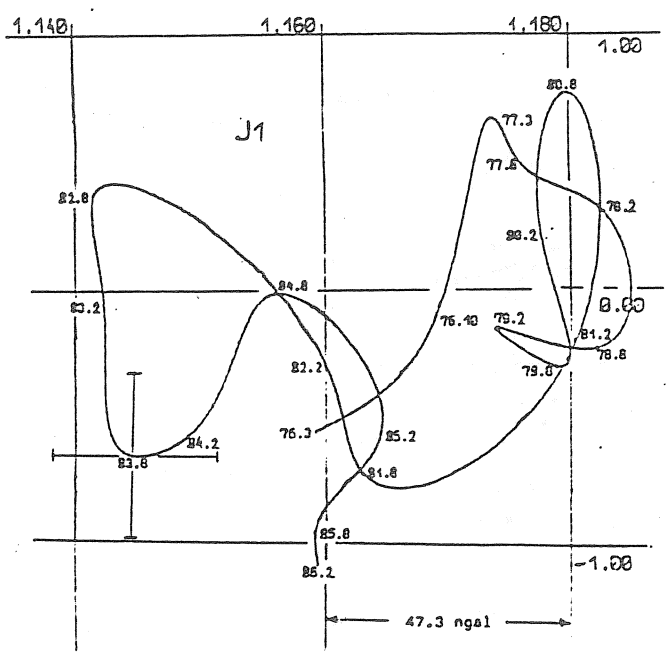
1.140
1.160
1.180
1.00
J1
0.00
-1.00
47.3 ngal

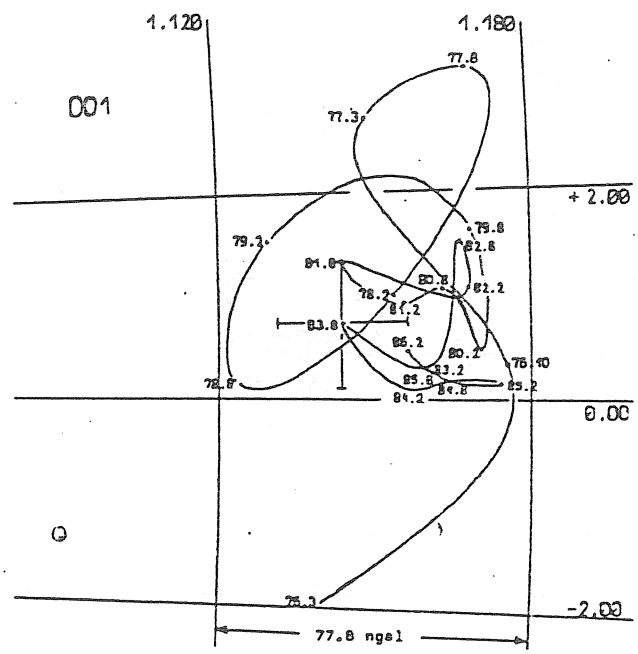
1.120
1.180
001
+ 2.00
0.00
-2.00
77.8 ngal

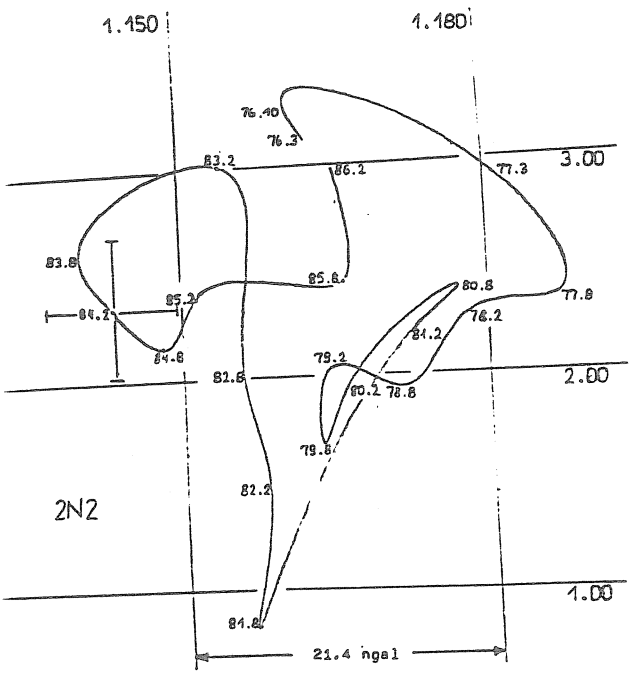
1.150
1.180
3.00
2.00
1.00
2N2
21.4 ngal

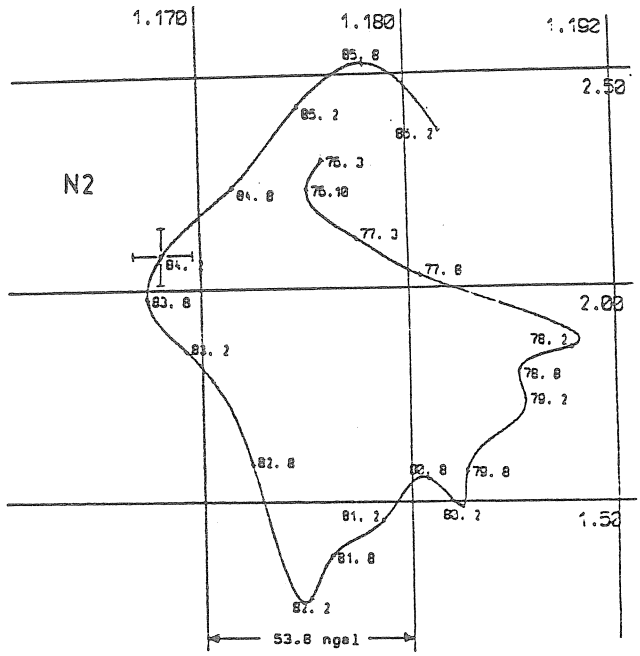
1.170
1.180
1.192
2.50
2.00
1.50
N2
53.8 ngal

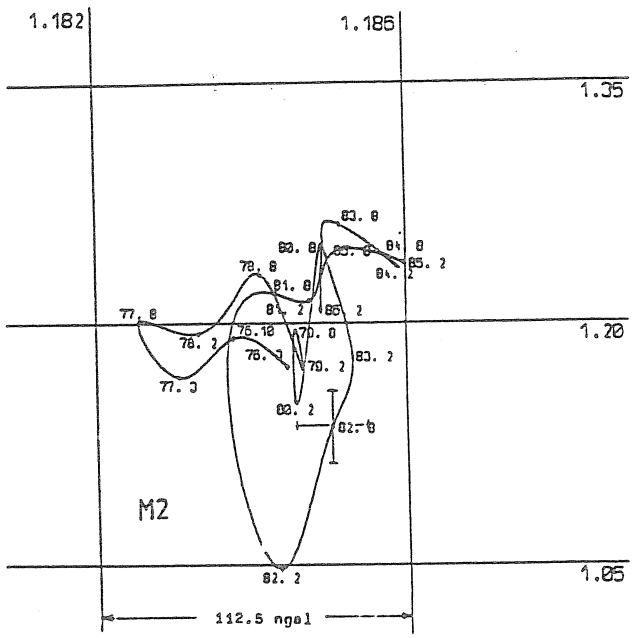
1.182
1.186
1.35
1.20
1.05
M2
112.5 ngal

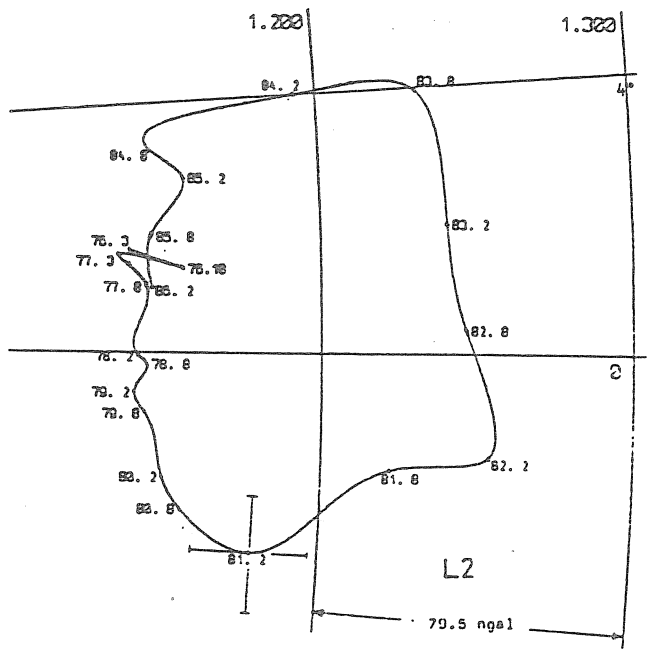
1.200
1.300
L2
79.5 ngal

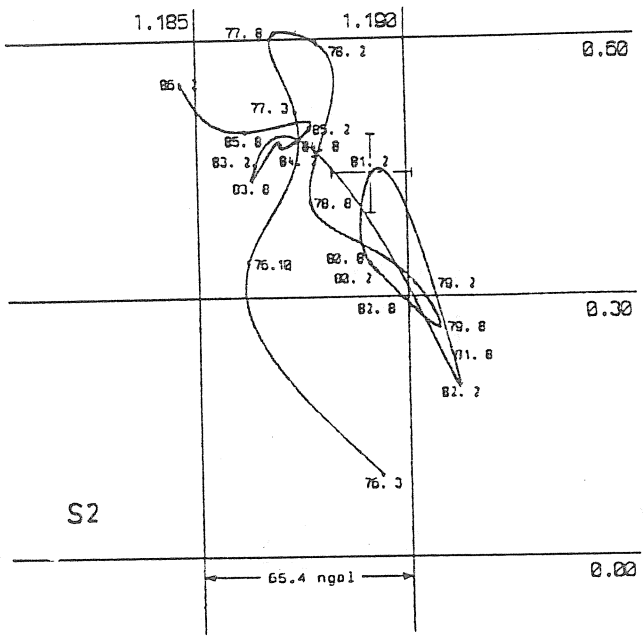
1.185
1.190
0.60
0.30
0.00
S2
65.4 ngal

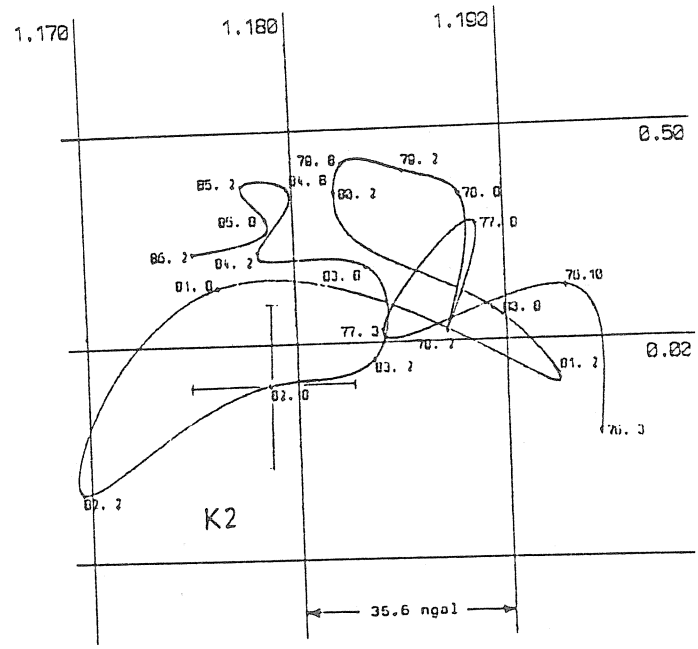
1.170
1.180
1.190
0.50
0.02
K2
35.6 ngal

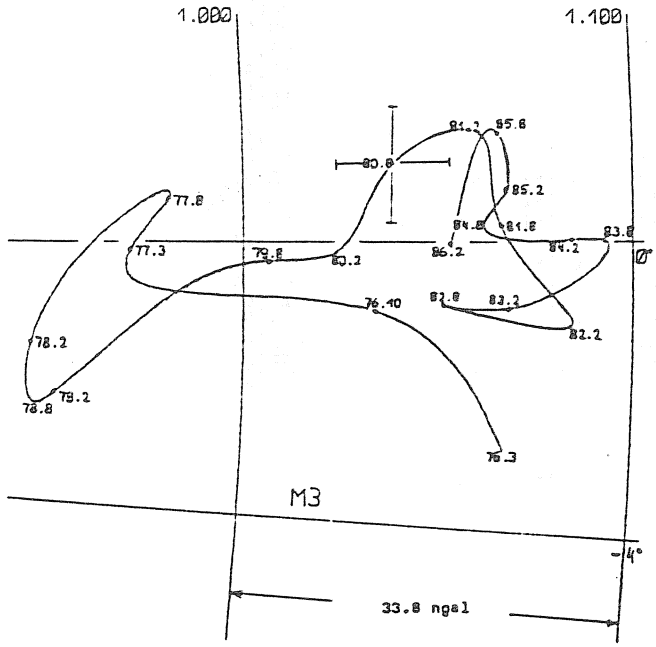
1.000
1.100
M3
33.8 ngal

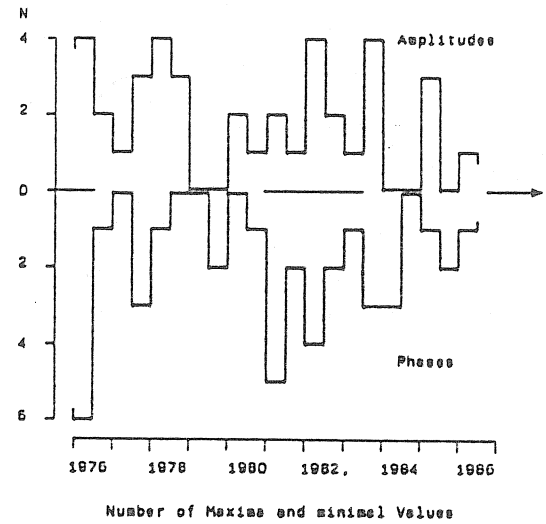
N
Amplitudes
Phases
1976
1978
1980
1982
1984
1986
Number of Maxima and minimal Values

WYROWNANIE KONCOWE - FINAL ADJUSTMENT ZENTRALINSTITUT FUER PHYSIK DER ERDE POTSDAM H.J. DITTFELD
CHOJNICKI METHOD

KONCOWE WYNIKI OBLICZEN - OCENA DOKLADNOSCI NA PODSTAWIE RESIDUUM
FINAL RESULTS OF COMPUTATIONS - ESTIMATION OF ACCURACY BASED ON RESIDUAL

0.0 1980 731 0 0 10001111 52,3809 +13,0676 82 0.0 981.261400

STATION POTSDAM 0764 VERTICAL COMPONENT GERMAN DEMOCR.REPUBLIC

ZENTRALINSTITUT FUER PHYSIK DER ERDE POTSDAM H.J. DITTFELD
GRAVIMETER ASKANIA GS-15 NO. 222 DIGITAL
ELECTROMAGNETIC CALIBRATION SENSITIVITY 0,0289 MKRGAL/DIGIT
INSTALLATION H.J. DITTFELD
MAINTENANCE H.J. DITTFELD, W. ALTMANN

LEAST SQUARE ANALYSIS IN CLASSICAL MANNER (CHOJNICKI)
FILTRATION OF OBSERVATIONS / FILTER 517 1438
POTENTIAL CARTWRIGHT-EDDEN-(DOODSON) / COMPLETE EXPANSION AND S3, M4, S4
COMPUTATION - ZENTRALINSTITUT FUER ASTROPHYSIK, K. ARLT-POTSDAM - COMPUTER ES 1040

74 3 22 0 - 74 4 13 21 / 74 4 18 0 - 74 6 19 21 / 74 6 25 0 - 74 7 13 21 / 74 7 19 0 - 74 11 4 21
74 11 12 0 - 74 12 14 21 / 75 6 22 0 - 75 10 27 21 / 75 11 5 0 - 76 1 6 21 / 76 1 12 0 - 76 9 17 21
76 9 22 0 - 76 11 1 21 / 76 12 2 0 - 78 5 4 21 / 78 5 10 0 - 81 2 9 22 / 81 2 14 21 - 81 5 9 4
81 5 15 13 - 82 2 14 4 / 82 2 26 0 - 86 10 29 4

TOTAL NUMBER OF DAYS 4604 103640 READINGS

ARGUMENT	WAVE GROUP N	SYMBOL	ESTIM. AMPL. VALUE	R.M.S.	AMPLITUDE VALUE	FACTOR R.M.S.	PHASE DIFFERENCE VALUE	R.M.S.	RESIDUALS AMPL.	PHASE	corrected phase lag
105,-11X.	14	SMQ1	0,14	0,00	1,14655	0,03769	-1,614	1.883	0,00	-113.5	-1,49
124,-125.	7	2Q1	0,78	0,01	1,16563	0,01149	2,213	0.565	0,03	54.1	+2,34
126,-129.	14	SIG1	0,87	0,01	1,15485	0,00949	-0,411	0.471	0,01	-172.4	-0,28
133,-135.	15	Q1	5,77	0,01	1,15030	0,00147	-0,375	0.073	0.06	-142.1	-0,24
136,-139.	15	RO1	1,04	0,01	1,14915	0,00769	-0,806	0.383	0,02	-124.3	-0,67
145,-146.	18	O1	29,72	0,01	1,15223	0,00027	-0,127	0.014	0.21	-162.1	+0,02
147,-149.	8	TAU1	0,52	0,01	1,16171	0,01828	0,539	0.901	0,00	81.8	+0,68
152,-155.	15	M1	3,20	0,01	1,14114	0,00296	-0,099	0.149	0,05	-174.0	+0,05
156,-158.	7	CHI1	0,45	0,01	1,14447	0,01797	-0,144	0.900	0,01	-169.6	+0,01
161,-162.	3	PI1	0,93	0,01	1,16656	0,00956	-0,079	0.470	0,01	-14.4	+0,07
163,-163.	7	P1	16,26	0,01	1,15143	0,00056	0,179	0.028	0,12	153.8	+0,33
164,-164.	3	S1	0,14	0,01	0,69155	0,03353	89,431	5.194	0,31	152.5	89,58
165,-165.	11	K1	44,15	0,01	1,15980	0,00019	0,007	0.010	0.80	179.6	+0,16
166,-166.	2	PSI1	0,39	0,01	1,17892	0,02352	-0,379	1.143	0,01	-22.5	-0,22
167,-168.	7	PHI1	0,71	0,01	1,19063	0,01305	3,147	0.628	0,04	66.1	+3,30
172,-173.	6	THE1	0,45	0,01	1,19758	0,01806	0,351	0.864	0,01	11.1	+0,51
174,-177.	16	J1	2,43	0,01	1,16070	0,00347	-0,538	0.171	0.02	-86.8	-0,38
181,-184.	8	SO1	0,56	0,01	1,15659	0,02179	2,535	1.079	0,02	95.2	+2,70
185,-186.	10	OO1	1,10	0,01	1,15846	0,00623	0,120	0.308	0.00	123.5	+0,26
191,-193.	19	NY1	0,17	0,00	1,16166	0,03209	-0,701	1,582	0,00	-83.5	-0,53
207,-22X.	21	EPS2	0,15	0,00	1,11292	0,01750	3,130	0.901	0.01	126.8	+3,41
233,-236.	10	2N2	0,87	0,00	1,16082	0,00543	1,650	0.268	0,02	89.6	+1,94
237,-23X.	10	MY2	0,95	0,00	1,16212	0,00452	2,233	0.223	0.04	86.6	+2,52
245,-246.	17	N2	6,59	0,00	1,17635	0,00071	1,643	0.035	0,21	64.9	+1,93
247,-248.	7	NY2	1,21	0,00	1,18455	0,00372	1,200	0.180	0.04	45.7	+1,49
252,-258.	26	M2	34,37	0,00	1,18491	0,00013	0,908	0.006	0.89	37.7	+1,20
262,-264.	5	LMB2	0,25	0,00	1,17127	0,01805	-0,425	0.883	0.00	-38.0	-0,12
265,-267.	12	L2	0,92	0,00	1,14958	0,00384	0,362	0.192	0,01	145.4	+0,66
271,-272.	2	T2	0,87	0,00	1,17937	0,00498	-0,466	0.242	0.02	-26.5	-0,16
273,-273.	4	S2	15,51	0,00	1,18775	0,00029	0,096	0.014	0.36	4.1	+0,40
274,-277.	12	K2	3,21	0,00	1,18216	0,00113	-0,138	0.055	0.06	-7.3	+0,17
282,-285.	15	ETA2	0,16	0,00	1,18919	0,01975	-1,006	0.952	0.00	-35.6	-0,69
292,-2X5.	14	2K2	0,04	0,00	1,12778	0,05818	3,589	2.956	0.00	116.1	+3,91
327,-375.	17	M3	0,48	0,00	1,02984	0,00662	-0,770	0.368	0.02	-159.8	-0,33
382,-382.	1	S3	0,02	0,00	0,17525	0,02242	-170,284	7.328	0,12	-178.6	-169,82
455,-455.	1	M4	0,01	0,00	0,11066	0,01868	83,373	9.670	0.01	83.4	83,96
491,-491.	1	S4	0,01	0,00	0,05950	0,01875	31,410	18.058	0.01	31.4	32,02

R.M.S.ERROR M-ZERO 0.6032 MIKRGAL

R.M.S.ERROR FOR BANDS D 1,7873 SD 0.8686 TD 0.5525 QD 0.4269

O1/K1 1.0109 1-O1/1-K1 1.0889 M2/O1 1.0280

REFERENCE EPOCH 1980 7 31 0,0 JULIAN DATE 2444451.50

Table 1: Final result of the series - standard resolution

```
STROJNAPIS KONCOWE - FINAL ADJUSTMENT                                   ANALYTICAL METHOD

KONCOWE WYNIKI OBLICZEN - OCENA DOKLADNOSCI NA PODSTAWIE RESIDUOW
FINAL RESULTS OF COMPUTATIONS - ESTIMATION OF ACCURACY BASED ON RESIDUAL

0.0   1980 731 0 0  10001111  52.3800 -11.0670   87   0.0              981.201400

STATION POTSDAM 0764          VERTICAL COMPONENT          GERMAN DEMOCR.REPUBLIC

ZENTRALINSTITUT FUER PHYSIK DER ERDE POTSDAM  H.J. DITTFELD
GRAVIMETER ASKANIA GS-15 NO. 222 DIGITAL
ELECTROMAGNETIC CALIBRATION:        SENSITIVITY 0.0289 MKRGAL/DIGIT
INSTALLATION  H.J. DITTFELD
MAINTENANCE   H.J. DITTFELD, W. ALTMANN

LEAST SQUARE ANALYSIS IN CLASSICAL MANNER (CHOJNICKI)
FILTRATION OF OBSERVATIONS / FILTER  S1/ 1438
POTENTIAL CARTWRIGHT-EDDEN-(DOODSON)       / COMPLETE EXPANSION AND S3, S4, S4
COMPUTATION - ZENTRALINSTITUT FUER ASTROPHYSIK, K, ABLT-POTSDAM - COMPUTER ES 1040

 74  3 22  0 - 74  4 15 21 / 74  4 18  0 - 74  6 19 21 / 74  6 25  0 - 74  7 15 21 / 74  7 19  0 - 74 11  4 21
 74 11 12  0 - 74 12 14 21 / 75  6 22  0 - 75 10 27 21 / 75 11  5  0 - 76  1  6 21 / 76  1 12  0 - 76  9 17 21
 76  9 22  0 - 76 11  1 21 / 76 12  2  0 - 78  5  4 21 / 78  5 10  0 - 81  2  9 22 / 81  2 14 21 - 81  5  6  4
 81  5 15 13 - 82  2 14  4 / 82  2 26  0 - 86 10 29  4

TOTAL NUMBER OF DAYS   4004        105640  READINGS
```

WAVE GROUP ARGUMENT	N	SYMBOL	ESTIM.AMPL. VALUE	R.M.S.	AMPLITUDE FACTOR VALUE	R.M.S.	PHASE DIFFERENCE VALUE	R.M.S.	RESIDUALS AMPL.	PHASE	corrected phase lag
105.-109.	3	130	0,02	0,00	0,65718	0,21423	0.106	13.009	0.00	170.6	+0,23
113.-115.	3	134	0,10	0,01	1,24282	0,10716	-1.800	4.940	0.01	-25.4	-1,67
116.-11X.	8	SMQ1	0,19	0,01	1,14127	0,04052	-1.038	2.034	0.01	-120.6	-1,51
124.-125.	7	2Q1	0,78	0,01	1,16583	0,01145	2.222	0.563	0.03	83.9	+2,35
126.-127.	8	SIG1	0,94	0,01	1,15467	0,00947	-0.419	0.470	0.01	-121.5	-0,29
128.-129.	6	159	0,07	0,01	1,04750	0,12878	3.651	7.018	0.01	140.9	+3,78
133.-134.	4	167	0,06	0,01	1,13257	0,16261	-4.036	8.227	0.00	-110.8	-3,90
135.-135.	11	M1	5,72	0,01	1,15026	0,00147	-0.376	0.073	0.06	-142.2	-0,24
136.-136.	5	183	0,06	0,01	0,67565	0,13358	-7.320	7.849	0.01	-147.2	-7,18
137.-137.	6	RO1	1,00	0,01	1,14949	0,00767	-0.809	0.382	0.02	-123.4	-0,67
138.-139.	4	191	0,03	0,00	0,99059	0,16156	-11.675	9.260	0.01	-131.9	-11,48
143.-144.	6	198	0,20	0,01	1,25573	0,06074	-1.920	2.816	0.01	-28.9	-1,78
145.-145.	10	O1	29,67	0,01	1,15220	0,00027	-0.127	0.014	0.21	-162.1	+0,02
146.-146.	2	211	0,08	0,01	0,99418	0,09351	-3.837	5.549	0.01	-156.4	-3,70
147.-149.	8	TAU1	0,52	0,01	1,16067	0,01873	0.572	0.980	0.01	87.4	+0,72
152.-154.	5	222	0,20	0,01	1,19181	0,03691	-0.299	1.774	0.01	-11.1	-0,15
155.-155.	10	P1	3,35	0,01	1,14075	0,00296	-0.100	0.164	0.06	-174.1	+0,05
156.-158.	7	CHI1	0,45	0,01	1,14479	0,01792	-0.140	0.897	0.01	-166.0	-0,04
161.-161.	1	242	0,04	0,01	1,23925	0,23347	-30.119	10.704	0.02	-98.1	-29,97
162.-162.	2	PI1	0,96	0,01	1,16569	0,00953	-0.059	0.466	0.00	-12.2	0,09
163.-163.	7	P1	16,20	0,01	1,15153	0,00050	0.179	0.028	0.12	153.9	+0,33
164.-164.	3	S1	0,14	0,01	0,60125	0,03342	89.450	3.145	0.31	152.5	89,60
165.-165.	11	K1	44,15	0,01	1,13980	0,00019	0.007	0.010	0.00	170.6	0,16
166.-166.	2	PSI1	0,39	0,01	1,17035	0,02344	-0.363	1.139	0.01	-21.2	-0,21
167.-167.	6	PHI1	0,74	0,01	1,19165	0,01302	3.140	0.638	0.04	85.5	+3,30
168.-168.	1	274	0,03	0,01	0,66567	0,22368	-5.584	15.274	0.01	-154.8	-5,43
172.-173.	6	TPE1	0,45	0,01	1,19760	0,01799	0.540	0.881	0.01	10.7	+0,00
174.-177.	16	J1	2,43	0,01	1,16068	0,00345	-0.339	0.170	0.02	-82.9	-0,30
181.-184.	8	SOI1	0,56	0,01	1,13665	0,02191	2.533	1.076	0.02	95.4	+2,70
185.-186.	10	OOI1	1,10	0,01	1,13852	0,00621	0.122	0.307	0.00	122.1	+0,29
191.-193.	8	317	0,09	0,01	1,24825	0,10007	0.990	4.806	0.21	13.8	+1,10
195.-195.	6	NY1	0,19	0,01	1,16210	0,03410	-0.689	1.681	0.00	-42.2	-0,52
1X3.-1X3.	2	329	0,02	0,01	0,64384	0,21577	-4.820	14.650	0.01	-167.5	-4,65
1X5.-1X5.	3	331	0,02	0,00	1,09030	0,25366	-8.632	13.214	0.00	-113.9	-8,46
207.-21X.	8	336	0,02	0,00	1,07257	0,09846	3.164	5.260	0.00	140.4	+3,44
225.-226.	5	342	0,10	0,00	1,15023	0,04748	3.684	2.347	0.01	92.5	+3,96
227.-228.	5	EPS2	0,22	0,00	1,10841	0,01885	2.999	0.974	0.02	132.5	+3,28
229.-22X.	3	353	0,04	0,00	1,07650	0,09651	3.999	5.134	0.00	138.8	+4,28
233.-236.	16	2N2	0,87	0,00	1,16056	0,00531	1.057	0.262	0.03	90.1	+1,94
237.-237.	4	MY2	1,03	0,00	1,16257	0,00443	2.225	0.218	0.04	88.2	+2,51
230.-234.	8	371	0,09	0,00	1,12755	0,06085	0.938	3.082	0.00	150.6	+1,22
243.-244.	4	378	0,07	0,00	1,14078	0,07754	0.330	3.804	0.00	147.4	+0,62
245.-245.	9	N2	6,59	0,00	1,17639	0,00069	1.042	0.034	0.21	66.9	+1,93
246.-246.	4	391	0,08	0,00	1,19544	0,06361	3.369	3.044	0.00	62.3	+3,36
247.-247.	5	MY2	1,26	0,00	1,18466	0,00364	1.202	0.176	0.04	45.6	+1,49
248.-248.	2	398	0,05	0,00	1,04161	0,07837	-0.775	4.311	0.01	-173.2	-0,48
252.-253.	5	GAM2	0,10	0,00	1,23025	0,04320	4.688	2.012	0.01	52.6	+4,38
254.-254.	3	ALF2	0,13	0,00	1,28567	0,03823	-10.148	1.796	0.02	-65.1	-9,85
255.-255.	10	M2	56,30	0,00	1,18449	0,00013	0.912	0.010	0.64	57.9	+1,21
256.-256.	2	BET2	0,11	0,00	1,21427	0,04316	17.541	2.035	0.03	90.3	17,84
257.-258.	6	DLT2	0,03	0,00	1,18041	0,07813	6.876	3.742	0.00	80.8	+5,12
262.-264.	5	LMB2	0,25	0,00	1,17214	0,01766	-0.450	0.863	0.00	-37.9	-0,16
265.-265.	9	L2	0,89	0,00	1,14046	0,00376	0.366	0.147	0.01	145.4	+0,07
267.-267.	3	439	0,03	0,00	1,12664	0,10139	-5.734	5.155	0.00	-115.9	-5,43
271.-271.	1	2T2	0,04	0,00	1,24468	0,11929	-0.633	5.640	0.00	-9.2	-0,33
272.-272.	1	T2	0,90	0,00	1,17035	0,00487	-0.488	0.257	0.02	-77.0	-0,18
273.-273.	6	S2	15,51	0,00	1,14779	0,00029	0.003	0.014	0.56	4.0	+0,40
274.-274.	5	R2	0,16	0,00	1,16764	0,02754	5.776	1.351	0.01	88.6	+5,50
275.-277.	9	K2	3,35	0,00	1,14758	0,00110	-0.138	0.053	0.66	-7.3	+0,17
282.-283.	7	KSI2	0,03	0,00	1,16674	0,10137	0.086	5.155	0.00	177.1	+0,40
285.-285.	8	ETA2	0,18	0,00	1,19066	0,01960	-1.030	0.963	0.01	-34.9	-0,72
292.-293.	4	476	0,03	0,00	1,21687	0,12302	9.427	6.475	0.01	66.3	+9,74
2X5.-2X5.	16	2K2	0,05	0,00	1,04061	0,06441	1.517	3.577	0.01	167.7	+1,64
327.-347.	6	M3	0,11	0,00	1,66066	0,02519	-3.612	1.551	0.01	-97.3	-3,17
353.-365.	7	M3	0,35	0,00	1,02910	0,00691	-0.542	0.345	0.01	-164.3	-0,10
375.-375.	6	K3	0,03	0,00	1,05704	0,05290	-0.978	2.871	0.00	-171.4	-0,48
382.-382.	1	S3	0,02	0,00	0,17536	0,07240	-170.543	7.320	0.12	-178.6	-169,88
455.-455.	1	M4	0,01	0,00	0,11062	0,01868	83.353	9.676	0.01	83.4	83,94
491.-491.	1	S4	0,01	0,00	0,05040	0,01876	31.472	18.005	0.01	31.5	32,08

```
R.M.S.ERROR M-ZERO      0.0014   MICROGAL

R.M.S.ERROR FOR BANDS                  D  1.7812    SD  0.8494    TD  0.5522
                                                                   GD  0.4270

SIGMA    1.0150          1-SIGMA-K1    1.0087          +/-01       1.0203

REFERENCE EPOCH    1980  7 31  0.0        JULIAN DATE  2444451.5
```

Table 2: Final result of the series - maximum resolution
69 wave groups

On the parameters of the nearly monthly modulation of the gravimetric M2-wave

SCHWAHN, W.*; ELSTNER, C.*; SAVIN, I.V.**

Abstract

The modulation of the M2 gravity tide with a nearly monthly period is investigated. An amplitude as well as a phase modulation are considered.

It may be shown by a demodulation procedure that a quasi-persistent modulation wave exists, which exhibits also sudden changes in amplitude and phase.

Using the tidal parameters of M2 and the FOURIER coefficients (both in amplitude and phase) of the residuals, the mean parameters of the temporal behaviour in the years 1982-1986 are presented.

The following values were obtained

period	27.14 ... 27.23 days	
most probable period	27.18 ... 27.19 days	
modulation factor	0.002 (Brussels)	0.003 (Potsdam)
modulation amplitude	60 ngal	80 ngal
phase deviation	0.128°	0.017°
phase amplitude	76 ngal	10 ngal.

Zusammenfassung

Es wird die Modulation der M2-Tide der Schwere mit einer nahezu monatlichen Periode untersucht. Es werden sowohl die Amplituden- als auch die Phasenmodulation betrachtet.

Es kann durch eine Demodulationsmethode gezeigt werden, daß eine quasi-persistente Modulation vorhanden ist, die aber auch plötzliche Änderungen in Amplitude und Phase ausweist.

Unter Verwendung der Gezeitenparameter für M2 und der FOURIER-Koeffizienten (sowohl für Amplitude als auch Phase) der Residuen kann ein Mittelwert für das zeitliche Verhalten in den Jahren 1982-1986 angegeben werden.

---

*) ELSTNER, C., Dr.; SCHWAHN, W., Dr.; Central Institute for Physics of the Earth, Potsdam, GDR.

**) SAVIN, I.V., Dr.; Institute of Physics of the Earth, Academy of Sciences of the USSR, Moscow, USSR.

Die Parameter sind folgende

Periode	27.14 ... 27.23 Tage		
wahrscheinlichste Periode	27.18 ... 27.19 Tage		
Modulationsfaktor	0.002 (Brüssel)	bzw.	0.003 (Potsdam)
Modulationsamplitude	60 nGal "	bzw.	80 nGal "
Phasenhub	0.128°(Brüssel)	bzw.	0.017°(Potsdam)
Phasenamplitude	76 nGal "	bzw.	10 nGal "

Introduction

In a first paper (SCHWAHN, ELSTNER, SAVIN (1989)) on the phenomenon of the modulation of the gravimetric M2-tide the following facts were obtained with respect to the nearly monthly modulation period

- amplitude in the order of 45...50 ngal
  (=0.045...0.050 µgal = 45...50 x E-11 ms^{-2})
- frequencies at 0.078978 and 0.082044

both for the stations Brussels and Potsdam. Fig.1 and fig. 2 represents again the spectral distribution of the residuals in the neighbourhood of the M2-wave. Significant lines occure.

As we take it this is the spectral representation of a modulation of the M2-wave ($\omega_o = 2\pi \times 0.0805\ 114$ [h^{-1}]). The main argument for this conception is the symmetric structure of the lines related to the M2-frequency and their nearly equal amplitudes for equal frequency distances.

Under the assumption of a periodic modulation the appropriate formula yields

$$(1)\quad y(t) = (A_o + A_1 \cos(\omega_1 t + \varphi_1)) \cos(\omega_o t + \varphi_o + \varepsilon \cos(\omega_1 t + \varphi_2))$$

with the angular frequencies ω_o for the carrier and ω_1 for the modulation and $\varphi_o, \varphi_1, \varphi_2$ as the phase angles. The formula expresses both an amplitude (parameters A_1, ω_1; $\varrho = A_1/A_o$ modulation factor) as well as a phase modulation (parameters ε, φ_2; ε phase deviation).

In the above mentioned paper (SCHWAHN, ELSTNER, SAVIN (1989)) we considered among others the pair of lines in a distance $\omega_1 = 2\pi \times 0.0015333$ [h^{-1}], i.e. for the modulation period of 27.18 days. The lines are situated in the N2- and L2-regions respectively.

In a first working hypothesis they were allocated to the harmonics 245.545 and 265.565 in the harmonic development of the third order terms. But a small delay was obtained and therefore we have concluded that these waves are not included in the set of tidal harmonics.

In this paper we undertake the attempt to describe in detail the characteristics of this probably non-tidal contributions.

1. The time domain

To obtain a more detailed insight in the character (periodic? aperiodic?, constant or time varying amplitude?) of the modulation we looked for their representation in the time domain. Using the expression (1) we get the following equations

$$(2)\quad y(t) = A_o(1+\rho\cos(\omega_1 t+\varphi_1)*$$
$$*(\cos(\omega_o t+\varphi_o)\cos(\varepsilon\cos(\omega_1 t+\varphi_2)-$$
$$-\sin(\omega_o t+\varphi_o)\sin(\varepsilon\cos(\omega_1 t+\varphi_2)).$$

In the case ρ , $\varepsilon \ll 1$ we neglect the higher terms in the sin- and cos- series and term with the product $\rho * \varepsilon$:

$$(3)\quad y(t) = A_o(1+\rho\cos(\omega_1 t+\varphi_1)*$$
$$*(\cos(\omega_o t+\varphi_o) - \sin(\omega_o t+\varphi_o)\varepsilon\cos(\omega_1 t+\varphi_2))$$
$$= A_o\cos(\omega_o t+\varphi_o)+$$
$$+A_o\rho\cos(\omega_1 t+\varphi_1)\cos(\omega_o t+\varphi_o)$$
$$-A_o\varepsilon\sin(\omega_o t+\varphi_o)\cos(\omega_1 t+\varphi_2).$$

We consider the residuals $y_R(t)$, i.e. the term $A_o\cos(\omega_o t+\varphi_o)$ was extracted by the adjustment

$$(4)\quad y_R(t) = y(t)-A_o\cos(\omega_o t+\varphi_o)$$
$$= A_o\rho\cos(\omega_1 t+\varphi_1)\cos(\omega_o t+\varphi_o)$$
$$-A_o\varepsilon\sin(\omega_o t+\varphi_o)\cos(\omega_1 t+\varphi_2).$$

The first term represents the amplitude modulation, the second one the phase modulation.

Multiplying $y_R(t)$ by $\cos\omega_o t$ or $\sin\omega_o t$ we obtain new series $y^{DC}{}_R(t)$ and $y^{DS}{}_R(t)$ respectively, for instance

$$(5)\quad y^{DC}{}_R(t) = (A_o\rho\cos(\omega_1 t+\varphi_1)\cos(\omega_o t+\varphi_o)$$
$$-A_o\varepsilon\sin(\omega_o t+\varphi_o)\cos(\omega_1 t+\varphi_2))\cos\omega_o t$$
$$= A_o\rho\cos(\omega_1 t+\varphi_1)(\cos\varphi_o\cos\omega_o t-\sin\varphi_o\sin\omega_o t)\cos\omega_o t$$
$$-A_o\varepsilon(\sin\omega_o t\cos\varphi_o+\cos\omega_o t\sin\varphi_o)\cos(\omega_1 t+\varphi_2)\cos\omega_o t.$$

Now we use the addition theorems

$$(6)\quad \cos\omega_o t\cos\omega_o t = 1/2(\cos(o)+\cos(2\omega_o t))$$
$$\sin\omega_o t\cos\omega_o t = 1/2(\sin(o)+\sin(2\omega_o t))$$

and so, after a low-pass-filtering suppressing the constituents $2\omega_o$ we obtain the time series

$$(7)\quad y^{DC}_{RF}(t) = A_o\rho/2\cos(\omega_1 t+\varphi_1)\cos\varphi_o - A_o\varepsilon/2\cos(\omega_1 t+\varphi_2)\sin\varphi_o$$

$$= A_1/2\cos(\omega_1 t+\varphi_1)\cos\varphi_o - A_o\varepsilon/2\cos(\omega_1 t+\varphi_2)\sin\varphi_o$$

and by adequate considerations,

$$(8)\quad y^{DS}_{RF}(t) = -A_o\rho/2\cos(\omega_1 t+\varphi_1)\sin\varphi_o - A_o\varepsilon/2\cos(\omega_1 t+\varphi_2)\cos\varphi_o.$$

$$= -A_1/2\cos(\omega_1 t+\varphi_1)\sin\varphi_o - A_o\varepsilon/2\cos(\omega_1 t+\varphi_2)\sin\varphi_o.$$

It means that after the multiplication and low-pass-filtering the time series y^{DS}_{RF}, y^{DC}_{RF} represents only the modulation function, the socalled "envelope" of the carrier frequency, (ANDEL (1984), SAVIN (1985, 1987) with the angular frequency ω_1 and their half amplitude A_1 and the half of the product of the phase deviation ε with the carrier amplitude A_o.

In the figure 3 the graphs of the time series y^{DC}_{RF} and y^{DS}_{RF} are represented for Brussels June 1982-October 1986 and for Frankfort/M. August 1981-April 1984.

It can be seen very clearly
- there is no persistent, constant periodic function
- in some time intervals a well-shaped sinusoid with a period of nearly 28 days appears (see, for instance, the time section winter 85 - spring 86 in the y^{DS}_{RF} for Brussels or the last half-year 1983 both y^{DS}_{RF} as well as y^{DC}_{RF} for Frankfort
- in some time intervals a sudden change in the course of the time series occurs
- especially in the y^{DC}_{RF} a stronger stochastic contribution is present.

From this we may conclude that here a nontidal, quasi-persistent wave exists. Because of the y^{DS}_{RF} component is predominant, a polarization ellipse with the major axis in the y^{DS}_{RF}-direction should be expected. As we know from the electrotechnics a polarization ellipse is the realization of an amplitude and phase modulation.

2. Spectral domain and the modulation parameter

To obtain the spectral representation of $y_R(t)$ we use equation (4). Using again addition theorems and the relation

$$\cos((\omega_1-\omega_o)t + \varphi_1-\varphi_o) = \cos((\omega_o-\omega_1)t - \varphi_1+\varphi_o)$$

the following equation yields

$$(9)\quad y_R(t) = A_o/2(\rho(\cos((\omega_o-\omega_1)t - \varphi_1+\varphi_o) +$$

$$+ \cos((\omega_o+\omega_1)t + \varphi_1+\varphi_o)$$

$$- \varepsilon(\sin((\omega_o-\omega_1)t + \varphi_o-\varphi_2) +$$

$$+ \sin((\omega_o+\omega_1)t + \varphi_o+\varphi_2)).$$

The arguments $\omega_o - \omega_1$ and $\omega_o + \omega_1$ show that the modulation yields two spectral lines in the distance ω_1 from the carrier frequency ω_o. Both the amplitude as well as the phase modulation for ϱ, $\varepsilon \ll 1$ contribute to the same spectral lines. For the equal phases φ_1 and φ_2 the contributions from the amplitude- and the phase modulation are related by the phase delay of $\pi/2$.

Further application of addition theorems and the grouping of the sin- and cos- terms for each of the frequencies $A = \omega_o + \omega_1$ and $B = \omega_o - \omega_1$ we obtain the components of the amplitude vector R and the phase angle ψ for the frequencies A and B

$$
\begin{aligned}
R_A \cos \psi_A &= A_o/2\,(\varrho \cos(\varphi_1 + \varphi_o) - \varepsilon \sin(\varphi_2 + \varphi_o)) \\
R_A \sin \psi_A &= A_o/2\,(\varrho \sin(\varphi_1 + \varphi_o) + \varepsilon \cos(\varphi_2 + \varphi_o)) \\
R_B \cos \psi_B &= A_o/2\,(\varrho \cos(\varphi_1 - \varphi_o) + \varepsilon \sin(\varphi_2 - \varphi_o)) \\
R_B \sin \psi_B &= A_o/2\,(-\varrho \sin(\varphi_1 - \varphi_o) + \varepsilon \cos(\varphi_2 - \varphi_o)).
\end{aligned} \tag{10}
$$

From the equations (10) four linear equations may be derived to determine the values for A_1, ε, φ_1 and φ_2.

$$
\begin{aligned}
A_1 &= (R_B^2 + R_A^2 + 2R_B R_A \cos(\psi_A + \psi_B - 2\varphi_o))^{1/2} \\
\varepsilon &= (R_B^2 + R_A^2 - 2R_B R_A \cos(\psi_A + \psi_B - 2\varphi_o))^{1/2}
\end{aligned}
$$

$$
\tan \varphi_1 = \frac{R_A \sin(\psi_A - \varphi_o) - R_B \sin(\psi_B - \varphi_o)}{R_A \cos(\psi_A - \varphi_o) + R_B \cos(\psi_B - \varphi_o)} \tag{11}
$$

$$
\tan \varphi_2 = \frac{R_B \cos(\psi_B - \varphi_o) - R_A \cos(\psi_A - \varphi_o)}{R_A \sin(\psi_A - \varphi_o) - R_B \sin(\psi_B - \varphi_o)}
$$

The equations in (11) give the transformation between the parameters R_A, R_B, ψ_A, ψ_B (amplitudes and phases) of the FOURIER-representation of $y_R(t)$ and the parameters of the amplitude (ϱ resp. A_1 and φ_1) and the phase (ε, φ_2) modulation.

Using equation (11) the modulation parameters for the nearly monthly modulation were determined. On the basis of the least squares adjustment of y(t) (CHOJNICKI-method, version A15K) we obtained the values A_o and φ_T, $\varkappa$ for the carrier M2 and by the FOURIER-analysis of $y_R(t)$ these of R_A, R_B, ψ_A, ψ_B. In Table 1 the results are given.

Table 1. The parameters for the nearly monthly modulation of the M2-wave
($\omega_1 \approx 2\pi$ *1.532 426 E-03 cph)
($\omega_{M2} = \omega_o = 2\pi$ *0.082 05114 cph)

	Brussels t_o = 1982 060301 UT	Potsdam t_o = 1982 022601 UT
Adjustment		
A_o	34 980 ngal	32 700 ngal
$\varphi_o = \varphi_T + \varkappa$	310.3 °	171.12 °
FOURIER-analysis		
R_A	48 ngal	35 ngal
R_B	50 ngal	45 ngal
ψ_A	317.5 °	321.6 °
ψ_B	45.4 °	21.9 °
Modulation		
A_1	61.44 ngal	79.99 ngal
$A_o \varepsilon$	76.38 ngal	10.03 ngal
ε	0.128 °	0.017 °
φ_1	301.9 °	326.61 °
φ_2	68.2 °	348.33 °

3. First consideration on the most probable freguencies

In chapter 2 we have discussed the parameters of the modulation, in chapter 3 the period (frequency) should be treated. It means as we see in equation (9), we must determine as accurate as possible the frequencies $A = \omega_o + \omega_1$ and $B = \omega_o - \omega_1$.

Here we used
- the high-resolution power spectral analysis on the basis of demodulation, low-pass-filtering and decimation, followed by the maximum-entropy method (SAVIN (1985, 1987)).
- the FOURIER-analysis.

In fig. 4 the power spectra for the stations Frankfort/Main, Brussels and Potsdam are compiled. To obtain a maximum sensitivity of the method, the parameters for Brussels and Potsdam were k = 240 (48*5, two-fold demodulation), m = 40 (order of the autoregressive model), whereas for Frankfort k = 96, m = 40 were used and therefore a more smoothed estimation was obtained. As we take it the line is significant, if its value exceeds the surrounding in the order of 20 ...30 dB, i.e. ten times the noise in the very near region.

The position of the maxima in the fig. 4 may be given in the order of 0.1 mm. Therefore the accuracy of the data for the position is +-2 E-06 in frequency or +-3 E-04 in the period. We obtained the maximum for

Frankfort	May 1981 - April 1984
Brussels	June 1982 - Oct. 1986
Potsdam	Febr.1982 - Oct. 1986

in the N2-region

Frankfort	0.078 992 cph	+- 2 E-06
Brussels	0.078 978 "	+- 2 E-06
Potsdam	0.078 979 "	+- 2 E-06

and in the L2-region

Frankfort	0.082 038 cph	+- 2 E-06
Brussels	0.082 043 "	+- 2 E-06
Potsdam	0.082 043 "	+- 2 E-06.

Using for the deviation 2 E-06 the combination (-) in the N2 region, (+) in the L2 region and vice versa we obtain a realistic estimate for the nearly monthly modulation

$$\omega_1 = 2\pi * (1.53018 \ldots 1.53412 \text{ E-03 cph})$$
$$T_1 = 27.16 \ldots 27.23 \text{ days.}$$

An independent estimation of the modulation frequency was obtained not on the basis the absolute position, but from the readings of the difference

$$\omega_1 = 1/2(A-B) = 1/2(\omega_o + \omega_1 - (\omega_o - \omega_1)).$$

The disadvantage is the large sensitivity with respect to the uncertainty at the scale factor of the figures. The values are (the value in the centre is the most probable value)

Frankfort	27.35 ... 27.39 ... 27.45	days
Brussels	27.14 ... 27.187 .. 27.21	"
Potsdam	27.14 ... 27.199 .. 27.21	".

Concerning the FOURIER-analysis, we refined the results, which are represented in fig. 1 and 2, by further computations in the region of the maxima. The aim was to find out the sharp absolute maximum. But the FOURIER-analysis showed "plateaus" characterized by the corner frequencies

	N2-region		L2-region	
Brussels	0.078 97834	0.078 98270	0.082 04119	0.082 04724
Potsdam	0.078 97958	0.078 98208	0.082 04119	0.082 04522

It should be proofed whether these plateaus are the effect of the leakage phenomenon due to the finite data lengths.

Using the pair of the "outer" (with respect to ω_o) corner frequencies and the pair of the "inner" corner frequencies we obtain the estimates for the modulation period

Brussels	27.154 ... 27.247 days
Potsdam	27.183 ... 27.241 days.

The draconic month (27.21 days) is in the range of these data. From all these estimations we can conclude, that the term $2\tau + -(s-N)$, i.e. the constituents with the DOODSON-numbers (245.545) and (265.565) can be included in the considerations on the source mechanisms for the above noted lines. In so far we must revise our previous statement (SCHWAHN, ELSTNER, SAVIN (1989)) basing on the knowledge of the "outer" corners only.

Concluding remark

For the derivation of equation (3) from equation (2) we considered very small ϱ ($< 10^{-3}$) and ε ($< 10^{-2}$). In other cases the term $\cos(\omega_o t...)$ can be written in the form

$$\cos(\omega_o t + \varphi_o + \varepsilon \cos(\omega_1 t + \varphi_2))$$

$$= \mathrm{Re}\left\{ e^{i\omega_o t}\, e^{i\varphi_0}\, e^{i\varepsilon \cos(\omega_1 t + \varphi_2)} \right\}$$

The last factor $\exp(i\varepsilon\cos(\omega_1 t + \varphi_2))$ can be expanded in series of BESSEL-functions of the first kind with the parameter $n*\omega_1$, $n = 1,2,...$ (WOSCHNI (1960)). The case $n = 1$ gives spectral lines, which we have considered. For $n = 2$ we should expect spectral lines in the distance $+-2\omega_1$ from ω_o, i.e. in the region of 2N2 and K2 for M2 and a nearly fortnightly period. The FOURIER-spectrum for Brussels (fig.2) exhibits indeed such significant lines above the noise level. For Potsdam we can remark the same result for the whole observation period 1974-1984 (see ASCH et al. (1986)).

But this explanation by larger phase modulation and $n = 2$ is a suggestion only with the respect to the position of the frequencies. An independent physical phenomenon with a modulation period in the order $T_2 = 2\pi(2\omega_1)^{-1}$ of $13.56 < T_2 < 13.60$ days should be taken into account also. The relation of the amplitudes in the regions of N2 and 2N2 and L2 and K2 respectively support this existence of an independent physical source, because the first estimation for $n = 2$ gives a complete different value. To differentiate the two cases further detailed considerations on the quantitative estimation of the amplitudes are needed.

Aknowledgement

We are much obliged to the colleagues Dr. DITTFELD (Potsdam), Dr. DUCARME (Brussels) and Dr. RICHTER (Frankfort/Main) to make available their gravimetric data series.

References

ANDEL, J.: Statistische Analyse von Zeitreihen. Berlin, Akademie Verlag 1984, 276 S..

ASCH, G.; C. ELSTNER; G. JENTZSCH; H.-P. PLAG (1986): On the estimation of significant periodic and aperiodic gravity variations in the time series of neighbouring stations - part I: Tidal signals. Proc. 10th Internat. Symp. Earth Tides, Sept. 23-27, 2985, Madrid (1986), 239-249.

SAVIN, I.V. (1985,1987): Analyse spectrale a bande etroite des observations de marees (Narrow-band analysis of tide observations).Marees Terr. BIM, Bruxelles (1987)100, 6987-7002, Vychislit. Seismolog., Moskva (1985)18, 217-228.

SCHWAHN, W.; C. ELSTNER; I.V. SAVIN (1989): On the modulation of the M2 gravity tide. Proc. 6th Internat. Symp. "Geodesy and Physics of the Earth", Potsdam Aug. 22-26, 1988, Veröff. Zentralinst. Physik Erde, Potsdam (1989)102 (in press).

List of figure captions

Fig. 1 Amplitude spectrum of the gravimetric residuals at Potsdam 1982-1986. The sharp spikes in the regions of the L2 and N2 tidal groups are caused predominantly by an amplitude modulation (80 ngal) of the M2-tide with a period of 27.183 ... 27.241 days.

Fig. 2 Amplitude spectrum of the gravimetric residuals at Brussels 1982-1986. Here the sharp spikes in the regions of the L2 and N2 tidal groups are caused by as well an amplitude (60 ngal) as a phase (75 ngal) modulation of the M2-tide with a period of 27.154 ... 27.247 days.

Fig. 3 The time series $y^{DS}_{RF}(t)$ and $y^{DC}_{RF}(t)$ after the demodulation by $\sin \omega_o t$ resp. $\cos \omega_o t$, filtering and decimation of the gravimetric time series y(t) for the stations Frankfort/M. and Brussels. Note the different sequence of y^{DS}_{RF} and y^{DC}_{RF} for both the stations.

Fig. 4 Power spectra following the maximum entropy method for the time series $y^{DS}_{RF}(t)$ and $y^{DC}_{RF}(t)$ (fig.3) for Frankfort/M., Brussels and Potsdam. Note the slight delay of the maxima for Frankfurt/M., probably due to the shift in the time interval under consideration.

Contribution No. 1767 of the Central Institute for Physics of the Earth, Potsdam

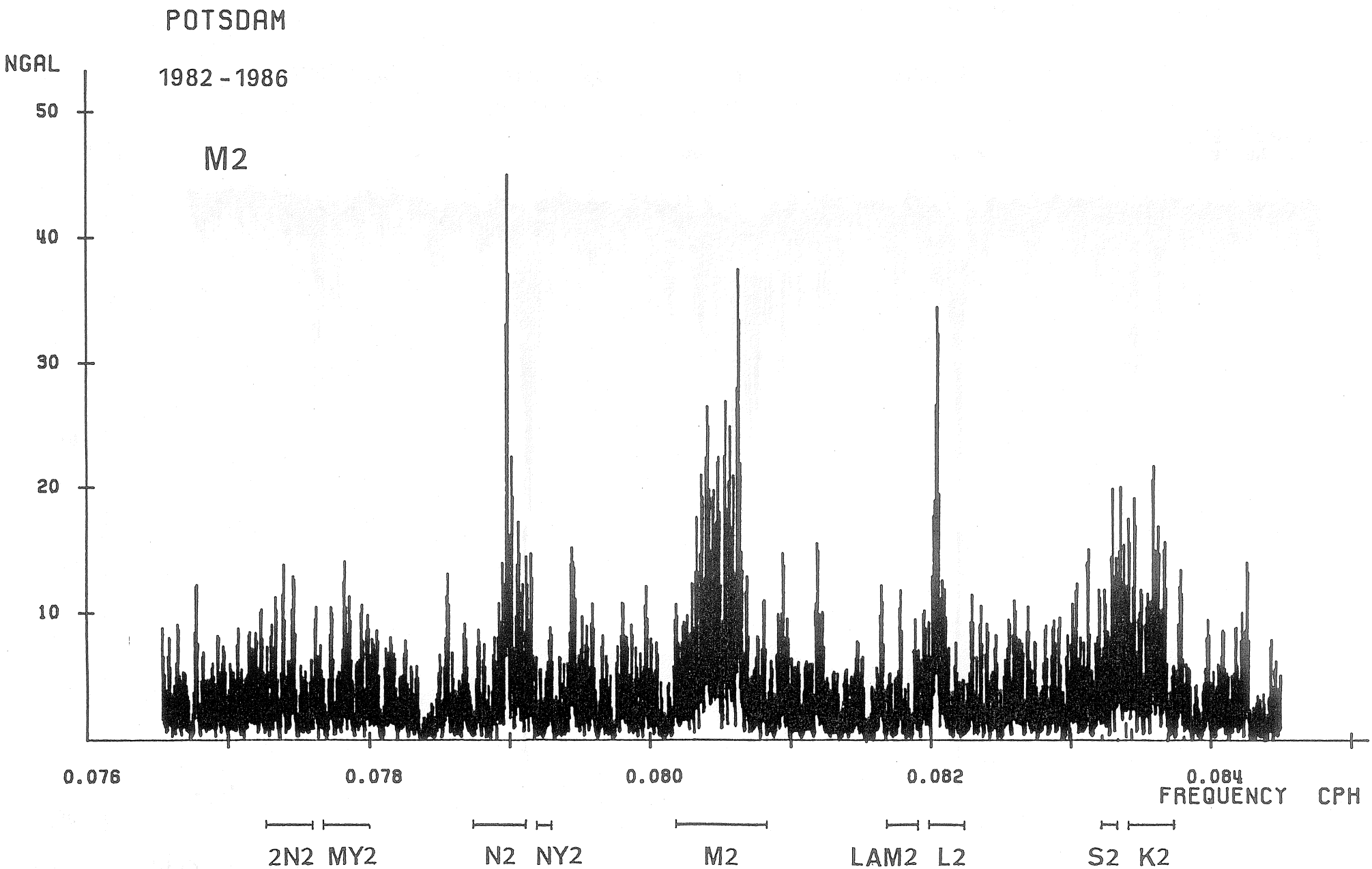
POTSDAM
1982 - 1986
M2
NGAL
50
40
30
20
10
0.076
0.078
0.080
0.082
0.084
FREQUENCY CPH
2N2 MY2
N2 NY2
M2
LAM2 L2
S2 K2

Fig. 1

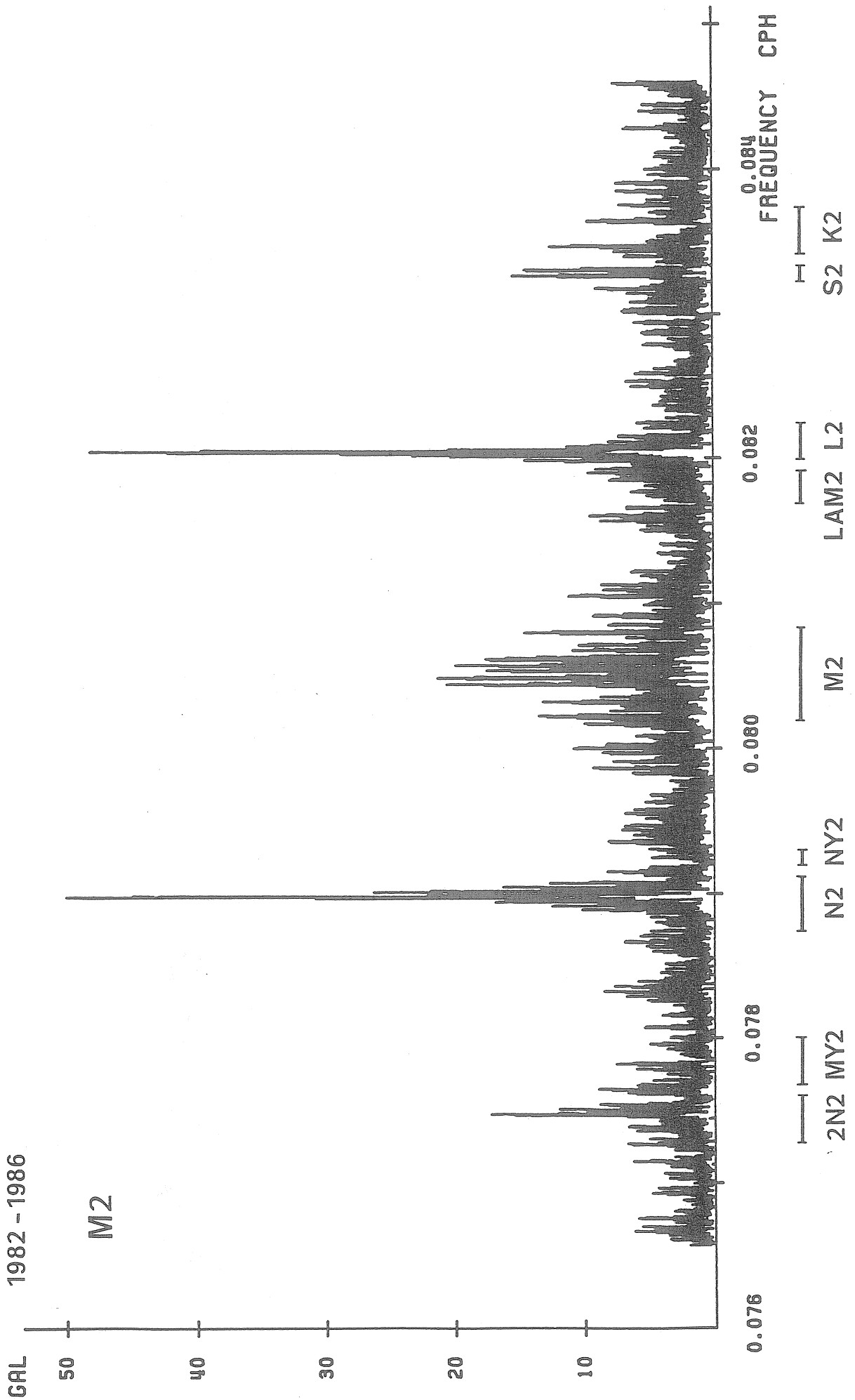
BRUSSELS
1982-1986
M2
NGAL
50
40
30
20
10
0.076
0.078
0.080
0.082
0.084
FREQUENCY CPH
2N2 MY2
N2 NY2
M2
LAM2 L2
S2 K2

Fig. 2

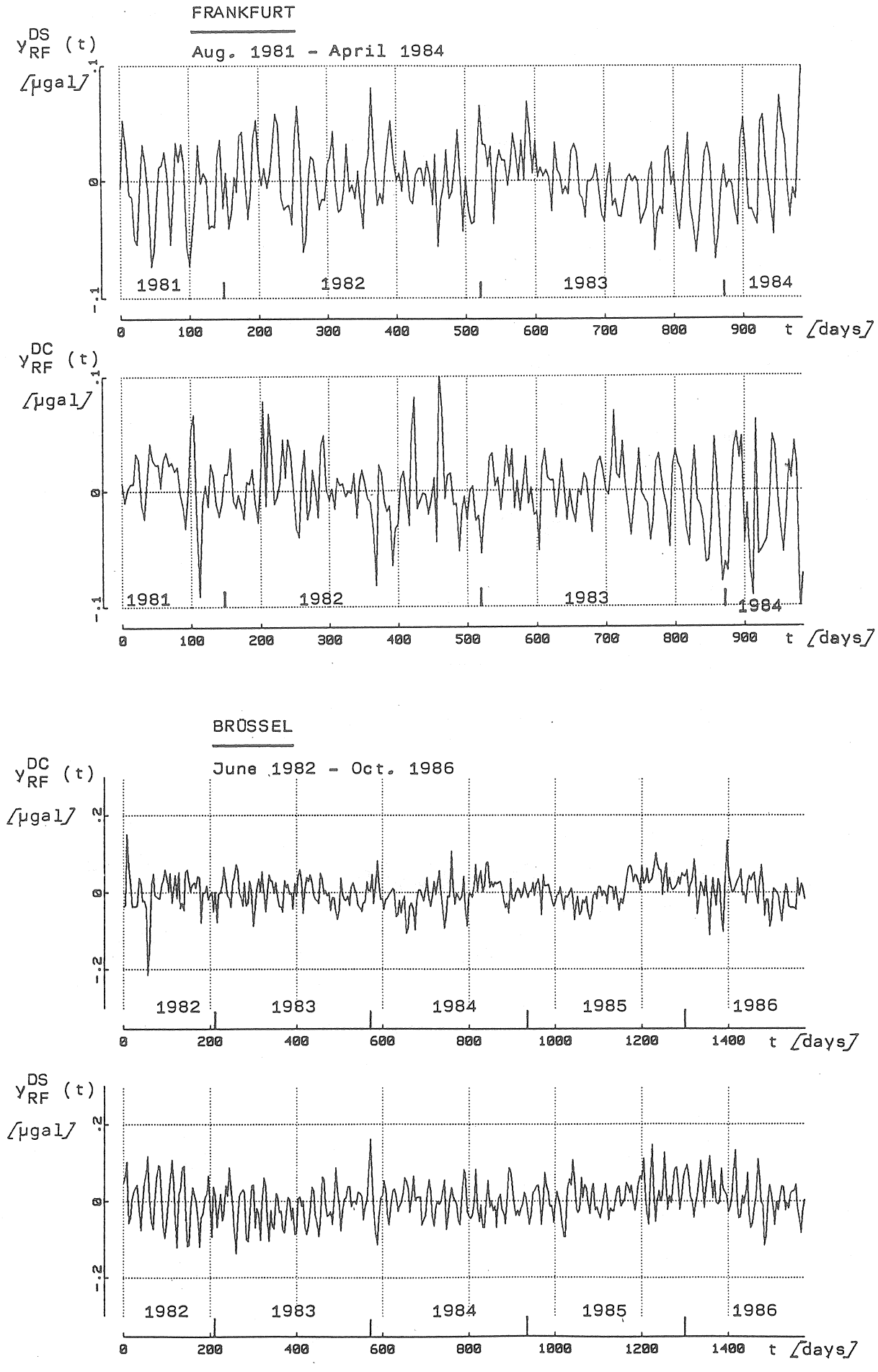
FRANKFURT
Aug. 1981 - April 1984
y^{DS}_{RF} (t)
[µgal]
.1
0
-.1
1981
1982
1983
1984
0 100 200 300 400 500 600 700 800 900 t [days]
y^{DC}_{RF} (t)
[µgal]
.1
0
-.1
1981
1982
1983
1984
0 100 200 300 400 500 600 700 800 900 t [days]
BRÜSSEL
June 1982 - Oct. 1986
y^{DC}_{RF} (t)
[µgal]
.2
0
-.2
1982
1983
1984
1985
1986
0 200 400 600 800 1000 1200 1400 t [days]
y^{DS}_{RF} (t)
[µgal]
.2
0
-.2
1982
1983
1984
1985
1986
0 200 400 600 800 1000 1200 1400 t [days]

Fig. 3

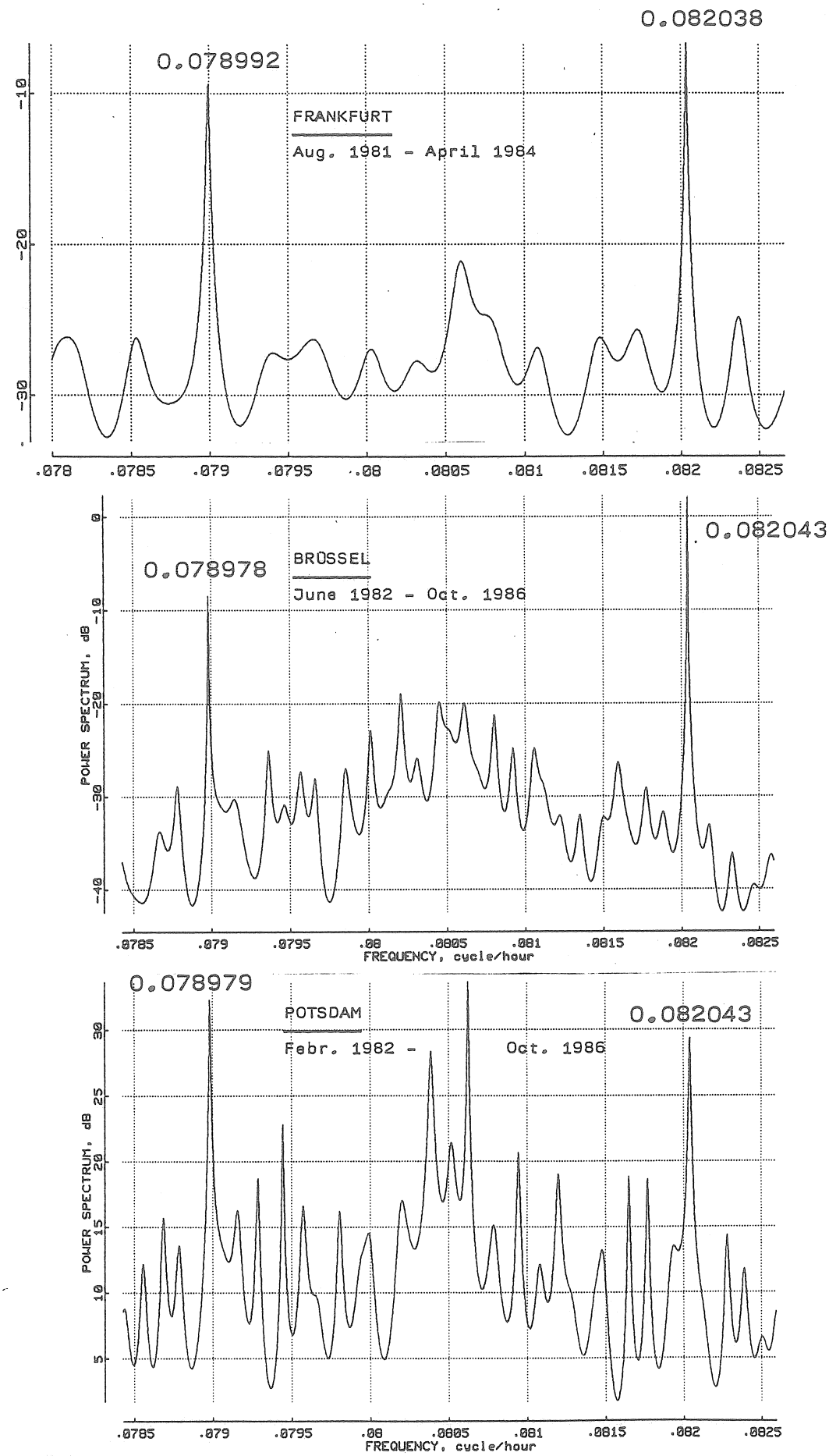
0.082038
0.078992
FRANKFURT
Aug. 1981 - April 1984
-10
-20
-30
.078
.0785
.079
.0795
.08
.0805
.081
.0815
.082
.0825
0.082043
0.078978
BRÜSSEL
June 1982 - Oct. 1986
POWER SPECTRUM, dB
0
-10
-20
-30
-40
FREQUENCY, cycle/hour
0.078979
POTSDAM
Febr. 1982 -
Oct. 1986
0.082043
POWER SPECTRUM, dB
5
10
15
20
25
30
FREQUENCY, cycle/hour

Fig. 4

RELATION BETWEEN EARTH TIDE OBSERVATIONS AND SOME OTHER DATA

Zd. Simon[1], Vl. Stanchev[2], C. De Toro[3], A.P. Venedikov[4], R. Vieira[5]

[1] V.U.G.T. a K., Prague
[2] University Kliment Ohridski, Sofia
[3] Instituto de Astronomia y Geodesia, Madrid
[4] Geophysical Institute, Sofia

1. Introduction.

Recently (Venedikov, 1988) it was proposed a new model for the study of the relation between Earth tide observations, say G and the air pressure data, say P. Here we shall give the results from the application of the model to a large record obtained in Pecny and to a shorter record in Sofia.

It is well known that the most important influence on the Earth tide observations is that of the ocean and sea tides. It is taken into account through computations made on a co-tidal map, now most often the map of Schwiderski. In such a way only the pure harmonic tidal oscillations of the water level are considered.

At a given coastal place it is certainly possible to have deviations in the water level. First, due to local particularities of the water bassin the tides may be shifted in amplitude and phase compared to the tides predicted by the cotidal map. Second, the level may be influenced by meteorological factors as air pressure and wind (meteorological tides). At the same time just the closest water masses have the strongest effect especially on the coastal Earth tide stations.

In principle, in the model mentioned above we can use as P any phenomenon which is expected to influence the Earth tide observations. In particular, for a coastal station, it could be interesting to use as P the water level. Thus we would obtain some direct estimates of the effect of the closest ocean or sea zones. It seems that this may be a helpful addition to the computations made on the co-tidal map.

We have realized such an experiment with the coastal gravity station Cueva de los Verdes (Lanzarote). The results are also given in the present paper.

2. The model used.

We shall briefly discuss the model with some precising explanations.

Let $\bar{S}$ be a vector representing a periodic component of P. We suppose that $\bar{S}$ generates a component Q with the same periodicity in the Earth tide record G. If $Q = |\bar{Q}|$ and $S = |\bar{S}|$ are the corresponding amplitudes and b is the angle (phase shift) between $\bar{S}$ and $\bar{Q}$ our hypothesis is

$$Q = B.S \ , \quad B = \text{const.} \quad \text{and} \quad b = \text{const.} \tag{1}$$

Let δ_s , χ_s

$$\xi_s = \delta_s \cos \chi_s \quad \text{and} \quad \eta_s = - \delta_s \sin \chi_s \tag{2}$$

are parameters of $\bar{S}$ defined in a similar way as usual Earth tide parameters. This statement means that if we analyse P formally as if P are Earth tide data we shall obtain some estimates of the quantities (2).

Let $\bar{A}$ (δ, χ) be an observed tidal component of G of the same type as $\bar{S}$, i.e. D, SD or TD. Observed means that $\bar{A}$ incorporates the effect $\bar{Q}$ of $\bar{S}$. And let A_o (δ_o, χ_o) be the same component free from this effect, i.e.

$$\bar{A}_o = \bar{A} - \bar{Q} \tag{3}$$

If we use the quantities

$$\xi = \delta \cos \chi, \quad \eta = - \delta \sin \chi \ ,$$

$$\xi_o = \delta_o \cos \chi_o \ , \quad \eta_o = - \delta_o \sin \chi_o \tag{4}$$

the following simple relations come from (1) and (3)

$$\xi = \xi_o + B_1 \xi_s - B_2 \eta_s$$

$$\eta = \eta_o + B_1 \eta_s + B_2 \xi_s \tag{5}$$

where $B_1 = B \cos b$ and $B_2 = B \sin b$ (6)

The quantities ξ and η as defined by the first equations of (4) are the unknowns used in the ordinary tidal analysis. If we want to take into the account the effect of P, respectively $\overline{S}$ and $\overline{Q}$, we have to replace ξ and η by the new unknowns ξ_o and η_o and include two more unknowns-the regression coefficients B_1 and B_2.

However this cannot be directly done through the expressions (5) with constant ξ_s and η_s. The equations used in the analysis will become linearily dependent. This reflects simply the fact that in principle there are no means to separate, from the tidal data a stable constant meteorological or any other kind of wave with a tidal frequency.

Nevertheless the expressions (5) can be used if we consider on the variation with time of $\overline{S}$, ξ_s and η_s.

In the first stage of the analysis we process a filtering of independent short intervals of the tidal record. Let T be the central epoch of a given filtered interval. Through the technics proposed by Venedikov (1981) and Xu Houze (1984) we can get ξ_s (T) and η_s (T) separately for D, SD and TD, through the filtering of the data P.

Let x_s and y_s be the mean values of ξ_s (T) and η_s(T) respectively and let

$$\Delta x_s\ (T) = \xi_s\ (T) - x_s, \Delta y_s\ (T) = \eta_s\ (T) - y_s \qquad (7)$$

Then the expressions (5) become

$$\begin{aligned} \xi &= \tilde{\xi}_o + B_1 \Delta x_s\ (T) - B_2 \Delta y_s\ (T) \\ \eta &= \tilde{\eta}_o + B_1 \Delta y_s\ (T) + B_2 \Delta x_s\ (T) \end{aligned} \qquad (8)$$

where

$$\begin{aligned} \bar{\xi}_o &= \xi_o + B_1 x_s - B_2 y_s \\ \bar{\eta}_o &= \eta_o + B_1 y_s + B_2 x_s \end{aligned} \qquad (9)$$

It is these equations (8) which can be used in the analysis. As results directly from the processing we shall obtain estimates of the quantities (9) which are still charged by the total effect of S, respectively of P. In the same time we shall get the estimates of the regression coefficients B_1 and B_2. Later we can get the corrected numbers ξ_o and η_o from (9) i.e.

$$\begin{aligned} \xi_o &= \tilde{\xi}_o - (B_1 x_s - B_2 y_s) \\ \eta_o &= \tilde{\eta}_o - (B_1 y_s + B_2 x_s) \end{aligned} \qquad (10)$$

3. Some results for the atmospheric pressure.

We have analysed formally as an Earth tide record a large air pressure series from Pecny prepared by Broz and Simon. It covers in total an interval of 15.9 years, 1.09.1970 - 30.07.1986 with the following important interruptions : 4.11.1971 - 30.01.1974, 20.08.1975 - 20.04.1976 and 1.09.1981 - 25.01.1982. The results - amplitudes, phases and mean square errors (R.M.S.) are presented in Table 1. The original data are given in 0.1 mm mercury, while the amplitudes are expressed in mm mercury. The phases are related to the corresponding theoretical tidal phases.

Statistically significant and relatively important amplitudes are observed only at the waves S1, S2, S3 and some close tides - (P1, S1, K1, PSI1, PHI1), (T2, S2, K2).
The evident conclusion is that the main oscillations in the atmosphere are of meteorological and non-tidal origin. The only clearly observed tidal wave is M2 with a small but very significant amplitude.

It is interesting that the relation D/SD/TD for the standard deviation is similar to this relation for the analysis of Earth tide data.

These series, after a corresponding reduction of the length, were processed together with a large record of the gravimeter GS 15/228 at the same station Pecny provided by S. Holub, J. Broz and Zd.Simon. It covers a time interval of 8.4 years, (22.04.1976 - 25.09.1984). The total amount of data is 48.708 hourly ordinates. The results are presented in Table 2.

With the same gravimeter GS 15/228 observations were made in Sofia during 1 year. A record 12.12.1981 - 4.12.1982 was processed together with parallel air pressure data from the meteorological station in Sofia. The results are presented also in Table 2.

If we take into account the precision in Sofia there is a rather good coincidence in the coefficients B_1 and B for D tides in the two stations. For SD the results in Sofia are not satisfactory.

The lower precision in the determination of the coefficients in Sofia can be only partly explained by the fact that the record is shorter.

4. Direct relation between Earth tide and sea tide observations.

The motivation for this experimental study was given in § 1.

In the station Cueva de los Verdes (Lanzarote) Earth tide observations are made with the gravimeter LaCoste and Romberg N° 434. The station is situated closely to a maregraphic station. We have used two parallel series from these stations with length 0.8 year - 11.07.1987 - 27.04.1988.

The maregraphic data were submitted to an analysis as gravity Earth tide data. The results are presented in Table 3 as they are outprinted by the computer. The amplitudes are expressed in cm.

The SD tides are more important and better determined than the D tides. Some of the D tides are statistically unsignificant: NO1, J1 and OO1. The SD tides as well as M3 are all significant. It is interesting that there is perfect coincidence in phase between M2 and the tidal potential.

The results from the analysis of the gravity data are presented in Table 4. It is very remarkable that with the exception of M3 all factors are very small, especially for SD. It is possible that this is due to the coastal situation of the station and a strong particular influence of the sea.

In the same Table 4 are given the coefficients B_1, B_2, B and the angle b which are determined by the common processing of both series of data. These coefficients are significant for D and SD.

It will be interesting to calculate the corrected parameters for the gravity M2 according to the expressions (10).

As the phase shift is small for M2 for both Earth and sea data from (10) we have approximately

M2 :

$$\delta_o(\text{corrected}) = \delta_o(\text{gravimetric}) - B_1.\delta\ (\text{maregraphic})$$

$$= 1.014 + 0.103 \times 1.130 = 1.130$$

This is still a somewhat low value of δ but, in our opinion, it is remarkable that the correction is in the right sense. It is easy to verify that the corrections according to (10) of all more important tides are in the sense to rise considerably the values of δ.

References.

Venedikov, A.P., 1981. Determination of the tidal parameters from short intervals in the analysis of Earth tide records. BIM 85, pp 5435 - 5441.

Venedikov, A.P., 1989. A model for the study of the effect of the air pressure on the Earth tide data. BIM 103, pp 7263-7373.

Xu Houze, 1984. Harmonic analysis for short data using Venedikov's filters (in chinese). Crustal deformations and Earthquake, V.4, N° 2, Wuhan.

Table 1

Station Pecny, Air pressure, tidal analysis.

wave	amplitude	R.M.S.	phase diff.	R.M.S.
		D tides		
SIGQ	0.005	±0.007	24.269	± 78.843
2Q1	0.005	0.007	144.091	89.179
SIG1	0.01	0.007	256.746	39.766
Q1	0.017	0.007	-11.963	23.244
RO1	0.017	0.007	111.915	23.423
O1	0.011	0.007	98.762	34.709
TAU1	0.011	0.006	15.312	33.368
NO1	0.006	0.005	180.944	53.832
CHI1	0.012	0.006	112.561	30.704
PI1	0.003	0.007	76.278	121.361
P1	0.054	0.007	249.291	6.942
S1	0.066	0.010	41.231	9.124
K1	0.038	0.007	203.246	10.143
PSI1	0.010	0.007	-44.816	38.088
PHI1	0.014	0.006	103.809	25.059
TETA	0.005	0.006	190.929	72.125
J1	0.011	0.006	-11.079	30.267
SO1	0.020	0.006	236.171	18.109
OO1	0.014	0.005	98.155	21.583
NU1	0.008	0.005	267.313	35.263
		SD tides		
EPS2	0.003	0.002	162.070	43.573
2N2	0.001	0.002	190.021	176.205
MU2	0.003	0.002	76.455	38.704
N2	0.001	0.002	11.905	98.759
NU2	0.005	0.002	64.106	21.820
M2	0.010	0.002	119.242	11.042
LAMB	0.002	0.002	107.308	61.656
L2	0.001	0.002	-30.095	63.038
T2	0.015	0.002	-48.854	7.237
S2	0.151	0.002	193.825	0.752
K2	0.020	0.002	184.632	5.159
ETA2	0.001	0.002	127.047	146.158
2K2	0.002	0.001	-1.850	29.157
		TD tides		
M3	0.001	0.001	13.929	112.531
S3	0.010	0.001	209.238	4.716

Standard deviations D 1.67, SD 0.52 TD 0.22

Note: the amplitudes are in mm mercury.

Table 2

		B_1	R.M.S.	B_2	R.M.S.	B	b
Station Pecny	D	-0.416	±0.007	0.024	±0.007	0.417	176.74°
	SD	-0.235	0.023	0.032	0.024	0.237	172.86
Station Sofia	D	-0.471	0.047	0.093	0.045	0.481	168.78
	SD	-0.081	0.110	0.057	0.112	0.099	144.69

The unit of the coefficients B_1 , B_2 and B is μgal/mbar

STATION DUNNEES MAREGRAPHYQUES ESPAGNE
29 9 0 N -13 26 0 E H 0M

LEAST SQUARE ANALYSIS/VENEDIKOV/74,PROG.SV.-ICET-CUCARME,MELCHIOR,VENEDIKOV
FILTERS ON 30 HRS,NR 102,202,301, ELIM.POWERS D 2 SD 1 TD 1
COMPONENTS S1 O1 S2 N2 M3
POTENTIAL CARTWRIGHT-TAYLER-EDDEN / COMPLETE DEVELOPMENT
COMPONENTS ORIENTATED TOWARDS THE ELLIPSOID (SKALSKY)
COMPUTER CENTRE UNIVERSITY COMPLUTENCE, MADRID
COMPUTER IBM 4381 PROCESSED ON 21.09.88

NORMALIZATION FACTOR -1.0000
INERTIAL CORRECTIONS INTRODUCED

TIME INTERVAL 0.8 YEARS 287.4 DAYS 5580 READINGS 8 BLCKS WEIGHTS
G*** 870711/870818 870903/871008 871011/871013 871110/871129
G*** 871202/880214 880218/880305 880307/880314 880316/880427

WAVE GROUP ARGUMENT	N	WAVE	ESTIMATED AMPL.	R.M.S.	AMPLIT. FACTOR	R.M.S.	PHASE DIFF.	R.M.S.	RESIDUALS AMPL.	PHASE
105.-139.	65	Q1	1.527	0.201	0.3018	0.0397	120.522	7.484	6.77	168.8
143.-149.	26	O1	4.348	0.214	0.1646	0.0081	77.047	2.809	29.95	171.9
152.-158.	22	NO1	0.252	0.190	0.1211	0.0913	-31.750	41.698	2.20	-176.5
161.-164.	13	P1	1.437	0.231	0.1169	0.0188	-27.185	9.401	12.92	-177.1
165.-168.	20	K1	5.335	0.216	0.1436	0.0058	-26.312	2.286	37.56	-176.4
172.-177.	22	J1	0.055	0.179	0.0263	0.0860	-89.978	187.254	2.41	-178.7
181.-1*3.	37	OO1	0.066	0.115	0.0580	0.1014	202.267	97.621	1.38	-179.0
207.-2*5.	155	M2	57.353	0.834	1.0020	0.0146	-1.820	0.781	9.26	-168.7
207.-23*.	41	2N2	1.778	0.052	1.2258	0.0362	33.340	1.690	1.00	101.4
243.-248.	24	N2	14.273	0.082	1.3024	0.0074	11.534	0.325	3.12	66.0
252.-258.	26	M2	64.674	0.090	1.1299	0.0016	0.000	0.079	1.73	180.0
262.-265.	14	L2	1.108	0.049	0.6846	0.0305	-21.290	2.567	0.94	-154.5
267.-274.	12	S2	23.854	0.078	0.8957	0.0029	-21.576	0.178	12.36	-134.8
275.-2*5.	38	K2	6.780	0.055	0.9357	0.0075	-17.564	0.463	2.82	-133.5
327.-382.	18	M3	0.274	0.029	0.2786	0.0294	237.592	5.854	1.14	-168.4

STANDARD DEVIATIONS D 12.02 SD 4.19 TD 1.31
O1/K1 1.1441 1-O1/1-K1 0.9756 M2/O1 6.8517

Table 4

29 10 0 N -13 26 0 E H 60M

CUEVA DE LOS VERDES (LANZAROTE) GRAVIMETRC LCR. 434

LEAST SQUARE ANALYSIS/VENEDIKOV/74,PROG.SV.-ICET-CUCARME,MELCHICR,VENEDIKCV
FILTERS ON 30 HRS,NR 102,202,301, ELIM.POWERS D 2 SD 1 TD 1
COMPONENTS S1 O1 S2 N2 M3
POTENTIAL CARTWRIGHT-TAYLER-EDDEN / COMPLETE DEVELOPMENT
COMPONENTS ORIENTATED TOWARDS THE ELLIPSOID (SKALSKY)
COMPUTER CENTRE UNIVERSITY COMPLUTENCE, MADRID
COMPUTER IBM 4381 PROCESSED ON 21.09.88

NORMALIZATION FACTOR -1.0000
INERTIAL CORRECTIONS INTRODUCED

TIME INTERVAL 0.8 YEARS 287.4 DAYS 5580 READINGS 8 BLCKS WEIGHTS
G*** 870711/870818 870908/871008 871011/871013 871110/871129
G*** 871202/880214 880218/880305 880307/880314 880316/880427

WAVE GROUP ARGUMENT	N	WAVE	ESTIMATED AMPL.	R.M.S.	AMPLIT. FACTOR	R.M.S.	PHASE DIFF.	R.M.S.	RESIDUALS AMPL.	PHASE
105.-139.	65	Q1	5.930	0.035	1.1721	0.0068	-0.309	0.379	0.07	-26.7
143.-149.	26	O1	29.958	0.057	1.1338	0.0021	-0.077	0.150	0.68	-176.6
152.-158.	22	NO1	2.363	0.027	1.1372	0.0132	0.156	0.676	0.05	171.8
161.-164.	13	P1	13.621	0.037	1.1077	0.0030	0.428	0.161	0.57	169.8
165.-168.	20	K1	41.296	0.039	1.1113	0.0010	0.581	0.053	1.07	156.8
172.-177.	22	J1	2.404	0.027	1.1572	0.0132	0.098	0.650	0.01	154.3
181.-1*3.	37	OO1	1.251	0.018	1.0990	0.0157	1.964	0.810	0.08	148.8
207.-2*5.	155	M2	63.227	0.406	1.1047	0.0071	1.557	0.345	3.63	151.7
B1= -0.0978 +- 0.0083 B2= -0.0132 +- 0.0070 E= 0.0987 BETA= 187.69										
207.-23*.	41	2N2	1.476	0.031	1.0175	0.0213	0.205	1.122	0.21	178.5
243.-248.	24	N2	11.122	0.077	1.0150	0.0070	2.387	0.365	1.67	163.9
252.-258.	26	M2	58.038	0.043	1.0140	0.0007	2.829	0.053	8.90	161.2
262.-265.	14	L2	1.605	0.027	0.9921	0.0164	3.654	0.859	0.29	159.6
267.-274.	12	S2	27.073	0.278	1.0167	0.0104	3.674	0.501	4.24	155.9
275.-2*5.	33	K2	7.390	0.069	1.0200	0.0095	3.556	0.469	1.13	156.0
B1= -0.1032 +- 0.0213 B2= -0.0413 +- 0.0213 E= 0.1112 BETA= 201.81										
327.-382.	18	M3	1.069	0.016	1.0888	0.0159	1.570	0.827	0.10	17.3
B1= -0.0313 +- 0.0285 B2= -0.0048 +- 0.0293 E= 0.0316 BETA= 188.67										

STANDARD DEVIATIONS D 1.68 SD 1.30 TD 0.62
O1/K1 1.0201 1-O1/1-K1 1.1988 M2/O1 0.8971

Modelling regional ocean tides

Hans-Georg Scherneck
Dept. of Geodesy
Uppsala University
Hällby, S-755 92 Uppsala, Sweden

(extended abstract)

Ocean tide modelling has been a domain for oceanographers for many decades. Researchers conducting geodynamic measurements use mainly global ocean tide models in order to compute the effect of ocean loading. However, sites that are located at short distance to the sea obtain a large fraction of the total load effect from their vicinity. In this case regional tidal models are needed, but not always available.

The aim of the work presented here is to provide an easy-to-use computer program for solving the discrete ocean tide equations in regional shelf areas. Demands to fulfill are

(a) automatisized grid mesh bathymetry and boundary setup at selectable resolution;

(b) uncritical conditions at open boundaries;

handling of shallow-water phenomena like

(c) bottom friction: both linear and quadratic terms;

(d) turbulence (eddy viscosity);

(e) nonlinear tide interaction and advection.

Put in this order, these demands require increasing oceanographic expertise; to fulfill them all is in conflict with the aim of providing an efficient, user-friendly program.

At level (e) for example, availability of nontidal ocean current (depth averaged transport) and meteorological data is required; in return, the predicted results would consist of a time series of the regional sea surface which comprises a more complete set of load relevant variations in addition to the harmonic tidal constituents.

At the current stage of program development, the following features have been implemented and successfully tested:

The ocean tide equations were formulated according to Krauss (1973) and the discrete scheme according to Sielecki (1967), using an implicit-explicit method on plane, staggered grids for surface elevation and mass transport. The grid is on the tangent plane, stereographic projection is used. Refinements, like frictional laws, tide-coupled water depth, and ocean tide self-attraction and self-loading were adopted according to Flather (1981) and Zahel (1978).

In the first preprocessing step, bathymetry and coastlines are determined from the World Data Center's global topographic data set. The preprocessing program attaches labels to the boundary cells, depending upon the coastline's geometry, or whether the boundary is open to the ocean, in which case auxiliary points are labelled for loading driving tide values from a global model.

In a second preprocessing step, the tidal potential is computed, comprising the luni-solar terms as well as the global contribution due to ocean self-attraction and self-loading, and the open-boundary reference flags are resolved (Schwiderski's model (1983) is used).

The solving program includes at the current stage feature (c) from the list above, and in addition:
(c') infrequent update of the driving potential to account for the self-potential of the modelled region in order to converge to consistency. This is done by Green's function convolution rather than parametrisation; (c") tide elevation-coupled water depth.

So far, only one tide constituent can be modelled at a time. During the test phase, the importance was realized to start from a finite-difference operator which corresponds as accurately as possible

with its continuous equivalent, before non-linear terms or other difficult extensions are added. It was found that the disperion relation can efficiently be turned by adjusting the model parameter g (gravity) such that the operators' eigenvalues coincide for the prevalent wavelength, given the time step size and the water depth.

References

Flather, R.A., 1981: Results from a model of the East Atlantic relating to the Norwegian coastal current. In: R. Saetre and M. Mork (eds): Proc. Norwegian Coastal Current Symposium, Geilo 1980, University of Bergen, 427-458.

Krauss, W., 1973: Methods and results of theoretical oceanography, Vol. 1: Dynamics of the homogeneious and the quasi-homogeneious ocean. Bornträger Berlin, 302 pp.

Schwiderski, E.W., 1983: Atlas of ocean tidal charts and maps, part 1: the semidiurnal principal lunar tide M_2. Marine Geodesy, Vol. 6, 219-265.

Sielecki, A., 1967: An energy conserving difference scheme for the storm surge equations. Monthly Weather Review, Vol. 96, No. 3.

Zahel, W., 1978: The influence of solid earth deformations on semidiurnal and diurnal oceanic tides. In: P. Brosche and J. Sündermann (eds): Tidal Friction and the Earth's Rotation, Springer, Berlin, 98-124.

Propagation of random ocean tide model errors into computed ocean loading effects

Hans-Georg Scherneck
Dept. of Geodesy
Uppsala University
Hällby, S-755 92 Uppsala, Sweden

(extended abstract)

The propagation of errors in the ocean tide models through the computation of loading effects was estimated. The purpose of this study is to provide confidence limits for the analysis of tidal residuals obtained with instruments, the accuracy of which is not the dominating limit.

Superconducting gravimeters allow determination of observed tidal amplitudes with an accuracy of better than 10 ngal (3σ), Richter (1987). This is probably a factor of 10 greater than the current limit of precision for modelling the direct, astronomical tide (Tamura, 1986).

Regardless of whether the analyst is interested in resolving ocean tide loading anomalies, body tide anomalies, or any other perturbing effect on the basis of observed residuals, the accuracy of the computed loading effects is crucial. It is therefore timely to ask how the ocean tide model errors on a global scale, which Schwiderski (1983) specified as $1\,\sigma = 5$ cm, influence the predicted load effect.

In the approach taken in this study, ocean tide model errors are assumed to be spatially correlated. This extends the work presented by Hsu (1987). Evidence for correlation stems from a comparison of Schwiderski's (1983) M_2 tide with the same tide modelled by Flather (1981) in the region of the North East Atlantic (Anderson et al., 1988). The result comes from evaluation of

$$R_{cor} = \sigma_{load\ effect}/\sigma_{tide\ err} = (G\rho)^2 \sum_{ij} G(\vartheta_i)\, G(\vartheta_i)\, cor\, |\zeta_i, \zeta_j|\, \Delta s_i\, \Delta s_j$$

where the sum is taken twice over the ocean model. The sum is approximated in terms of an outer sum and an inner integral over the sphere, of which the latter contains the convolution of the correlation function with the loading Green's function G. Spherical harmonic analysis is applied to carry out the convolution, and corrections are introduced to mimic the effect of the inherent multiplication of G with the geographic ocean function. Special treatment is required to prevent spurious load effects from convolving cor with the pole of G at zero distance: The integral excludes a small "island" with the site at its centre, implying perturbed orthogonality of the Legendre polynomials. A method by Paul (1973) is used to cope with this problem.

The correlation model used so far is

$$cor \sim (1 - 2t\cos\vartheta + t^2)^{-\frac{1}{2}}$$

However, work on the more appropriate choice in terms of the propagation of errors in linear finite difference (ocean tide) model algorithms,

$$cor \sim q^{-\vartheta}$$

is under completion.

Preliminary results suggest $R_{cor}/R_{uncor} \approx 1$ µgal/m e.g. for the Bad Homburg site. This results in a 95% confidence interval of $1.96 \times 0.05 \times 1 = 0.1$ µgal for $\sigma_{tide\ err} = 5$ cm.

References

Anderson, A.J., G. Marquart, and H.G. Scherneck, 1988: Arctic Geodynamics: A satellite altimeter experiment for the European Space Agency Earth Remote-Sensing Satellite. EOS Trans. AGU, Vol. 69, No. 39. 873-881.

Flather, R.A., 1981: Results from a model of the East Atlantic relating to the Norwegian coastal current. In: R. Saetre and M. Mork (eds): Proc. Norwegian Coastal Current Symposium, Geilo 1980, University of Bergen, 427-458.

Hsu, H.T., 1986: Error estimation of gravity loading correction. B.I.M., 99, 6880-6896.

Paul, M.K., 1973: A method for evaluating the truncation error coefficients for geoidal height. Bull. Gëod., 110, 413-425.

Richter, B., 1987: Das supraleitende Gravimeter. Dissertation. Deutsche Geod. Komm., Bayer. Akad. d. Wiss., Reihe C, Heft 329, Verlag d. Inst. f. angew. Geodäsie, Frankfurt/M, 126 pp.

Schwiderski, E.W., 1983: Atlas of ocean tidal charts and maps, part 1: the semidiurnal principal lunar tide M_2. Marine Geodesy, Vol. 6. 219-265.

Tamura, Y., 1986: A harmonic development of the tide-generating force. B.I.M., 99, 6813-6855.

Tidal loading in the shelf area around Denmark

by
Thomas Jahr *

1. Introduction

From April 1984 to November 1988 earth tide measurements were carried out in Denmark. The aims of this project were: The estimation of tidal residuals for the main tidal waves in the diurnal and semidiurnal frequency bands, for correction of geodetical precise measurements. Existing ocean tide models for M2 and O1 for the areas East North Sea, German Bight, Skagerrak, Kattegat, Belt Sea and south-western part of the Baltic Sea were investigated and compared. The influences of nontidal load-effects, caused by windfields and nonlinear signals, due to tidal water level changes at the North Sea coast were estimated.

2. Experimental work

For the Earth tide measurements three gravimeters, two ASKANIA GS-15 (No. 206 and No. 210) and one LaCoste & Romberg Earth tide gravimeter (No. 18) were available. The ASKANIA gravimeters were calibrated by reference recordings in the Earth tide observatory "Insulaner" in Berlin. The LaCoste & Romberg gravimeter was calibrated on the vertical baseline in Hannover. Fig. 1 shows the distribution of the new recording stations in Denmark and some other stations in South Scandinavia and North Germany, where results of Earth tide measurements exist. It was intended to reach a noise level of the residuals of less than 0.1 µgal for the semidiurnal frequencies. This required recording periods of more than half a year at each station.

The digital data were sampeled with intervalls of 30 seconds. After the preprocessing, the data reduction to hourly values was carried out by low pass filtering. All time series were analysed for 13 tidal waves applying a modified program originally written by Chojnicki.

---

* Geologisches Institut Bonn, Nußallee 8, 5300 Bonn 1, GFR

Fig. 1: Distribution of Earth tide stations in South Scandinavia and North Germany. The new stations in Denmark are marked with circles.

The estimated Amplitude, the tidal parameter and the phase yield to the observed ocean load effect. Corresponding to the expectation the loading amplitudes of M2 are in the order of ≈ 1 µgal in Denmark.

3. Load calculation

The calculation of the theoretical load effects were carried out according to the method of Farrell (1972). The theoretical load is discribed by an integral over the Green´s function and the modelled ocean tide. The influence of different Green´s functions, due to various Earth models or changes in the modelling of the Lithosphere, were investigated. The result shows that these differences have only small influences of less than 5 % to the calculated load vector, whereas the ocean tide model plays the decisive role. The Green´s function, used for the load calculation in Denmark (Moho ≈ 30 km) is based on results of the seismic project from the European Geotraverse in 1985 (EGT, 1988).

For the theoretical load calculation of M2 four different ocean tide models of the North Sea and the shelf area around Denmark were available (Fig. 2):

- The original model of Schwiderski provides amplitudes and phases of the main tidal waves in 1° by 1° grid over all oceans (Schwiderski, 1980).

- Mathisen´s model was developed specially for calculations along the Norwegian coast, but it reachs southward to the North Sea and the Channel, too (Mathisen et al., 1983).

- The ocean tide model from Flather for the British Seas and the North Sea is constructed in a more detailed grid of $1/2^\circ$ in longitude by $1/3^\circ$ in latitude (Flather, 1976).

- Flather´s model was improved by amplitudes and phases of the tides in German Bight, calculated by the German Hydrographical Institute (DHI; Soetje et al., 1983). On one side this model was extended eastwards for the Skagerrak, Kattegat, Belt Sea and the south Baltic Sea, on the other side the North Sea coast was improved by a more detailed grid structure (Jahr, 1989).

These local models were adopted to the global model of Schwiderski by introducing a transition zone. For connecting different ocean tide models, the conservation of the watermass moved by tides is another important point. According to the regional problem of the measurements in Denmark, the massconservation was realized as normalisation to the model of Schwiderski

1. Schwiderski

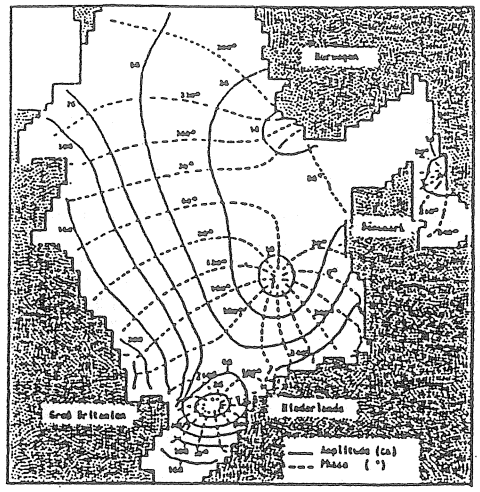

2. Mathisen et al.

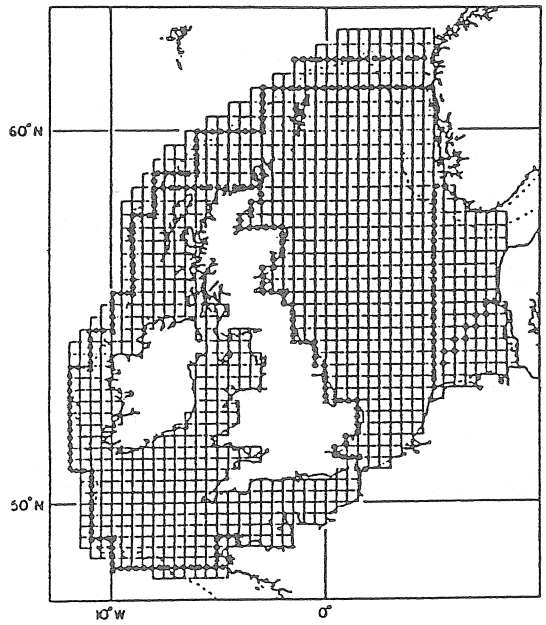

3. Flather

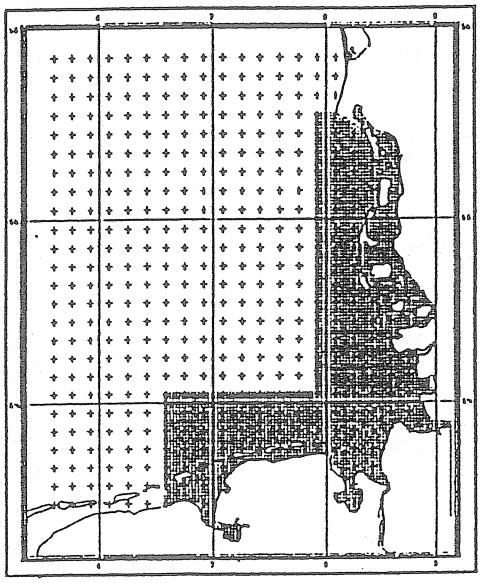

4. German Hydro-graphical Institute

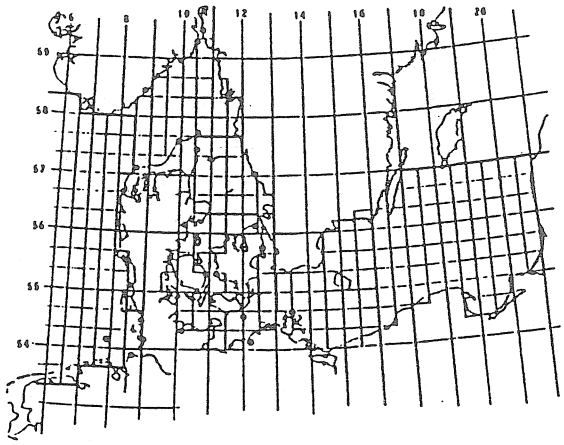

5. Modell extension eastwards

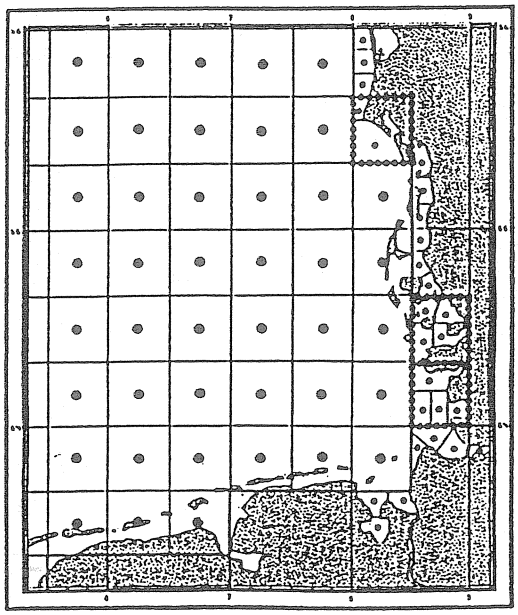

6. Improved gridstructure

Fig. 2: Ocean tide modells for the North Sea and the shelf area around Denmark.

Observed and theoretical ocean load effect of M2							
Earth tide station	Observ.	Theoretical load					
	Amplitude B[µgal] Phase B[µgal]	Schwiderski (original) L [µgal] λ [°]	Mathisen (original) L [µgal] λ [°]	Flather (original) L [µgal] λ [°]	Flather (Mk) L [µgal] λ [°]	OHI (Mk) L [µgal] λ [°]	Schelf (Mk) L [µgal] λ [°]
Møgeltønder	1.396 ± .225 86.3 ± 9.3	0.741 70.2	1.529 112.0	1.182 113.9	1.116 102.8	1.135 96.5	1.277 98.2
Varde	1.324 ± .087 64.1 ± 3.8	0.956 77.9	1.335 92.1	1.382 106.3	1.344 95.2	1.358 90.8	1.262 84.6
Mønsted	1.070 ± .094 71.7 ± 5.0	0.917 70.2	1.125 81.0	0.971 80.3	1.027 69.4	1.043 68.7	1.080 67.4
Ålborg	0.987 ± .105 52.1 ± 6.1	0.857 67.9	1.015 74.8	0.846 76.1	0.898 66.0	0.908 65.5	0.960 60.8
Rolfsted	1.059 ± .141 66.5 ± 7.6	0.849 62.5	1.054 85.0	0.911 78.8	0.946 70.1	0.970 68.8	1.003 71.6
Kopenhagen	0.751 ± .035 73.8 ± 2.7	0.790 60.4	0.935 86.4	0.817 69.0	0.851 62.1	0.862 61.7	0.855 60.1

Tab. 1: Comparison of the theoretical loadvectors of different ocean tide models with the observed ocean tide loadings (Mk = Massconservation).

for the same ocean area. The normalisation of the modified M2-model from Flather was carried out by adding a small constant tide to each cell, with an amplitude of 0.6 cm and a constant phase.

4. Results

The results of the new measurements show, that the effect depends mainly on the distance between the station and the German Bight, where tidal water level changes are considerably high. Therefore we can assume that the M2 loading amplitude of ≈ 0.6 µgal for Büsum is too low, whereas the values of Århus (≈ 1.4 µgal) and Bornholm (≈ 1.1 µgal) seem to be too high.

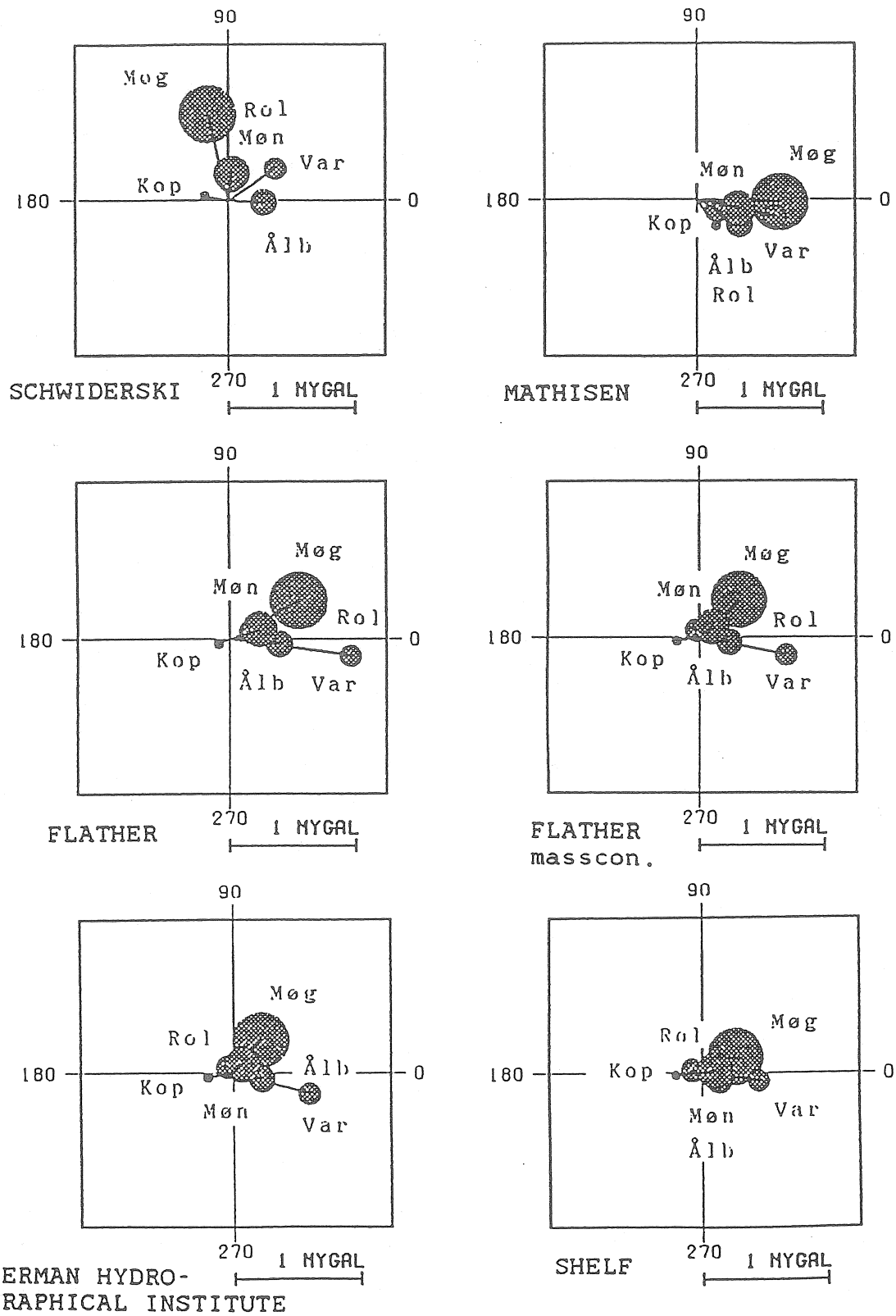

Fig. 3: Restvectors, which are the differences of theoretical and observed load vectors, for different ocean tide models.

The results of the theoretical load calculations for the different ocean tide models compared to the observed load vectors are shown in Tab. 1. The restvectors, discribing the differences of the observed and the calculated load vectors, are plotted in Fig. 3.

The amplitudes of the loadvectors calculated by Schwiderski's model are generally smaller than the observed ones. Although the phases are in good agreement with the observations, the amplitudes of the restvectors are relatively big (Fig. 3).

The theoretical and observed load amplitudes of Mathisen's and Falther's models are more correlated, but the phases of the theoretical vectors are in the order of 10°-30° bigger than the observed phases. Specially the restvectors of Mathisen's model show nearly same phases for all stations, which point to some mistakes in the model. The massconservation of Flather's model leads to a significant improvement of the correlation (Tab. 1).

The agreement of theoretical and observed loadvectors is increased by using the values of the German Hydrographical Institute and the model extension eastwards. Especially the observed load effects in Mønsted and Rolfsted are explained by this ocean tide model. This result is confirmed in the amplitudes of the restvectors, which are the smallest for the so called "shelf" model.

5. Discussion

To get some ideas for further improvements of this ocean tide model (M2), amplitudes and phases of the different ocean patches were systematically changed. The best agreement between the observed and theoretical loadvectors are obtained by increased ocean tide phases (≈ 20° in the East North Sea and the Shelf Area, ≈ 10° in the German Bight), and decreased amplitudes (≈-5 cm in the East North Sea,≈-20 cm in the Shelf Area, ≈-10 cm in the German Bight). The load amplitudes of the ajacent sea areas, Skagerrak, Kattegat, Belt Sea and Baltic Sea are smaller than 0.08 µgal (M2) for all stations in Denmark. These effects are less than the observed noise level of the residuals in the semidiurnal frequency band, except the results of the record of

the LaCoste & Romberg gravimeter in the station in Kopenhagen.

The investigations of nonlinear signals, due to tidal water level changes at the North Sea coast were carried out by the calculation of the coherence functions and the phase differences of the timeseries for Varde (≈16 km from the coast) and for Møgeltønder (≈8 km from the coast) and a theoretical timeseries with nonlinear signals. The results show, that there is no significant signals in higher harmonicals to be found. But a stable coherence with correlated phases of the timeseries in Møgeltønder point to a signal with a period 3 hours and 15 minutes. This seems to be a local effect because it is not obtained at any other station.

The investigation on nontidal load effects in the observed time series were carried out for three different high water levels at the North Sea coast, produced by windfields and storms. Amplitudes of more than 150 cm over the normal high water level

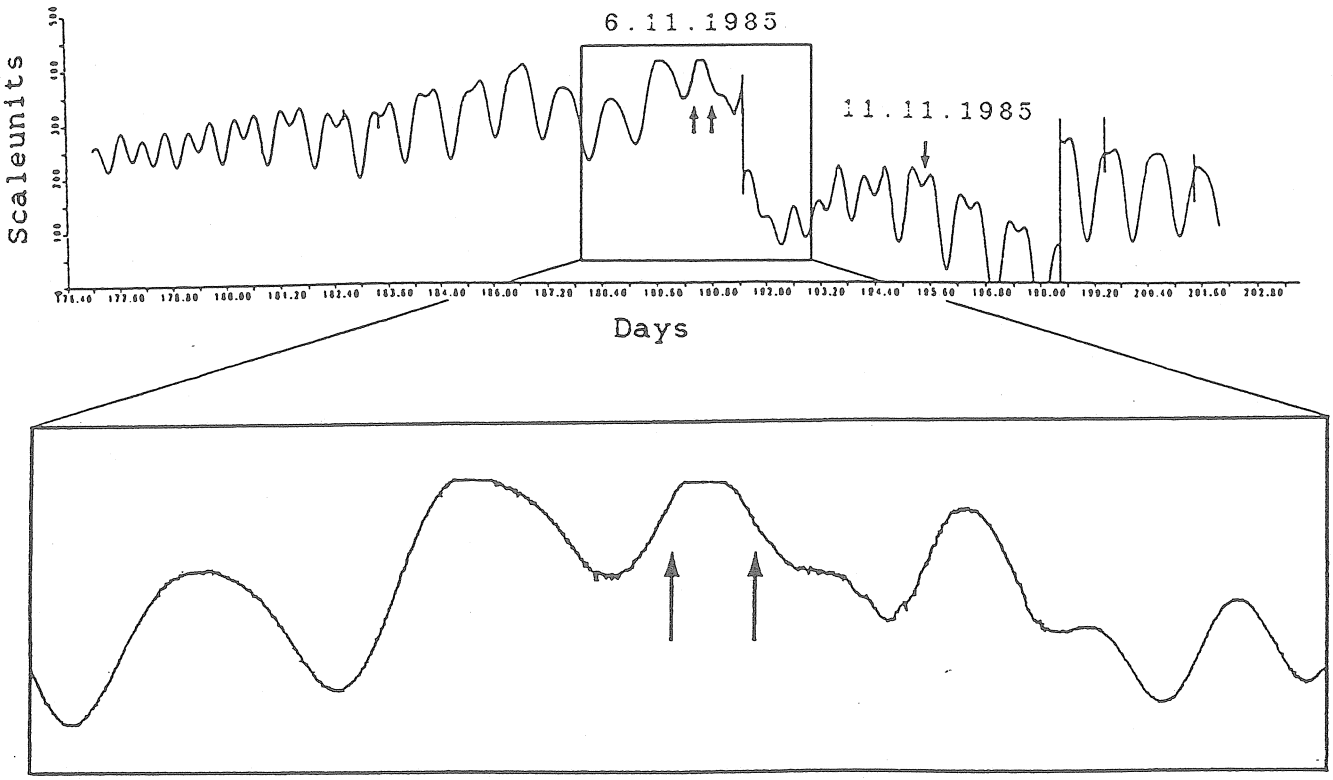

Stepcorrected part of the recording in Varde

Fig. 4: Earth tide recording at the Station in Varde during high water levels (November 1985).

should produce additional loadeffects in the order of 1-2 µgal which are a superimposed drift in the recordings. The separation of this small drift effects presuppose the knowledge of the drift, due to the instrument. If we assume, that the instrumental drift is approximated sucessfully, stronger drift-gradients can be established one day before the maximum amplitude of the high water level is observed (Fig. 4). The amplitudes of this additional drifts are much bigger than the expected 1-2 µgal. The reasons therefore are maybe some further load-effects due to the windfields at the North Sea or the North Atlantic ocean, or some other infuences of meteorological effects like wind or airpressure changes.

6. Acknowledgement

The experimental work was carried out in cooperation with the Danish Geodetic Institute in Kopenhagen. I would like to thank N. Andersen and Dr. O. Remmer for their support of the field work.

Prof. M. Bonatz (Bonn) and Prof. J. Zschau (Kiel) made their ASKANIA gravimeters available to the measurements in Denmark.

Our colleagues from the German Hydrographical Institute (DHI, Hamburg) K. C. Soetje, S. Müller-Navarra and R. Anutsch support the model calculation with their ocean tide model of the German Bight, and the informations about extrem high water levels.

I am thankfull for the help and discussions of all mentioned colleagues, especially Prof. G. Jentzsch, who applied this project (Je 107/10-1 and 10-2) to the German Research Soc. (Deutsche Forschungsgemeinschaft). We thank the German Research Soc. for the financial support.

7. References

EUGENO-S Working Group (ESWG), 1988: Crustal structure and tectonic evolution of the transition between the Baltic Shield and the North German Caledonides (the EUGENO-S Project). - Tectonophysics, Special Issue EGT, Part 4, Vol. 150, p.253-348.

Farrell, W.E., 1972: Deformation of the Earth by surface loads. - Rev. Geophys. Space Physics, 10, 761-797.

Flather, R.A., 1976: A tidal model of the north-west European continental shelf. - Mem. Soc. R. Sci. Liege, 10, 141-164.

Jahr, T., 1989: Gezeitengravimetrie in Dänemark. - Berliner Geowiss. Abhandlungen, Reihe B, in press.

Mathisen, J.P., and O. Johansen, 1983: A Numerical Tidal and Storm Surge Model of the North Sea. - Marine Geodesy, Volume 6, Number 3-4.

Schwiderski, E.W., 1980: On Charting Global Ocean Tides. - Review of Geophysics and Space Physics, 18, 243-268.

Soetje, K.C., and Ch. Brockmann, 1983: An operational numerical model of the North Sea and the German Bight. - North Sea Dynamics, Springer Verlag Berlin, Heidelberg.

Tidal Influences on VLBI Observations

H. Schuh
Geodetic Institute
University of Bonn
Nussalle 17
D-5300 Bonn 1, FRG

Abstract: The tides due to gravitational attraction of the Sun and Moon cause deformations of the solid Earth and influence the Earth rotation paramaters. The following paper will give an overview about all aspects related to to the tides which have to be taken into account in today's high precision geodetic observing techniques, such as Very Long Baseline Interferometry, Satellite Laser Ranging (SLR) and Lunar Laser Ranging (LLR).

1. Introduction

Over the past fifteen years the method of Very Long Baseline Interferometry (VLBI) has been proved to be one of the most accurate modern techniques. It can be used for the measurements of the Earth's rotation, polar motion and of tectonic plate motion, as well as for astrometry and inertial celestial reference system studies. Intercontinental baselines have been measured by VLBI with an accuracy of a few centimeters. Significant changes of the distances between the North American tectonic plate and the Eurasian plate, between the North American plate and the Pacific plate as well as between the Pacific plate and the Eurasian plate have been derived from several years of regular baseline measurements.
The second important aspect of VLBI is the observation of the parameters which define the orientation of the Earth's axes, i.e. polar motion and UT1. At present, VLBI networks of project IRIS (International Radio Interferometric Surveying) produce the most precise measurements of the Earth rotation parameters.
All studies which are based on these measurements address fundamental questions of geophysics such as the cause of crustal movements and earthquakes and the nature of the convection of the mantle. There are also close relations to atmospheric and oceanographic sciences. Moreover, astrometry and the establishing and maintenance of an inertial

reference coordinate frame are fundamental disciplines in geodesy and astronomy.

2. Influences of the tides on the VLBI observables

2.1 Displacements of the radio telescopes

In VLBI data analysis all influences which affect the observed delay τ, i.e the well-known geometric relation between the baseline vector b and the unit vector in source direction k have to be considered besides other effects such as instrumental variations and the retardation of signals by the propagation medium.

2.1.1 Effects of the solid Earth tides

The first order, direct effect of the Sun and Moon causes the solid Earth tides. The resulting displacements of the observing stations, i.e. VLBI as well as Laser stations, are in the range of a few decimeters and are applied in all data analysis programs.
For the calculation of vertical and horizontal displacements (u_r, u_θ, u_λ), besides the tide-generating potential W_T, its derivations $\partial W_T/\partial\theta$, $\partial W_T/\partial\lambda$ the following well known equations are used:

$$u_r = h \cdot W_T/g \quad ,$$
$$u_\theta = l \cdot (\partial W_T/\partial\theta) \,/\, g \quad ,$$
$$u_\lambda = l \cdot (\partial W_T/\partial\lambda) \,/\, (g\cdot\cos\theta) \quad .$$

The evaluation of the tidal potential in the time domain from lunar and solar ephemerides is a very precise method. However, this requires the availability of a homogeneous set of ephemerides and appropriate interpolation programs. Therefore, a second, very simple method using the harmonic expansion of the potential is preferred in most of the VLBI data analysis programs. Moreover, a significant amount of CPU-time can be saved by this method. For the implementation in the 'Bonn VLBI Software System' BVSS, developed at the Geodetic Institute in Bonn, the 'Earth Tides Model Bonn' (ETMB-model) (Buellesfeld, 1985) has been reduced from 665 to 93 constituents, all of which belong to the second degree potential (Buellesfeld and Schuh, 1986). With this version of the ETMB model tidal station displacements can be generated which agree within 1 mm with those computed from the most precise presently available ephemerides.

Another advantage of the harmonic tidal development is the possibility of a direct consideration of frequency dependent Love numbers. While the nominal values $h_2 = 0.609$ and $l_2 = 0.0852$ (Wahr, 1981) are used for the frequency independent Love number h_2 and the Shida number l_2 in accord with the MERIT Standards (Melbourne et al., 1983), the frequency dependent h_{K1} from Wahr's theory $h_{K1} = 0.5203$ is taken for the K1-tide. Thus a rather complicated two-step solution, combining the ephemeris method with an harmonic development for some tides, as recommended by the MERIT Standards, can be avoided without any loss of accuracy.

2.1.2 Effects of the ocean tides

As a secondary tidal effect the solid earth deforms - mainly elastically - under the load exerted on the Earth's crust by the oceanic tides. The observable components of the deformational response, e.g. the displacements of the surface, are subsummed under the term ocean tidal loading effects. The uplift or subsidence of the Earth due to ocean tidal loading is generally of the order of a few centimeters. However, for stations near coastlines or on islands the size of the effect can be one order of magnitude larger. In geophysical models the deformation of the terrain, i.e. the displacement of the station is a function of the ocean tide heights, the areal shape and depth of the oceans, and the rheology of the oceanic and continental lithosphere between the loading masses and the station on the solid Earth. In the past decade, displacements due to ocean tidal loading have been computed by several authors (Goad, in 'Project MERIT Standards', Melbourne et al., 1983; Agnew, 1983; Scherneck, 1983; Pagiatakis et al., 1984; Sato and Hanada, 1985), most of them using methods similar to that described by Farrell (1972) and based on global representations of the ocean tides like those by Schwiderski (1980).
In all of these models the locally referenced displacement vector E in the vertical (radial), N-S and E-W local coordinate system at time t can be computed as a sum of the contributions of n individual ocean tides

$$E(t) = \sum_{i=1}^{n} \begin{Bmatrix} A_i^r \cdot \cos(\omega_i \cdot t + \varphi_i - \delta_i^r) \\ A_i^{NS} \cdot \cos(\omega_i \cdot t + \varphi_i - \delta_i^{NS}) \\ A_i^{EW} \cdot \cos(\omega_i \cdot t + \varphi_i - \delta_i^{EW}) \end{Bmatrix} ,$$

where ω_i is the frequency of the tidal constituents and φ_i the corresponding astronomical argument.
The amplitudes A_i^r, A_i^{NS}, A_i^{EW}, and the Greenwich phase lags δ_i^r, δ_i^{NS}, δ_i^{EW} of each tidal component are determined by the particular model assumed for the deformation of the Earth.
For most of the published results the station displacements derived by the different authors agree within 10 - 20% of the total effect. The differences are caused by taking into account a different number of tides, by using different topographic maps for coastline areas or by adding improved ocean tidal models for those parts of the oceans which are near the coast. Also the choice of the Earth model, and consequently of the loading Green's Function, may change the results as well as the algorithm employed to carry out the surface integral, i.e. the convolution of the load distribution with the Green's kernel. As pointed out by Pagiatakis et al. (1984) the elastic response modeling is as yet inadequate for locations close to the oceans.
Concerning the data analysis of VLBI and Laser observations, the MERIT Standards (Melbourne et al., 1983), on which most of the present analysis software programs are based, contain the ocean loading site displacements compiled by Goad according to Goad (1980). These are tidal loading height displacements of the observing stations due to the 9 main ocean tides (four semi-diurnal tides, four diurnal tides and the fortnightly (Mf) tide). The horizontal displacements which are on the order of 30% of the radial components (Scherneck, 1983) are not yet included in the MERIT Standards.
The load term of degree 0 (n=0) has been excluded by Goad (1980) to impose mass conservation. According to Pagiatakis et al. (1984) the differences of the station displacements between inclusion and exclusion of the n=0 term are less than 0.2 cm, which is not relevant for the present level of accuracy.
Although the model contained in the MERIT Standards has been implemented in most of the present VLBI data analysis programs, the corrections have not yet been applied to the observed delays and delay rates in published standard VLBI solutions (Carter et al., 1985; Herring et al., 1986; Ryan and Ma, 1987).

2.2 Variations of the Earth rotation parameters caused by the tides

2.2.1 Influences of the solid Earth tides on the Earth rotation parameters

Variations of the Earth's rotation caused by the tidal deformation of the polar moment of inertia have been theoretically derived by several authors, for example by Woolard (1959) and by Yoder et al. (1981). The periods and phases of the fluctuations of UT1 are well determined by the motions of the moon and the sun, but the amplitudes are uncertain because of the imperfections in the model for the tidal deformations of the liquid core and the oceans and because of the probable inelasticity of the Earth's mantle (Zschau and Wang, 1986) which has not been taken into account in previous investigations. Yoder et al. (1981) have tabulated all periodic terms in UT1 with amplitudes greater than 0.002 msec. 41 variations have periods between 5 and 35 days and 21 terms have periods longer than three months.

2.2.2 Influences of the ocean tides on the Earth rotation parameters

Oceanic tides with short periods cause variations of the Earth rotation parameters which are qualitatively different from the ones caused by solid Earth tides: with respect to the mechanism (relative water motion), the phase (phase lag to the phase of the tidal force) and sometimes with respect to the very existence of variations at all (e.g. in the case of the M_2 tide) (Brosche et al., 1989, this issue). Hydrodynamical models of the following partial tides have been evaluated for the angular momentum content of the oceans: M2, S2, N2; K1, O1, P1; Mf, Mf'; Mm. The axial angular momentum content of the oceans is presented in two parts: 1. the part P_r due to relative motions of the water, 2. the part P_θ due to changing moment of inertia connected with the water elevations. Both these contributions and their sum P can be represented by a sinusoidal wave in dependence on the total phase. The quantity of the resulting UT1 variations is in the 0.1 msec range (see also Brosche et al., 1989, this issue) and has to be taken into account in VLBI data analysis.

References

Agnew, D.C., Conservation of mass in tidal loading computations, Geophys. J. Roy. Astron. Soc.,72,321-325, 1983.

Brosche, P., Seiler, U., Suendermann, J. and Wuensch, J., Periodic Changes in Earth's Rotation due to Oceanic Tides, this issue, 1989.

Buellesfeld, F.J., Ein Beitrag zur harmonischen Darstellung des gezeitenerzeugenden Potentials, DGK Reihe C, Nr. 365, 1985.

Buellesfeld, F.J. and Schuh, H., New Harmonic Development of the Tide-Generating Potential ETMB 85 with Application on VLBI Data Analysis, Proc. of the Tenth International Symposium on Earth Tides, Madrid, 1985, ed. by R. Vieira, C.S.I.C., 933-942, 1986.

Carter, W.E., Robertson D.S. and MacKay, J.R., Geodetic Radio Interferometric Surveying: Applications and Results. J. Geophys. Res., 90, 4577-4587, 1985.

Farrell, W.E., Deformation of the Earth by surface loads. Rev. Geophys. Space Phys., 10, 761-797, 1972.

Goad, C.C., Gravimetric Tidal Loading Computed from Integrated Green's Functions, J. Geophys. Res., 85, 2679-2683, 1980.

Herring, T.A., Gwinn, C.R. and Shapiro, I.I., Geodesy by Radio Interferometry: Studies of the Forced Nutations of the Earth 1. Data Analysis, J. Geophys. Res., 91, 4745-4754, 1986.

Melbourne, W.R. et al., Project MERIT Standards, U.S. Naval Observatory, Circular No. 167, 1983.

Pagiatakis, S.D., Langley, R.B. and Vanicek, P., Ocean Tide Loading: A Global Model for the Analysis of VLBI Observations, Proc. of the 3rd International Symposium on the Use of Artificial Satellites for Geodesy and Geodynamics, Ermioni, Greece, Sept. 1982, ed. by G. Veis, Publication of the National Techn. Univ. Athens, 328-340, 1984.

Ryan, J.W. and Ma, C., Crustal Dynamics Project Data Analysis-1987, NASA Technical Memorandum 100682, 1987.

Sato, T. and Hanada, H., A Program for the Computation of Oceanic Tidal Loading Effects 'GOTIC', Proc. of the International Conference on Earth Rotation and the Terrestrial Reference Frame, Columbus, 1985, Dept. of Geodetic Science and Surveying, Ohio State Univ. Columbus, Ohio 43210-1247, Vol. 2, 742-748, 1985.

Scherneck, H.G., Crustal Loading Affecting VLBI Sites, University of Uppsala, Institute of Geophysics, Dept. of Geodesy, Report No. 20, Uppsala, Sweden, 1983.

Schwiderski, E.W., On charting global ocean tides, Rev. Geophys. Space Phys., 18, 243-268, 1980.

Wahr, J.M., The Forced Nutations of an Elliptical, Rotating, Elastic, and Oceanless Earth, Geophys. Journ. Roy. Astron. Soc., 64, 705-728, 1981.

Woolard, E.W., Inequalities in mean solar time from tidal variations in the rotation of the earth, Astron. Journ., 64, No.1269, 140-142, 1959.

Yoder, C.F., Williams, J.G. and Parke, M.E., Tidal Variations of Earth Rotation, J. of Geophys. Res., 86, 881-891, 1981.

Zschau, J. and Wang, R., Incomplete Elasticity in the Earth's mantle, Consequences for Earth Tides, Joint meeting of the European Geophys. Soc. and the European Seismol. Comm., Aug. 1986, Kiel FRG, abstract in Terra cognita, Vol. 6, No. 3, 464, Summer 1986.

Periodic Variations in Earth's Rotation Caused by Oceanic Tides

P. Brosche[1], U. Seiler[2], J. Sündermann[2], J. Wünsch[1]

[1] Sternwarte der Universität Bonn,
Auf dem Hügel 71,
D-5300 Bonn 1, F.R. Germany

[2] Institut für Meereskunde
der Universität Hamburg
Troplowitzstr. 7
D-2000 Hamburg 54, F.R. Germany

Abstract

Hydrodynamical models of the following partial tides have been evaluated for the angular momentum content of the oceans:

M_2, S_2, N_2; K_1, O_1, P_1; Mf, Mf'; Mm.

Not only angular momentum changes due to changes of the tensor of inertia have been considered, but also changes due to relative motions in the oceans. From the resulting angular momentum balances, we derive changes in Earth's rotation which amount together to about 0.1 msec in universal time. A manuscript containing the details has been submitted to "Astronomy and Astrophysics".

These theoretical terms are within reach of present VLBI accuracy. The signal of these terms is being sought for in IRIS VLBI experiments. This work is in progress.

Figure 1 shows the theoretical UT1-variations caused by the 9 partial tides listed above for a time interval of 12 days, where JD0 corresponds to 1985 December 1, 0h UT. The part of the long period tides Mf, Mf' and Mm which is in phase with the

equilibrium tide, is presumably partially included in the series for corrections to UT1 due to zonal tides (Yoder et al. 1981).

References

Accad, Y., Pekeris, C. L.: 1978, Phil. Trans. Roy. Soc. London Vol. A 290, 235

Baader, H.-R., Brosche, P., Hövel, W.: 1983, Zeitschrift für Geophysik 52, 140

Baader, H.-R.: 1982, in "Tidal Friction and the Earth's Rotation II" (eds. P. Brosche, J. Sündermann), Berlin-Heidelberg-New York, p. 122

Backhaus, J. O.: 1983, Continental Shelf Research , Vol. 2 p. 243

Brosche, P.: 1982, Proc. VIth Europ. Regional Meeting in Astronomy "Sun and Planetary Systems" (eds. W. Fricke, G. Teleki), Dordrecht, p. 179

Schwiderski, E. W.: 1978, Naval Surface Weapon Center, NSWC/DL TR-3888, Dahlgren, Virginia

Sündermann, J.: 1982, in "Tidal Friction and the Earth's Rotation II" (eds. P. Brosche, J. Sündermann), Berlin-Heidelberg-New York, p. 165

Yoder, C. F., Williams, J. G., Parke, M. E.: 1981, J. Geophys. Res. 86, 881

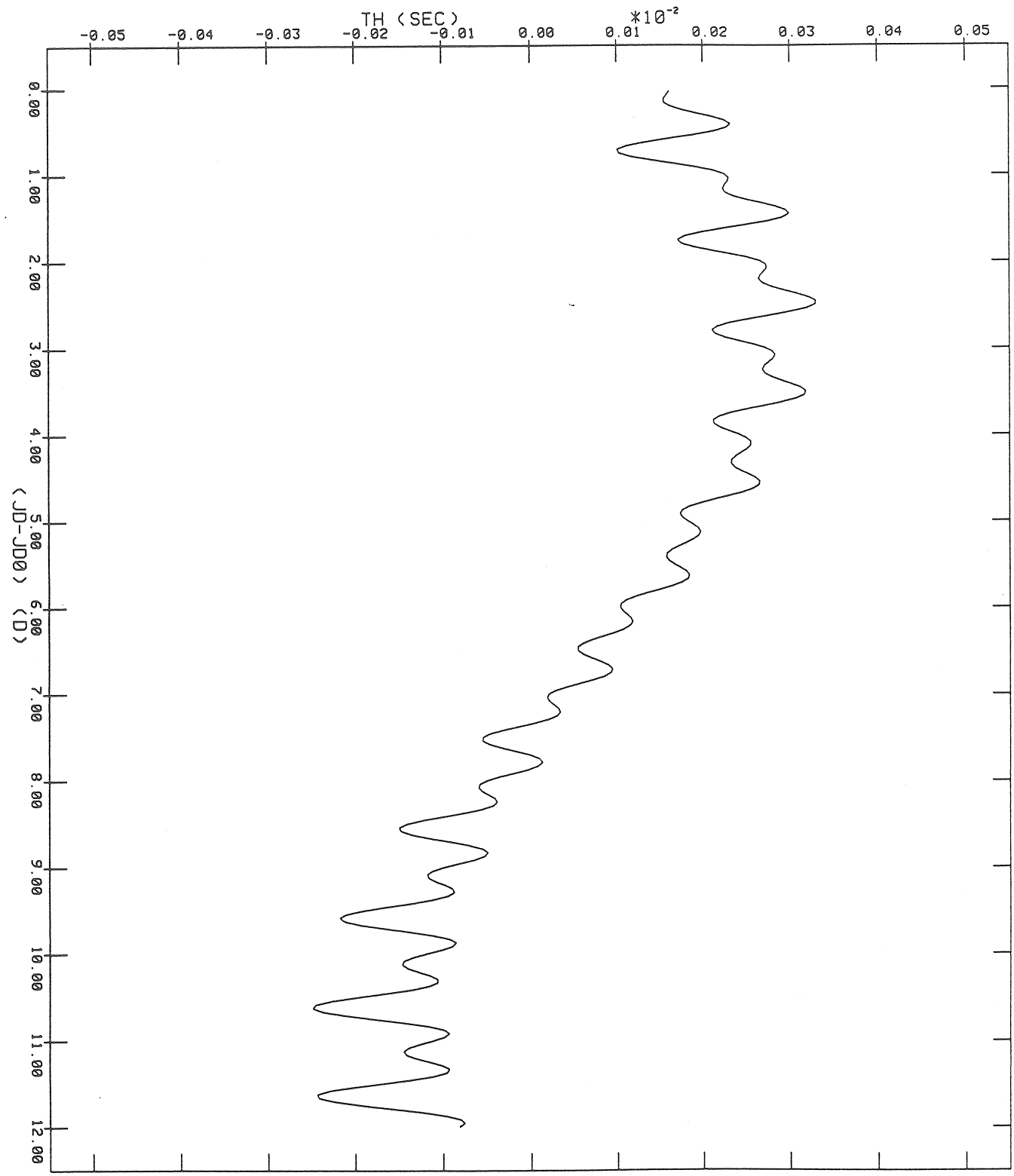

Figure 1: The theoretical UT1- variations for a time interval of 12 days; JD0 corresponds to 1985 December 1, 0h UT.